Discovery and Assessment of Endogenous Biomarkers of CYP2D6 Activity for Application in Clinical Studies

Jessica C. Sontheimer

A dissertation

submitted in partial fulfillment of the

requirements for the degree of

Doctor of Philosophy

University of Washington

2015

Reading Committee:

Yvonne S. Lin, Chair

Nina Isoherranen

Danny D. Shen

Program Authorized to Offer Degree:

Pharmaceutics

University of Washington

Abstract

Discovery and Assessment of Endogenous Biomarkers of CYP2D6 Activity for Application in Clinical Studies

Jessica C. Sontheimer

Chair of Supervisory Committee:
Assistant Professor Yvonne S. Lin, Ph.D.
Pharmaceutics

The activity of cytochrome P450 2D6 (CYP2D6) is highly variable due to genetic and environmental influences. Assessing CYP2D6 activity may aid in initial dosing of drugs metabolized by CYP2D6, help maximize therapeutic efficacy or minimize adverse events. Traditionally, probe drugs, such as dextromethorphan (DM), metoprolol and atomoxetine, are administered to determine CYP2D6 activity. The primary aim of this dissertation was the discovery and evaluation of endogenous biomarkers of CYP2D6 activity as a non-invasive means of phenotyping. We developed two liquid chromatography mass spectrometry methods to

quantify selected endocannabinoids and indolethylamines, previously reported as *in vitro* substrates of CYP2D6. Preliminary results suggest no difference between plasma anandamide concentrations at baseline and following CYP2D6 inhibition in healthy adults (P=0.61), although a possible difference in 5-MT/serotonin ratio was observed between two urine samples. With further refinement, these assays will allow evaluation of the endocannabinoid and indolethylamine substrates and metabolites as biomarkers of CYP2D6 and potentially other cytochromes P450 in clinical samples. Using global metabolomics, we detected a novel ion (M1) with *m/z* 444.3 eluting at 6.5 min. M1 was absent in the urine of CYP2D6 poor metabolizers and present in all other CYP2D6 phenotypes. In adults, M1 decreased on average 4- and 9-fold in plasma and urine, respectively after potent CYP2D6 inhibition and was negatively correlated with the DM parent-to-metabolite metabolic ratio (P=0.012). Furthermore, urinary M1 was correlated with the oral clearance of metoprolol in women studied during pregnancy and postpartum, and atomoxetine in children with attention deficit hyperactivity disorder. Our data suggest that M1 may be a product of a reaction catalyzed by CYP2D6. Following development of large-scale semi-purification of M1 in urine, characterization of M1 by multiple stage mass spectrometry was performed. Though the structure of M1 remains unknown, future efforts should focus on the identification of M1 and its parent. Validation of the M1 biomarker alone or in combination with its parent may provide a useful endogenous biomarker of CYP2D6 activity. Clinical application of endogenous biomarkers may have benefits of safety, cost, time and convenience over traditional phenotyping methods, and may permit the assessment of CYP2D6 activity in population-based studies.

Dedication

For my parents, Yulinda and Yong, and my sister, Suzanne, who have always believed in me. For my best friend and eternal companion, Clayton, who is a constant source of encouragement and inspiration.

Table of Contents

Chapter 1. Introduction

1.1 Background

Cytochromes P450 are a superfamily of enzymes that play a major role in the phase I metabolism of drugs. Cytochrome P450 2D6 (CYP2D6) is one of these drug metabolizing enzymes (DME) involved in the biotransformation of many clinically used drugs, such as antidepressants, antipsychotics, opioid analgesics, antiarrhythmics, β-blockers, antihistamines, and selective estrogen receptor modulators [1, 2]. Although the hepatic content of CYP2D6 is only about one to four percent of the total cytochrome P450 protein, this enzyme is responsible for the primary elimination of approximately 15-20% of clinically used drugs primarily metabolized by this family of enzymes [3, 4]. CYP2D6 protein has also been observed in the brain [5-7] and small intestine [8], but at lower concentrations than in the liver.

1.2 CYP2D6 genetics

CYP2D6 is highly polymorphic; there are more than 100 allelic variants and subvariants identified to date (www.cypalleles.ki.se/cyp2d6.htm). The various genotypes result in four phenotypic categories: poor metabolizers (PM), carriers of null alleles that lack of function; intermediate metabolizers (IM), carriers of one functional allele or two partial activity alleles; extensive metabolizers (EM), who have the reference phenotype; and ultra-rapid metabolizers (UM), who have multiple copies of functional alleles. About 5-10% of the European Caucasian population are poor metabolizers [9-11], whereas the frequency is lower among other ethnicities [12, 13]. The *CYP2D6*4* allele, which harbors a splice site mutation, is the most common null allele in Caucasians (20% in a Germans) [14], but is virtually absent in the Asian and African populations [12, 15]. Other common null alleles include frame shifts: *CYP2D6*3* [16], and *CYP2D6*6* [17], and a gene deletion: *CYP2D6*5* [18]. Partially functional alleles occur in all major races. The *CYP2D6*10* and *CYP2D6*17* are present in up to 30% of Africans and 50% of Asians, respectively [19, 20]. *CYP2D6*41* is more common among Caucasians (10-15%) and results in only a fraction of correctly spliced mRNA due to an erroneous intron SNP [21]. Multiple copies of alleles occur in about 5% of Caucasians [22] and more frequently (~10-30%) in Arabian and Eastern African populations [23, 24]. However, not all duplications are comprised of functional genes, there can be duplications of partially functional and nonfunctional alleles [25].

1.3 Genotype-to-phenotype predictions

Restriction fragment length polymorphism (RFLP) in conjunction with polymerase chain reaction (PCR) is the reference standard for determining *CYP2D6* genotype. Commercial genotyping assays are available and the most comprehensive, the AmpliChip CYP450 Test (Roche), checks for the presence of 33 *CYP2D6* alleles [26]. The highly polymporphic nature of *CYP2D6* combined with the presence of pseudogenes, unexpected recombinations and failure to account for important variants due to ethnicity make genotype-to-phenotype predictions both challenging and complex. In addition, the activity of the enzyme resulting from reduced functional alleles can be substrate specific. For example, the turnover of metoprolol and codeine in homozygous African subjects [19] and haloperidol *in vitro* [27] by *CYP2D6*17* was more rapid than what was expected based on other CYP2D6 substrates such as dextromethorphan. The majority of *CYP2D6* variants have not been evaluated for substrate specificity. In addition, there is a large degree of interindividual variability within each genotype, as subjects with identical genotypes may exhibit differences in enzyme activity which may span two orders of magnitude [28-30]. Gaedigk et al. proposed an activity score system to reduce the complexity of genotype data by combining genotypes into a small number of groups that include individuals with comparable predicted activities. In a cohort of over 600 Caucasians and African American subjects, *CYP2D6* activity score explained 55% of the variability in the urinary metabolic ratio of dextromethorphan, yet residual interindividual variability within each activity score remained [31].

1.4 CYP2D6 phenotyping

It has been proposed that environmental factors such as diet [24, 32] and disease [33-37] may play a role in CYP2D6 variability within the population. DME phenotyping captures both genotype and environmental effects on enzyme activity. Phenotyping of CYP2D6 activity is performed by the administration of exogenous substrates. Enzyme activity is reflected in the clearance of a drug exclusively metabolized by CYP2D6 or in the partial clearance of the parent drug to the CYP2D6-mediated metabolite.

Decreased clearance of debrisoquine and sparteine were first described in the late 1970s [9, 38, 39]. The distribution of debrisoquine and sparteine clearance in Caucasians was bimodal [38] and trimodal [40], respectively. These drugs can be used as markers of CYP2D6 activity [41-43], but their utility is limited as debrisoquine and sparteine are not approved for use in some countries. More contemporary drugs used for CYP2D6 phenotyping include metoprolol and dextromethorphan.

Metoprolol is primarily metabolized by CYP2D6 (70-90% of the dose) [44, 45]. The α-hydroxylation of metoprolol occurs almost exclusively by CYP2D6, whereas the O-demethylation occurs by CYP2D6 jointly with other enzymes [46]. Metoprolol is administered as a racemic mixture and metabolism of metoprolol by CYP2D6 EMs and PMs is stereoselective [47]. The metoprolol/α-hyrdoxymetoprolol or the S/R-metoprolol metabolic ratios have been used as markers of CYP2D6 activity [41, 47-50]. However, these metabolic ratios did not match debrisoquine results in some ethnic groups [51-53]. In addition, the metorpolol/α-hyrdoxymetoprolol metabolic ratio may be influenced by urinary pH [54].

Dextromethorphan (DM) is a well-established, over-the-counter drug that has been used with its O-demethylated product, dextrorphan (DX) for phenotyping [42, 43, 55]. The DM metabolic ratio (DM/DX), defined as the molar ratio of DM/[DX + DX glucuronide], has an anti-mode at a value of 0.3, distinguishing IMs/EMs from PMs [55]. DM MR is well correlated with both debrisoquine and sparteine metabolic ratios (r^2 = 0.78 and 0.82, respectively) [55, 56]. However, there is some evidence that DM/DX and DM oral clearance are only weakly correlated [57] and urinary pH may be a significant source of variation in DM/DX [54].

1.5 Common CYP2D6 substrates and reactions

As reviewed by Wang et al., substrates of CYP2D6 are classically planar, aromatic, lipophilic bases with a protonatable (at physiological pH) nitrogen 5-7 Å from the active site [58]. CYP2D6 has a well-defined active site approximately 540 $Å^3$ in volume and has been described to appear in the shape of a right foot [59]. Common CYP2D6 reactions include hydroxylation (for desipramine and debrisoquine), and dealkylation, including demethylation (for codeine and dextromethorphan) [38, 58].

1.6 Inhibition and induction of CYP2D6

CYP2D6 inhibitors may influence therapeutic outcomes of a co-administered drug [60]. Potent inhibition of CYP2D6 is exhibited by drugs such as paroxetine, fluoxetine, fluvoxamine and quinidine *in vivo*, resulting in a change from EM to PM phenotypes in some subjects [61-63]. While CYP2D6 is generally considered non-inducible by xenobiotics, there are conflicting reports of the effects of rifampin on CYP2D6 activity. Caraco et al. reported a 2- to 12- fold increase in codeine O-demethylation in healthy adult subjects following a 3-week treatment of rifampin (600 mg) [64]. However, others concluded that rifampin had little to no inductive effect on CYP2D6 [39, 65]. CYP2D6 activity has been shown to be induced in pregnancy with reports of a 26-48% increase in dextromethorphan O-demethylation [66], and a 2- to 13-fold increase in the apparent oral clearance of metoprolol during the third trimester of pregnancy as compared to postpartum [67].

1.7 Endogenous substrates of CYP2D6

In addition to the oxidation and dealkylation of many clinically used drugs, CYP2D6 may also be involved in the metabolism of endogenous substrates. CYP2D6 has been implicated in the metabolism of trace amines found in the brain. The metabolism of pinoline and 5-methoxy-N,N-dimethyltryptamine (5-MeO-DMT) have been shown to be selectively catalyzed by recombinant CYP2D6 [68]. In addition, it was found that pinoline metabolism was well correlated with CYP2D6 activity and content (r^2 = 0.93 and 0.82, respectively) and was inhibited by quinidine in human liver microsomes [69]. Similarly, CYP2D6 was responsible for the metabolism of 5-

methoxytryptamine (5-MT) to serotonin in recombinant CYP2D6 and hepatic microsomes from wild-type and CYP2D6-humanized mice [70]. Anandamide, a neuroprotective, anti-inflammatory and anti-nociceptive fatty acid cannabinoid found in the brain and several other tissues [71-74], has been shown to be hydroxylated and epoxygenated by recombinant CYP2D6 and in brain microsomal and mitochondria preparations [75]. Recently, serotonin, 5-hydroxyindoleacetic acid, L-carnitine, acetyl-L-carnitine, pantothenic acid, 2'-deoxycytidine diphosphate, anandamide, and N-acetylglucosaminylamine have been shown to be up-regulated and stearoyl-L-carnitine was found to be down-regulated in CYP2D6-humanized mice as compared to control mice [76]. Other reported *in vitro* endogenous CYP2D6 substrates include tryptamine [77] and steroids such as testosterone [78], estrogens [79], and allopregnanolone [80]. Development and use of endogenous substrates for *in vivo* CYP2D6 phenotyping is still work in progress.

1.8 Pediatric drug metabolism

In pediatric liver samples, CYP2D6 expression is detectable during fetal stages and increases with postnatal age [81]. By 2 weeks of age, CYP2D6 activity is significantly associated with genotype, suggesting that genotype is a greater determinant of CYP2D6 variability than is ontogeny [82]. However, knowledge of drug metabolism and appropriate therapeutic dosing in children lags far behind that of adults. In 2009, it was estimated that only 41% of clinically used drugs had some pediatric labeling information [83]. Lack of pediatric dosing guidelines have led to allometric scaling based on body weight or surface area; however, studies have shown deficiencies in these methods [84, 85].

The pharmacokinetics of drugs may be subject to physiological changes in the pediatric population. For example, renal function does not reach maturity until 1 year of age [86]. In addition, children have a higher ratio of total body water to fat as compared with adults [87]. Gastric pH is higher in neonates and young children and does not decrease to adult levels until age 2 [88-90]; this may affect acid labile drugs. Understanding complexities such as physiological development and genetic variation in children may improve drug therapy.

1.9 Metabolomics for clinical applications

Over the past two decades, advances in nuclear magnetic resonance (NMR) and mass spectrometry techniques has allowed the simultaneous measurement of a large number of analytes in a single biological sample [91]. These advances in analytical technology have been utilized in the field of metabolomics—the analysis of a complete set of small molecules in a biological sample under a given set of conditions [92, 93]. Metabolomics can capture the genetic, proteomic, metabolic and environmental interactions in a biological system [94]. The compounds in a metabolome may include endogenous and exogenous compounds such as amino acids, carbohydrates, sugars, vitamins, drugs and dietary components [93]. Using statistical analyses and chemometrics, differences in metabolomic profiles can be identified between perturbed and unperturbed states, such as case and control patients [91]. Metabolomics has been applied to studies in toxicology [95], plant research [96, 97], and biomarker discovery [98-101], and aided in understanding diseases [102, 103].

1.10 **Dissertation aims**

The aim of this dissertation was to explore non-invasive biomarkers of CYP2D6 activity by evaluating previously reported endogenous CYP2D6 substrates and metabolites, as well as discovering novel CYP2D6 biomarkers. Endogenous biomarkers of CYP2D6 activity have advantages over exogenous markers. Biomarkers would eliminate the risk of adverse events that may come with the administration of drug probes currently used for phenotyping. Phenotyping with endogenous biomarkers would be an attractive option in all populations, but especially for vulnerable populations such as children, pregnant women and the elderly. In addition, endogenous biomarkers might be more convenient and cost-effective by eliminating the need for timed sample collections.

A number of endogenous indolethylamines, such as 5-MT, 5-MeO-DMT and pinoline, and the fatty acid, anandamide have been shown to be metabolized by CYP2D6 *in vitro*. However, to our knowledge, there have been no human studies investigating the ability of these compounds to reflect changes in CYP2D6 activity. To support this assessment, our first goal was to develop analytical methods for the evaluation of reported CYP2D6 substrates and products as biomarkers of human CYP2D6 activity. In Chapter 2, we developed an analytical LC-MS/MS method capable of simultaneously quantifying anandamide and two *in vitro* CYP2D6 products, 20-hydroxyeicosatetraenoic acid ethanolamide (20-HETE-EA) and 14,15-epoxyeicosatrienoic acid ethanolamide (14,15-EET-EA) in human plasma. We used this method to analyze clinical plasma samples from adults at baseline and following CYP2D6 inhibition. In parallel, as described in Chapter 3, we developed an LC-MS/MS method to analyze three reported CYP2D6 substrates, 5-MT, 5-MeO-DMT and pinoline, and two metabolites, serotonin and bufotenine, in human urine.

In Chapter 4, we used a global metabolomics approach to detect M1, a novel endogenous biomarker, in CYP2D6-phenotyped and genotyped children. An independent set of children was used to validate M1 as a biomarker of CYP2D6. Moreover, we assessed the effect of CYP2D6 inhibition by multiple doses of fluoxetine on urinary M1 concentrations in adult subjects. In Chapter 5, we ascertained the relationships between M1 and various CYP2D6 probes. The association of M1 and metoprolol clearance was evaluated in urine samples from women during pregnancy and postpartum. Second, we compared plasma and urinary M1 concentrations with dextromethorphan clearance and its urinary metabolic ratio in adult subjects participating in a drug-drug interaction study with fluoxetine. Third, we evaluated the association of M1 with atomoxetine clearance and *CYP2D6* activity score in children with attention deficit hyperactivity disorder.

Finally, in Chapter 6, we describe our attempts to semi-purify M1 from human urine using large-scale liquid-liquid extractions and semi-preparative column chromatography. We used various techniques, such as high-resolution mass spectrometry, multiple stage mass spectrometry (MS^n) and NMR, to yield information about the accurate *m/z* of M1 and to obtain clues of the identity of M1.

1.11 References

1. Zhou SF: Polymorphism of human cytochrome P450 2D6 and its clinical significance: Part I. *Clinical pharmacokinetics* 48(11), 689-723 (2009).

2. Zhou SF: Polymorphism of human cytochrome P450 2D6 and its clinical significance: part II. *Clinical pharmacokinetics* 48(12), 761-804 (2009).

3. Zanger UM, Turpeinen M, Klein K, Schwab M: Functional pharmacogenetics/genomics of human cytochromes P450 involved in drug biotransformation. *Analytical and bioanalytical chemistry* 392(6), 1093-1108 (2008).

4. Zanger UM, Schwab M: Cytochrome P450 enzymes in drug metabolism: regulation of gene expression, enzyme activities, and impact of genetic variation. *Pharmacology & therapeutics* 138(1), 103-141 (2013).

5. Dutheil F, Dauchy S, Diry M *et al.*: Xenobiotic-metabolizing enzymes and transporters in the normal human brain: regional and cellular mapping as a basis for putative roles in cerebral function. *Drug metabolism and disposition: the biological fate of chemicals* 37(7), 1528-1538 (2009).

6. Siegle I, Fritz P, Eckhardt K, Zanger UM, Eichelbaum M: Cellular localization and regional distribution of CYP2D6 mRNA and protein expression in human brain. *Pharmacogenetics* 11(3), 237-245 (2001).

7. Miksys S, Rao Y, Hoffmann E, Mash DC, Tyndale RF: Regional and cellular expression of CYP2D6 in human brain: higher levels in alcoholics. *Journal of neurochemistry* 82(6), 1376-1387 (2002).

8. Paine MF, Hart HL, Ludington SS, Haining RL, Rettie AE, Zeldin DC: The human intestinal cytochrome P450 "pie". *Drug metabolism and disposition: the biological fate of chemicals* 34(5), 880-886 (2006).

9. Eichelbaum M, Spannbrucker N, Steincke B, Dengler HJ: Defective N-oxidation of sparteine in man: a new pharmacogenetic defect. *European journal of clinical pharmacology* 16(3), 183-187 (1979).

10. Niewinski P, Orzechowska-Juzwenko K, Hurkacz M *et al.*: CYP2D6 extensive, intermediate, and poor phenotypes and genotypes in a Polish population. *European journal of clinical pharmacology* 58(8), 533-535 (2002).

11. Rideg O, Haber A, Botz L *et al.*: Pilot study for the characterization of pharmacogenetically relevant CYP2D6, CYP2C19 and ABCB1 gene polymorphisms in the Hungarian population. *Cell biochemistry and function* 29(7), 562-568 (2011).

12. Myrand SP, Sekiguchi K, Man MZ *et al.*: Pharmacokinetics/genotype associations for major cytochrome P450 enzymes in native and first- and third-generation Japanese populations: comparison with Korean, Chinese, and Caucasian populations. *Clinical pharmacology and therapeutics* 84(3), 347-361 (2008).

13. Agundez JA, Ramirez R, Hernandez M, Llerena A, Benitez J: Molecular heterogeneity at the CYP2D gene locus in Nicaraguans: impact of gene-flow from Europe. *Pharmacogenetics* 7(4), 337-340 (1997).

14. Sachse C, Brockmoller J, Bauer S, Roots I: Cytochrome P450 2D6 variants in a Caucasian population: allele frequencies and phenotypic consequences. *American journal of human genetics* 60(2), 284-295 (1997).

15. Wan YJ, Poland RE, Han G *et al.*: Analysis of the CYP2D6 gene polymorphism and enzyme activity in African-Americans in southern California. *Pharmacogenetics* 11(6), 489-499 (2001).

16. Kagimoto M, Heim M, Kagimoto K, Zeugin T, Meyer UA: Multiple mutations of the human cytochrome P450IID6 gene (CYP2D6) in poor metabolizers of debrisoquine. Study of the functional significance of individual mutations by expression of chimeric genes. *The Journal of biological chemistry* 265(28), 17209-17214 (1990).

17. Saxena R, Shaw GL, Relling MV *et al.*: Identification of a new variant CYP2D6 allele with a single base deletion in exon 3 and its association with the poor metabolizer phenotype. *Human molecular genetics* 3(6), 923-926 (1994).

18. Gaedigk A, Blum M, Gaedigk R, Eichelbaum M, Meyer UA: Deletion of the entire cytochrome P450 CYP2D6 gene as a cause of impaired drug metabolism in poor metabolizers of the debrisoquine/sparteine polymorphism. *American journal of human genetics* 48(5), 943-950 (1991).

19. Wennerholm A, Dandara C, Sayi J *et al.*: The African-specific CYP2D617 allele encodes an enzyme with changed substrate specificity. *Clinical pharmacology and therapeutics* 71(1), 77-88 (2002).

20. Sakuyama K, Sasaki T, Ujiie S *et al.*: Functional characterization of 17 CYP2D6 allelic variants (CYP2D6.2, 10, 14A-B, 18, 27, 36, 39, 47-51, 53-55, and 57). *Drug metabolism and disposition: the biological fate of chemicals* 36(12), 2460-2467 (2008).

21. Toscano C, Klein K, Blievernicht J *et al.*: Impaired expression of CYP2D6 in intermediate metabolizers carrying the *41 allele caused by the intronic SNP 2988G>A: evidence for modulation of splicing events. *Pharmacogenetics and genomics* 16(10), 755-766 (2006).

22. Ingelman-Sundberg M: Genetic polymorphisms of cytochrome P450 2D6 (CYP2D6): clinical consequences, evolutionary aspects and functional diversity. *The pharmacogenomics journal* 5(1), 6-13 (2005).

23. Aklillu E, Persson I, Bertilsson L, Johansson I, Rodrigues F, Ingelman-Sundberg M: Frequent distribution of ultrarapid metabolizers of debrisoquine in an ethiopian population carrying duplicated and multiduplicated functional CYP2D6 alleles. *The Journal of pharmacology and experimental therapeutics* 278(1), 441-446 (1996).

24. Mclellan RA, Oscarson M, Seidegard J, Evans DA, Ingelman-Sundberg M: Frequent occurrence of CYP2D6 gene duplication in Saudi Arabians. *Pharmacogenetics* 7(3), 187-191 (1997).

25. Gaedigk A, Twist GP, Leeder JS: CYP2D6, SULT1A1 and UGT2B17 copy number variation: quantitative detection by multiplex PCR. *Pharmacogenomics* 13(1), 91-111 (2012).

26. Rebsamen MC, Desmeules J, Daali Y *et al.*: The AmpliChip CYP450 test: cytochrome P450 2D6 genotype assessment and phenotype prediction. *The pharmacogenomics journal* 9(1), 34-41 (2009).

27. Bogni A, Monshouwer M, Moscone A *et al.*: Substrate specific metabolism by polymorphic cytochrome P450 2D6 alleles. *Toxicology in vitro : an international journal published in association with BIBRA* 19(5), 621-629 (2005).

28. Gaedigk A, Bradford LD, Marcucci KA, Leeder JS: Unique CYP2D6 activity distribution and genotype-phenotype discordance in black Americans. *Clinical pharmacology and therapeutics* 72(1), 76-89 (2002).

29. Griese EU, Zanger UM, Brudermanns U *et al.*: Assessment of the predictive power of genotypes for the in-vivo catalytic function of CYP2D6 in a German population. *Pharmacogenetics* 8(1), 15-26 (1998).

30. Luo HR, Gaedigk A, Aloumanis V, Wan YJ: Identification of CYP2D6 impaired functional alleles in Mexican Americans. *European journal of clinical pharmacology* 61(11), 797-802 (2005).

31. Gaedigk A, Simon SD, Pearce RE, Bradford LD, Kennedy MJ, Leeder JS: The CYP2D6 activity score: translating genotype information into a qualitative measure of phenotype. *Clinical pharmacology and therapeutics* 83(2), 234-242 (2008).

32. Aklillu E, Herrlin K, Gustafsson LL, Bertilsson L, Ingelman-Sundberg M: Evidence for environmental influence on CYP2D6-catalysed debrisoquine hydroxylation as demonstrated by phenotyping and genotyping of Ethiopians living in Ethiopia or in Sweden. *Pharmacogenetics* 12(5), 375-383 (2002).

33. Hara H, Adachi T: Contribution of hepatocyte nuclear factor-4 to down-regulation of CYP2D6 gene expression by nitric oxide. *Molecular pharmacology* 61(1), 194-200 (2002).

34. Frye RF, Zgheib NK, Matzke GR *et al.*: Liver disease selectively modulates cytochrome P450--mediated metabolism. *Clinical pharmacology and therapeutics* 80(3), 235-245 (2006).

35. Jones AE, Brown KC, Werner RE *et al.*: Variability in drug metabolizing enzyme activity in HIV-infected patients. *European journal of clinical pharmacology* 66(5), 475-485 (2010).

36. Jetter A, Fatkenheuer G, Frank D *et al.*: Do activities of cytochrome P450 (CYP)3A, CYP2D6 and P-glycoprotein differ between healthy volunteers and HIV-infected patients? *Antiviral therapy* 15(7), 975-983 (2010).

37. Girardin F, Daali Y, Gex-Fabry M *et al.*: Liver kidney microsomal type 1 antibodies reduce the CYP2D6 activity in patients with chronic hepatitis C virus infection. *Journal of viral hepatitis* 19(8), 568-573 (2012).

38. Mahgoub A, Idle JR, Dring LG, Lancaster R, Smith RL: Polymorphic hydroxylation of Debrisoquine in man. *Lancet* 2(8038), 584-586 (1977).

39. Eichelbaum M, Mineshita S, Ohnhaus EE, Zekorn C: The influence of enzyme induction on polymorphic sparteine oxidation. *British journal of clinical pharmacology* 22(1), 49-53 (1986).

40. Bock KW, Schrenk D, Forster A *et al.*: The influence of environmental and genetic factors on CYP2D6, CYP1A2 and UDP-glucuronosyltransferases in man using sparteine, caffeine, and paracetamol as probes. *Pharmacogenetics* 4(4), 209-218 (1994).

41. Horai Y, Taga J, Ishizaki T, Ishikawa K: Correlations among the metabolic ratios of three test probes (metoprolol, debrisoquine and sparteine) for genetically determined oxidation polymorphism in a Japanese population. *British journal of clinical pharmacology* 29(1), 111-115 (1990).

42. Alvan G, Bechtel P, Iselius L, Gundert-Remy U: Hydroxylation polymorphisms of debrisoquine and mephenytoin in European populations. *European journal of clinical pharmacology* 39(6), 533-537 (1990).

43. Droll K, Bruce-Mensah K, Otton SV, Gaedigk A, Sellers EM, Tyndale RF: Comparison of three CYP2D6 probe substrates and genotype in Ghanaians, Chinese and Caucasians. *Pharmacogenetics* 8(4), 325-333 (1998).

44. Frank D, Jaehde U, Fuhr U: Evaluation of probe drugs and pharmacokinetic metrics for CYP2D6 phenotyping. *European journal of clinical pharmacology* 63(4), 321-333 (2007).

45. Anderson GD, Carr DB: Effect of pregnancy on the pharmacokinetics of antihypertensive drugs. *Clinical pharmacokinetics* 48(3), 159-168 (2009).

46. Otton SV, Crewe HK, Lennard MS, Tucker GT, Woods HF: Use of quinidine inhibition to define the role of the sparteine/debrisoquine cytochrome P450 in metoprolol oxidation by human liver microsomes. *The Journal of pharmacology and experimental therapeutics* 247(1), 242-247 (1988).

47. Lennard MS, Tucker GT, Silas JH, Freestone S, Ramsay LE, Woods HF: Differential stereoselective metabolism of metoprolol in extensive and poor debrisoquin metabolizers. *Clinical pharmacology and therapeutics* 34(6), 732-737 (1983).

48. Hogstedt S, Lindberg B, Rane A: Increased oral clearance of metoprolol in pregnancy. *European journal of clinical pharmacology* 24(2), 217-220 (1983).

49. Sohn DR, Kusaka M, Shin SG, Jang IJ, Chiba K, Ishizaki T: Utility of a one-point (3-hour postdose) plasma metabolic ratio as a phenotyping test using metoprolol in two east Asian populations. *Therapeutic drug monitoring* 14(3), 184-189 (1992).

50. Bozkurt A, Basci NE, Isimer A, Sayal A, Kayaalp SO: Metabolic ratios of four probes of CYP2D6 in Turkish subjects: a cross-over study. *European journal of drug metabolism and pharmacokinetics* 21(4), 309-314 (1996).

51. Al-Hadidi HF, Irshaid YM, Rawashdeh NM: Metoprolol alpha-hydroxylation is a poor probe for debrizoquine oxidation (CYP2D6) polymorphism in Jordanians. *European journal of clinical pharmacology* 47(4), 311-314 (1994).

52. Lennard MS, Iyun AO, Jackson PR, Tucker GT, Woods HF: Evidence for a dissociation in the control of sparteine, debrisoquine and metoprolol metabolism in Nigerians. *Pharmacogenetics* 2(2), 89-92 (1992).

53. Simooya OO, Njunju E, Hodjegan AR, Lennard MS, Tucker GT: Debrisoquine and metoprolol oxidation in Zambians: a population study. *Pharmacogenetics* 3(4), 205-208 (1993).

54. Labbe L, Sirois C, Pilote S *et al.*: Effect of gender, sex hormones, time variables and physiological urinary pH on apparent CYP2D6 activity as assessed by metabolic ratios of marker substrates. *Pharmacogenetics* 10(5), 425-438 (2000).

55. Schmid B, Bircher J, Preisig R, Kupfer A: Polymorphic dextromethorphan metabolism: co-segregation of oxidative O-demethylation with debrisoquin hydroxylation. *Clinical pharmacology and therapeutics* 38(6), 618-624 (1985).

56. Capon DA, Bochner F, Kerry N, Mikus G, Danz C, Somogyi AA: The influence of CYP2D6 polymorphism and quinidine on the disposition and antitussive effect of dextromethorphan in humans. *Clinical pharmacology and therapeutics* 60(3), 295-307 (1996).

57. Borges S, Li L, Hamman MA, Jones DR, Hall SD, Gorski JC: Dextromethorphan to dextrorphan urinary metabolic ratio does not reflect dextromethorphan oral clearance. *Drug metabolism and disposition: the biological fate of chemicals* 33(7), 1052-1055 (2005).

58. Wang B, Yang LP, Zhang XZ, Huang SQ, Bartlam M, Zhou SF: New insights into the structural characteristics and functional relevance of the human cytochrome P450 2D6 enzyme. *Drug metabolism reviews* 41(4), 573-643 (2009).

59. Rowland P, Blaney FE, Smyth MG *et al.*: Crystal structure of human cytochrome P450 2D6. *The Journal of biological chemistry* 281(11), 7614-7622 (2006).

60. Alfaro CL, Lam YW, Simpson J, Ereshefsky L: CYP2D6 inhibition by fluoxetine, paroxetine, sertraline, and venlafaxine in a crossover study: intraindividual variability and plasma concentration correlations. *Journal of clinical pharmacology* 40(1), 58-66 (2000).

61. Jeppesen U, Gram LF, Vistisen K, Loft S, Poulsen HE, Brosen K: Dose-dependent inhibition of CYP1A2, CYP2C19 and CYP2D6 by citalopram, fluoxetine, fluvoxamine and paroxetine. *European journal of clinical pharmacology* 51(1), 73-78 (1996).

62. Vandel S, Bertschy G, Baumann P *et al.*: Fluvoxamine and fluoxetine: interaction studies with amitriptyline, clomipramine and neuroleptics in phenotyped patients. *Pharmacological research : the official journal of the Italian Pharmacological Society* 31(6), 347-353 (1995).

63. Brosen K, Gram LF, Haghfelt T, Bertilsson L: Extensive metabolizers of debrisoquine become poor metabolizers during quinidine treatment. *Pharmacology & toxicology* 60(4), 312-314 (1987).

64. Caraco Y, Sheller J, Wood AJ: Pharmacogenetic determinants of codeine induction by rifampin: the impact on codeine's respiratory, psychomotor and miotic effects. *The Journal of pharmacology and experimental therapeutics* 281(1), 330-336 (1997).

65. Glaeser H, Drescher S, Eichelbaum M, Fromm MF: Influence of rifampicin on the expression and function of human intestinal cytochrome P450 enzymes. *British journal of clinical pharmacology* 59(2), 199-206 (2005).

66. Tracy TS, Venkataramanan R, Glover DD, Caritis SN: Temporal changes in drug metabolism (CYP1A2, CYP2D6 and CYP3A Activity) during pregnancy. *American journal of obstetrics and gynecology* 192(2), 633-639 (2005).

67. Hogstedt S, Lindberg B, Peng DR, Regardh CG, Rane A: Pregnancy-induced increase in metoprolol metabolism. *Clinical pharmacology and therapeutics* 37(6), 688-692 (1985).

68. Yu AM, Idle JR, Herraiz T, Kupfer A, Gonzalez FJ: Screening for endogenous substrates reveals that CYP2D6 is a 5-methoxyindolethylamine O-demethylase. *Pharmacogenetics* 13(6), 307-319 (2003).

69. Jiang XL, Shen HW, Yu AM: Pinoline may be used as a probe for CYP2D6 activity. *Drug metabolism and disposition: the biological fate of chemicals* 37(3), 443-446 (2009).

70. Yu AM, Idle JR, Byrd LG, Krausz KW, Kupfer A, Gonzalez FJ: Regeneration of serotonin from 5-methoxytryptamine by polymorphic human CYP2D6. *Pharmacogenetics* 13(3), 173-181 (2003).

71. Eljaschewitsch E, Witting A, Mawrin C *et al.*: The endocannabinoid anandamide protects neurons during CNS inflammation by induction of MKP-1 in microglial cells. *Neuron* 49(1), 67-79 (2006).

72. Pacher P, Batkai S, Kunos G: The endocannabinoid system as an emerging target of pharmacotherapy. *Pharmacological reviews* 58(3), 389-462 (2006).

73. Ozdemir B, Shi B, Bantleon HP, Moritz A, Rausch-Fan X, Andrukhov O: Endocannabinoids and inflammatory response in periodontal ligament cells. *PloS one* 9(9), e107407 (2014).

74. Snider NT, Walker VJ, Hollenberg PF: Oxidation of the endogenous cannabinoid arachidonoyl ethanolamide by the cytochrome P450 monooxygenases: physiological and pharmacological implications. *Pharmacological reviews* 62(1), 136-154 (2010).

75. Snider NT, Sikora MJ, Sridar C, Feuerstein TJ, Rae JM, Hollenberg PF: The endocannabinoid anandamide is a substrate for the human polymorphic cytochrome P450 2D6. *The Journal of pharmacology and experimental therapeutics* 327(2), 538-545 (2008).

76. Cheng J, Zhen Y, Miksys S *et al.*: Potential role of CYP2D6 in the central nervous system. *Xenobiotica; the fate of foreign compounds in biological systems*, (2013).

77. Hiroi T, Imaoka S, Funae Y: Dopamine formation from tyramine by CYP2D6. *Biochemical and biophysical research communications* 249(3), 838-843 (1998).

78. Hiroi T, Kishimoto W, Chow T, Imaoka S, Igarashi T, Funae Y: Progesterone oxidation by cytochrome P450 2D isoforms in the brain. *Endocrinology* 142(9), 3901-3908 (2001).

79. Lee AJ, Cai MX, Thomas PE, Conney AH, Zhu BT: Characterization of the oxidative metabolites of 17beta-estradiol and estrone formed by 15 selectively expressed human cytochrome p450 isoforms. *Endocrinology* 144(8), 3382-3398 (2003).

80. Kishimoto W, Hiroi T, Shiraishi M *et al.*: Cytochrome P450 2D catalyze steroid 21-hydroxylation in the brain. *Endocrinology* 145(2), 699-705 (2004).

81. Stevens JC, Marsh SA, Zaya MJ *et al.*: Developmental changes in human liver CYP2D6 expression. *Drug metabolism and disposition: the biological fate of chemicals* 36(8), 1587-1593 (2008).

82. Blake MJ, Gaedigk A, Pearce RE *et al.*: Ontogeny of dextromethorphan O- and N-demethylation in the first year of life. *Clinical pharmacology and therapeutics* 81(4), 510-516 (2007).

83. Sachs AN, Avant D, Lee CS, Rodriguez W, Murphy MD: Pediatric information in drug product labeling. *JAMA : the journal of the American Medical Association* 307(18), 1914-1915 (2012).

84. Johnson TN: The problems in scaling adult drug doses to children. *Archives of disease in childhood* 93(3), 207-211 (2008).

85. Bouzom F, Walther B: Pharmacokinetic predictions in children by using the physiologically based pharmacokinetic modelling. *Fundamental & clinical pharmacology* 22(6), 579-587 (2008).

86. Arant BS, Jr.: Developmental patterns of renal functional maturation compared in the human neonate. *The Journal of pediatrics* 92(5), 705-712 (1978).

87. Friis-Hansen B: Water distribution in the foetus and newborn infant. *Acta paediatrica Scandinavica. Supplement* 305, 7-11 (1983).

88. Krasilnikoff PA, Rodbro P, Christiansen PM: Gastric secretion in early childhood. *Acta paediatrica Scandinavica*, Suppl 177:110+ (1967).

89. Rodbro P, Krasilnikoff PA, Christiansen PM: Parietal cell secretory function in early childhood. *Scandinavian journal of gastroenterology* 2(3), 209-213 (1967).

90. Agunod M, Yamaguchi N, Lopez R, Luhby AL, Glass GB: Correlative study of hydrochloric acid, pepsin, and intrinsic factor secretion in newborns and infants. *The American journal of digestive diseases* 14(6), 400-414 (1969).

91. Madsen R, Lundstedt T, Trygg J: Chemometrics in metabolomics--a review in human disease diagnosis. *Analytica chimica acta* 659(1-2), 23-33 (2010).

92. Tolstikov VV, Fiehn O, Tanaka N: Application of liquid chromatography-mass spectrometry analysis in metabolomics: reversed-phase monolithic capillary chromatography and hydrophilic chromatography coupled to electrospray ionization-mass spectrometry. *Methods Mol Biol* 358, 141-155 (2007).

93. Wishart DS: Applications of metabolomics in drug discovery and development. *Drugs in R&D* 9(5), 307-322 (2008).

94. Kumar B, Prakash A, Ruhela RK, Medhi B: Potential of metabolomics in preclinical and clinical drug development. *Pharmacological reports : PR* 66(6), 956-963 (2014).

95. Garcia-Sevillano MA, Garcia-Barrera T, Navarro F, Montero-Lobato Z, Gomez-Ariza JL: Shotgun metabolomic approach based on mass spectrometry for hepatic mitochondria of mice under arsenic exposure. *Biometals : an international journal on the role of metal ions in biology, biochemistry, and medicine*, (2015).

96. Sudre D, Gutierrez-Carbonell E, Lattanzio G *et al.*: Iron-dependent modifications of the flower transcriptome, proteome, metabolome, and hormonal content in an Arabidopsis ferritin mutant. *Journal of experimental botany* 64(10), 2665-2688 (2013).

97. Scognamiglio M, D'abrosca B, Esposito A, Fiorentino A: Chemical Composition and Seasonality of Aromatic Mediterranean Plant Species by NMR-Based Metabolomics. *Journal of analytical methods in chemistry* 2015, 258570 (2015).

98. He Y, Hogrefe CE, Grapov D *et al.*: Identifying individual differences of fluoxetine response in juvenile rhesus monkeys by metabolite profiling. *Translational psychiatry* 4, e478 (2014).

99. Basak T, Varshney S, Hamid Z, Ghosh S, Seth S, Sengupta S: Identification of metabolic markers in Coronary Artery Disease using an untargeted LC-MS based metabolomics approach. *Journal of proteomics*, (2015).

100. Liu X, Zheng P, Zhao X *et al.*: Discovery and validation of plasma biomarkers for major depressive disorder classification based on liquid chromatography-mass spectrometry. *Journal of proteome research*, (2015).

101. Rahmioglu N, Le Gall G, Heaton J *et al.*: Prediction of variability in CYP3A4 induction using a combined 1H NMR metabonomics and targeted UPLC-MS approach. *Journal of proteome research* 10(6), 2807-2816 (2011).

102. Armstrong AW, Wu J, Johnson MA *et al.*: Metabolomics in psoriatic disease: pilot study reveals metabolite differences in psoriasis and psoriatic arthritis. *F1000Research* 3, 248 (2014).

103. Zhang W, Zhou L, Yin P *et al.*: A weighted relative difference accumulation algorithm for dynamic metabolomics data: long-term elevated bile acids are risk factors for hepatocellular carcinoma. *Scientific reports* 5, 8984 (2015).

Chapter 2. Development of a liquid chromatography-tandem mass spectrometry assay to support the evaluation of endogenous ethanolamides as phenotypic indicators of CYP2D6

2.1 Introduction

The importance of cytochrome P450 2D6 (CYP2D6) in the metabolism of clinically used drugs has been widely recognized [1-3]. Variations in an individual's CYP2D6 activities may in part determine the outcome of therapy for drugs primarily eliminated by this enzyme [4-6]. However, the *in vivo* involvement of CYP2D6 in the metabolism of endogenous substrates is not well understood. Suggested endogenous substrates of CYP2D6 include a number of compounds found in the brain, such as 5-methoxytryptamine, 5-methoxy-*N*,*N*-dimethyltryptamine, pinoline, tyramine, tryptamine and progesterone [7-13]. CYP2D6 is one of the major cytochrome P450 enzymes in the human brain [14-16], but it is present at lower levels in this tissue than in the liver [16]. In the brain, differences in the catalytic activities between wild-type and variant CYP2D6 could lead to altered product formation from endogenous substrates and neurological function. If an endogenous compound is found to be circulating in the body, it may be used as an indicator of hepatic CYP2D6 phenotype.

Anandamide (AEA), also known as arachidonyl ethanolamide, circulates at low nanomolar concentrations [17] and is highly bound to albumin (fu ~ 0.01) [18]. It is an endogenous, fatty acid cannabinoid that has physiological roles which include neuroprotective, anti-nociceptive, anti-inflammatory, cardiovascular and immunologic functions [19-22]. As ascertained *in vitro*, AEA undergoes oxidation by a number of cytochromes P450 (Figure 2-1). These reactions include hydroxylation at C-20 (20-hydroxyeicosatetraenoic acid ethanolamide (20-HETE-EA)) and epoxidation at carbon double bonds (5,6-epoxyeicosatrienoic acid ethanolamide (5,6-EET-EA), 7,8-epoxyeicosatrienoic acid ethanolamide (7,8-EET-EA), 11,12-epoxyeicosatrienoic acid ethanolamide (11,12-EET-EA), and 14,15-epoxyeicosatrienoic acid ethanolamide (14,15-EET-EA)) [23-27]. Several investigators demonstrated that altering CYP2D6 activity resulted in decreased AEA metabolism. Formation of AEA ethanolamide products in human brain mitochondrial preparations were decreased upon incubation with an inhibitory antibody against CYP2D6 [24]. Sridar et al. reported decreased formation of 14,15-EET-EA and 20-HETE-EA from AEA for an expressed variant of CYP2D6, CYP2D6.34 (C296A), compared to wild-type CYP2D6 protein: products were greatly reduced in an incubation with the variant[25]. In a recent *in vivo* metabolomics analysis involving CYP2D6 humanized mice, investigators reported that AEA levels were higher in the cerebrospinal fluid of CYP2D6 humanized mice as compared to wild-type mice [28]. The authors suggested that higher AEA in the CYP2D6 humanized mice as compare to the wild-type mice may be due to the relatively minor role that CYP2D6 plays in the metabolism of AEA in comparison with hydrolysis by fatty acid amide hydrolase [28]. The major products of AEA metabolism by expressed CYP2D6 are the hydroxylation and epoxidation products, 20-hydroxyeicosatetraenoic acid ethanolamide (20-HETE-EA) and 14,15-epoxyeicosatrienoic acid ethanolamide (14,15-EET-EA), respectively [25, 27]. We hypothesized that the parent-to-metabolite metabolic ratio of AEA to 14,15-EET-EA or 20-HETE-EA might be an indicator of CYP2D6 phenotype if these reactions occurred *in vivo* and if the metabolites were measurable in accessible biofluids. As reviewed by Zoerner et al., the majority of reports indicate that AEA concentrations in human plasma are below 5 nM [17] and it is unknown if 14,15-EET-EA and 20-HETE-EA are circulating metabolites *in vivo*. Anandamide is low (< 0.004 nM) [29] or not detectable in human urine [30].

We sought to develop an LC-MS/MS method for the simultaneous quantification of AEA, 14-15-EET-EA and 20-HETE-EA in human plasma. In our search for endogenous biomarkers of CYP2D6 activity, we investigated anandamide and two of its ethanolamide metabolites to determine whether these parent and CYP2D6 metabolites are altered in individuals after receiving multiple doses of fluoxetine, a potent CYP2D6 inhibitor.

2.2 **Materials and Methods**

2.2.1 *Chemicals and materials*

AEA (50 mg/mL), 14,15-EET-EA (100 µg/mL), 20-HETE-EA (100 µg/mL) and d_8-AEA (1 mg/mL) were purchased as methanolic solutions from Cayman Chemical (Ann Arbor, MI). HPLC-grade ethyl acetate, methyl tert-butyl ether (MTBE), hexane, toluene, methanol, water, glacial acetic acid, and potassium phosphate (monobasic and dibasic) were purchased from Fisher Scientific (Pittsburg, PA). Bovine serum albumin was purchased from Sigma-Aldrich (St. Louis, MA). Phosphate-buffered saline was purchased from Thermo Fisher Scientific (Waltham, MA). Blank plasma was obtained from the centrifugation of expired whole blood that was purchased from the Puget Sound Blood Center (Seattle, WA).

2.2.2 *Method development and selection of chemical extraction solvent*

Ethyl acetate, MTBE, toluene and hexane were selected as potential organic solvents for AEA, 14,15-EET-EA and 20-HETE-EA plasma extraction. In order to compare the extraction efficiency of the organic solvents, extraction of blank human plasma (human plasma that was not spiked) and spiked human plasma (final concentrations: 14.4 nM AEA, 13.7 nM 14,15-EET-EA and 13.7 nM 20-HETE-EA) was conducted using each solvent. The deuterated internal standard, d8-AEA (10 ng), was added to 2 mL of blank and spiked plasma samples. A double extraction was performed. We added 2 mL of ice-cold organic solvent to each sample. Samples were placed in a horizontal shaker for 10 min at low speed and centrifuged at 1700 x G at 4°C for 5 min. The organic layer was transferred to a polypropylene tube and set on ice. Another 2 mL of cold organic was added to each sample and samples were vortexed for 30 seconds. The samples were centrifuged at 1700 x G at 4°C for 5 min and the organic layer was transferred to the tube containing the first organic layer. Combined organic layers were evaporated under a gentle stream of nitrogen. Samples were reconstituted in 10 µL DMSO, followed by 40 µL of 5:1:4 of water:methanol:acetonitrile. Samples were analyzed by LC-MS/MS as described below.

2.2.3 *Selection of calibration and quality control sample matrix*

Samples of AEA, 14,15-EET-EA and 20-HETE-EA (0, 1.5, 2.5 and 5 nM) were prepared in 2 mL of water, phosphate-buffered saline, bovine serum albumin (30 mg/mL), potassium phosphate buffer (0.1 M, pH 7.4), or plasma. D8-AEA (7.03 nM, final concentration) was added as internal standard to each sample. Each sample was extracted and analyzed as described below on an AB Sciex (Framingham, MA) LC-MS/MS system.

2.2.4 *Ethanolamide calibration and quality control samples*

All standard stock dilutions were prepared in methanol. Intermediate stock solutions of 1.44 µM AEA, 1.37 µM 14,15-EET-EA, and 20-HETE-EA were made. These stock solutions were used for a mix of AEA and 20-HETE-EA each at a concentration of 100 nM and subsequently used for working standards at final concentrations of 0.05, 0.1, 0.5, 2 and 5 nM in blank human plasma. The 14,15-EET-EA standard curve working standards were created separately at 0.05, 0.1, 0.5, 2 and 5 nM. The 2 and 5 nM 14,15-EET-EA standards were used to measure accuracy on day 1, but not used during other experiments or sample analysis. Quality controls (QCs) were prepared in blank plasma with 1 nM AEA, 0.2 nM 14,15-EET-EA and 1 nM 20-HETE-EA. These working standards and QCs were aliquoted for single use and stored at -80°C in 15 mL conical polypropylene centrifuge tubes. A working internal standard (IS) solution of 500 nM d8-AEA was prepared in methanol. Small aliquots were stored at -80°C in amber, conical polypropylene microcentrifuge tubes for single use. A neat solution containing 5 nM AEA, 5 nM 14,15-EET-EA, 5 nM 20-HETE-EA and 50 nM d8-AEA was prepared for the purpose of direct repeat injections over multiple days of analysis. These instrument QC aliquots were stored at -80°C until analysis.

2.2.5 *Clinical samples*

Ten healthy adults (five females, five males) were recruited at the University of Washington for a drug-drug interaction study to evaluate the effects of fluoxetine and norfluoxetine on CYP3A4, CYP2D6 and CYP2C19. Study procedures, patient demographics and results were previously described in detail [31]. Briefly, participants were genotyped to exclude CYP2D6 poor metabolizers. Subjects were administered a phenotyping probe cocktail that contained dextromethorphan, a CYP2D6 probe, on Days 1 and 16 of the study. Subjects received a 20 mg oral dose of fluoxetine on Day 5 and 60 mg daily doses on Days 6 through 18. Plasma samples were obtained during the control and treatment phases (Days 1 and 16). Secondary analysis of these samples was approved by the University of Washington Human Subjects Review Board.

2.2.6 *Ethanolamide sample extraction*

Working standards, QCs, study plasma samples and IS were thawed on ice. Study plasma samples (1 mL) were aliquoted into a 15 mL conical polypropylene centrifuge tubes. Internal standard (10 µL) was spiked into each standard, QC and study sample. Samples were extracted using 2 mL of ice-cold toluene and tubes were agitated on a horizontal shaker at low speed for 15 minutes. Samples were centrifuged at 1700 x G at 4°C for 5 min. The organic layer was transferred to a polypropylene culture tube on ice. An additional 2 mL of ice-cold toluene was added to the remaining aqueous layer. Samples were agitated on a horizontal shaker at low speed for 10 min and centrifuged at 1700 x G at 4°C for 5 min. The organic layer was transferred to the tube containing the first organic layer. The combined organic layers were evaporated under a gentle stream of nitrogen. Samples were reconstituted in 50 µL of 5:1:4 of water:methanol:acetonitrile and subsequently transferred to a polypropylene LC insert in an amber LC vial. Analysis by LC-MS/MS was performed immediately following sample preparation.

2.2.7 *Ethanolamide LC-MS/MS Analysis*

All AEA, 14,15-EET-EA and 20-HETE-EA analyses were performed using a Waters (Milford, MA) Acquity UPLC coupled to a Waters Xevo TQ-S QqQ MS, except for initial method development and stability experiments, which were performed on an AB Sciex API 4000 triple quadrupole (QqQ) MS. Samples were separated using a Waters Cortecs UPLC C18 (50 x 2.1 mm x 1.6 µm) column fitted with a Phenomenex (Torrance, CA) SecurityGuard C18 precolumn. The mobile phases consisted of 0.05% acetic acid in water (mobile phase A) and 0.05% acetic acid in 4:1 methanol:acetonitrile (mobile phase B). The method employed a flow rate of 0.3 mL/min throughout and a gradient elution of 50% B for 1.5 min, then an increase to 100% B by 5 min holding until 6 min, followed by a rapid decrease to 50% B by 6.1 min, and finally re-equilibration to initial conditions until 8 min. Samples were maintained at 4°C in the autosampler and 20 µL was injected. Analyte signal intensities were measured in positive electrospray ionization mode (ESI) with unit resolutions in Q1 and Q3. Multiple reaction monitoring transitions and voltages are listed in Table 2-1. MS acquisition parameters were set as the following: capillary voltage 3.5 kV, source offset 50 V, source temperature 150°C, desolvation temperature: 500°C, cone gas flow 150 L/hr, desolvation gas flow 1000 L/hr, collision gas flow: 0.15 mL/min, nebulizer gas flow: 7 bar, and dwell time: 32 msec.

2.2.8 *Ethanolamide analyte accuracy, precision and stability*

QCs were used to evaluate the accuracy of the AEA, 14,15-EET-EA and 20-HETE-EA standard curve. Accuracy was estimated using QC samples on three separate days for 1 nM AEA and 1 nM 20-HETE EA, The accuracy for 14,15-EET-EA was only estimated on two days at 1 nM (day 1) and 0.2 nM (day 3). Standard curves on these days ranged from 0 - 5 nM for each analyte, except on day 3, for which 14,15-EET-EA standard curve ranged from 0 - 0.5 nM. Due to limited sample volume of the extracted QC, separate repeat injections of neat instrumental QCs were used to measure intraday precision. Accuracy was calculated as percent error: $\frac{|observed-calculated|*100}{calculated}$ |, and precision was calculated as percent relative standard deviation

(RSD): $\frac{standard\ deviation*100}{mean}$. Acceptable error and RSD criteria was less than or equal to 15%. Stability of the ethanolamides in the plasma matrix was assessed after five hours by repeated injections of the same samples. The samples were analyzed immediately following sample preparation and the samples were kept at 4°C in the autosampler.

2.2.9 *Data analysis*

Peak integration was performed using Waters MassLynx with QuanLynx software (version 4.1). The peak area of AEA, 14,15-EET-EA and 20-HETE-EA were normalized to the d_8-AEA IS to determine peak area ratios (PARs). In order to correct for endogenous AEA in the blank plasma matrix used for the working standards and QCs, the AEA/d_8-AEA PAR in the 0 nM standard was subtracted from each calibration point PAR. No correction was made for endogenous 14,15-EET-EA and 20-HETE-EA. The lower limit of quantitation (LLOQ) was determined as the lowest calibration with a back calculated error ≤ 15%. A quadratic equation was used to estimate the relationship between PARs and the molar concentration of each analyte, and subsequently used to calculate the concentration in the clinical plasma samples. GraphPad Prism (version 5.04, GraphPad Software, San Diego, CA) was used to compare AEA concentration between baseline and treatment groups in paired, two-tailed t-tests. $P < 0.05$ was considered significant.

2.2.10 *In vitro-in vivo predictions of metabolism of AEA to AEA metabolites*

For each AEA metabolite, *in vitro* V_{max} and K_m values determined in recombinant enzyme or human liver microsome incubations were obtained from published literature (Table 2-6). Assuming $S << K_m$, intrinsic clearance was calculated as:

$$CL_{int,in\ vitro} = \frac{V_{max}}{K_m} \quad \text{(Equation 1)}$$

To scale in vitro intrinsic clearance to hepatic clearance:

$$CL_{int,in\ vivo} = CL_{int,in\ vitro} \times MPPGL \times liver\ weight, \quad \text{(Equation 2)}$$

where milligrams of protein per gram liver (MPPGL) was set to 50 mg protein/g liver and the liver weight was 2100 g liver/kg body weight, and a 70 kg individual was assumed. Reference values for the liver expression of various cytochromes P450 (CYP3A4, CYP2D6, CYP2B6 and CYP4F2 in Caucasians) were obtained from the literature [32, 33]. Metabolism of AEA by CYP4X1 was not accounted for due to the lack of a liver abundance scaling factor for this isoform. The well-stirred model was used to scale the *in vivo* intrinsic clearance to hepatic clearance (CL_H):

$$CL_H = \frac{Q \cdot fu \cdot CL_{int,in\ vivo}}{Q + fu \cdot CL_{int,in\ vivo}}, \quad \text{(Equation 3)}$$

where Q is hepatic blood flow (1.5 L/min) and f_u is the fraction unbound (~0.01) [18]. For each AEA metabolite, the fraction metabolized (f_m) by each cytochrome P450 isoform was calculated by dividing CL_H for that enzyme by the total CL_H (sum of the scaled clearances).

2.3 **Results**

2.3.1 *Ethanolamide method development*

A variety of bioanalytical LC-MS/MS methods, including those that use liquid-liquid extractions, have been reported for the analysis of AEA in human plasma. These liquid-liquid extraction methods use a variety of solvents including acetonitrile, chloroform, methanol, heptane, ethyl acetate, and toluene, either as pure solvent or as a mixture [30, 34-38]. In order to select an appropriate solvent to use for simultaneous extraction of AEA, 14,15-EET-EA and 20-HETE-EA, we explored a variety of water immiscible solvents with a spectrum of polarities. Listed from most polar to least polar, ethyl acetate, MTBE, toluene and hexane were selected as potential extraction solvents. All ethanolamide analytes were detectable in spiked plasma when using ethyl acetate, MTBE and toluene. AEA and 14,15-EET-EA were detectable and 20-HETE-EA was undetectable in spiked plasma when using hexane. In blank plasma samples, AEA was detectable using toluene and hexane, whereas 14,15-EET-EA and 20-HETE-EA were absent irrespective of the solvent used. Samples extracted using hexane emulsified during the shaking process and only a small amount of organic was recovered. Ultimately, toluene was chosen as the extraction solvent due to the practicality of sample preparation and the detection of all analytes in spiked plasma and AEA in blank plasma. The recovery from spiked urine was calculated for the extraction with toluene. The recovery was estimated to be 238%, 74% and 7% for AEA/d_8-AEA, 14,15-EET-EA and 20-HETE-EA, respectively.

Consistent with previously reported methods of LC-MS/MS quantitation of AEA [39-43], all analytes were sufficiently ionized in ESI+ mode. Analytes ionized poorly in ESI- mode (data not shown). The dynamic range of the assay standard curve (0.05 - 5 nM) was chosen based on literature reports of plasma AEA concentrations in this range [17, 29, 39, 44, 45]. Pilot standard curves and QCs lacked linearity and accuracy on the original AB Sciex API 4000 MS platform used for method development. Thus, the method was transferred to a more sensitive Waters Xevo

TQ-S MS system using the same LC-MS/MS parameters. Figure 2-2 shows a representative chromatogram of each analyte in a spiked plasma sample. Satisfactory chromatographic resolution of all analyte peaks was achieved. The elution times were 2.68 min for 20-HETE-EA, 3.68 min for 14,15-EET-EA, and 4.72 min for both AEA and d_8-AEA. The LLOQ from a 20 µL injection of prepared spiked plasma was 0.05 nM for 14,15-EET-EA and AEA, and 0.1 nM for 20-HETE-EA using the final method described herein (Supplemental Figure 2-1).

2.3.2 *Calibration curve and QC samples*

We tried to find an ethanolamide-free source of plasma or an alternative matrix to plasma for the preparation of calibration curves and QC samples to account for matrix effects in sample extraction. Stock ethanolamides (0, 1.25, 2.5 and 5 nM) and IS were spiked into different matricies (water, 30 mg/mL bovine serum albumin, 0.1 M potassium phosphate buffer and PBS); the slopes or quadratic coefficients of the PAR-concentration curve were compared between the alternative matrix and spiked plasma. None of the alternative matrices produced comparable coefficients to the spiked plasma, indicating reasonably similar extraction (Figure 2-3). Therefore, we prepared stock calibration curves and QCs in a lot of blank plasma (Supplemental Figure 2-2) that contained acceptably low levels of AEA (between LLOD and LLOQ), and aliquots were stored at -80°C until use. The AEA PAR in the 0 nM calibration point was subtracted from the PAR of each of the AEA calibration points and quality control samples in order to obtain corrected calibration points. 14,15-EET-EA and 20-HETE-EA were <LLOD in the blank calibration and QC matrix so correction for endogenous concentrations for these analytes was unnecessary. Representative calibration curves for each ethanolamide analyte are presented in Figure 2-4. Injection of a prepared water sample showed no peaks at analyte retention times (Supplemental Figure 2-3).

2.3.3 *Intraday accuracy, precision and stability*

Intraday accuracy (Table 2-2) was determined using QC samples prepared alongside a calibration curve on three different days. On Day 2, 14,15-EET-EA was inadvertently left out of the analysis. Intraday bias ranged between -2.86 to -4.79%, +6.47 to +10.7%, and -5.25 to +14.5% for AEA, 14,15-EET-EA and 20-HETE-EA, respectively. Data from at least three injections over the course of a run are needed in order to calculate intraday precision. This was not feasible in the QC samples due to the limited volume following reconstitution and the relatively large injection volume used. Therefore, a neat solution of the ethanolamide analytes and IS was prepared and repeatedly injected on two separate days (days 2 and 3) for the determination of RSD of the instrument. Intraday precision (Table 2-2) was acceptable for AEA, 14,15-EET-EA and 20-HETE-EA, on days 2 and 3 respectively. The accuracy and precision of each ethanolamide analyte were within the acceptable 15% bias and RSD criteria set for this assay.

Bench-top stability of ethanolamides and IS in the plasma matrix at 4°C was assessed after 5 hours. This length of time was chosen to encompass the time needed to analyze the clinical samples. As shown in Table 2-3, no appreciable degradation was observed for any of the analytes; however, an appreciable increase in 20-HETE-EA and d_8-AEA was observed after 5 hours. Preliminary experiments suggest that the ethanolamide analytes were not stable after 24 hours (data not shown), and additional stability studies are needed for run times greater than 5 hours.

2.3.4 *Quantitation of ethanolamides in clinical samples*

AEA concentrations for each individual at baseline and following CYP2D6 inhibition by oral fluoxetine treatment are reported in Table 2-4. 14,15-EET-EA and 20-HETE-EA were not detected in the plasma of any subject (Supplemental Figure 2-4). The mean AEA fold-change of treatment phase/baseline was 1.0 ± 0.46. Plasma AEA concentrations of healthy adult volunteers did not differ between baseline and treatment phases (P=0.61, Figure 2-5).

2.3.5 *Prediction of intrinsic and hepatic clearances*

Based on anandamide metabolism in human liver microsomes reported by Snider et al. 2007 [23], 8,9-EET-EA, 20-HETE-EA and 5,6-EET-EA are the major products formed by cytochrome P450 oxidation (Table 2-5). 11,12-EET-EA and 14,15-EET-EA were predicted minor metabolites.

As shown in Table 2-6, the predicted hepatic clearance of AEA suggests CYP3A4 is primarily responsible for oxidation to 8,9-EET-EA, 11,12-EET-EA and 14-15-EET-EA ($f_{m\text{CYP3A4}}$ were 0.76, 0.67 and 0.94, respectively). CYP2B6 is also involved to a lesser extent in the metabolism of 8,9-EET-EA and 11,12-EET-EA. CYP3A4 and CYP2B6 were predicted equal contributors to the formation of 5,6-EET-EA *in vivo*. The predicted metabolism of AEA to 20-HETE-EA is mediated mostly by CYP4F2 with a minor contribution by CYP2D6 ($f_{m\text{CYP4f2}}$ = 0.92 and $f_{m\text{CYP2D6}}$ = 0.08). The predicted relative clearance pathways of AEA metabolism by cytochrome P450 enzymes is summarized in Figure 2-6.

2.4 **Discussion**

We developed an LC-MS/MS assay for the simultaneous quantification of AEA, 14,15-EET-EA and 20-HETE-EA using a double liquid-liquid extraction method for sample preparation. Overall, the interday and intraday variability was acceptable for all analytes (<15%). One limitation of the study is that we did not detect 14,15-EET-EA and 20-HETE-EA in plasma samples. Only one paper has reported the detection of 20-HETE-EA in serum of healthy adults (0.021 ± 0.013 nM) [46]. These results suggest that these metabolites may not be circulating in plasma as the detection of 14,15-EET-EA has not been reported, or could be present at low fM concentrations. It is possible that the sensitivity of our assay (LLOQ = 0.05 and 0.1 nM for 14,15-EET-EA and 20-HETE-EA, respectively) was not sufficient for the quantitation of these AEA metabolites. An additional factor may be that anandamide has been shown to readily adsorb to plastic more than glass in a temperature dependent manner [47] and therefore it is plausible the metabolites might also have adsorbed to the plastic tubes used. Further studies may be required to improve the LC-MS/MS conditions or extraction efficiency to optimize the detection of 14,15-EET-EA and 20-HETE-EA.

Our goal was to determine if anandamide might be a suitable biomarker of CYP2D6 activity. Sager et al. reported an average 27-fold increase in dextromethorphan AUC after fluoxetine treatment, indicative of potent inhibition of CYP2D6 in these subjects [31]. Plasma AEA concentrations were not altered by CYP2D6 inhibition. Despite strong *in vitro* evidence that AEA is metabolized by CYP2D6 [25] and *in vivo* support that cerebrospinal fluid AEA concentrations differ between wild-type and humanized CYP2D6 mice [28], our findings suggest that plasma AEA concentrations alone are not sufficient for phenotypic differentiation of CYP2D6 activity. A likely explanation for the lack of association is that CYP2D6 represents a minor pathway of AEA metabolism compared to other metabolizing enzymes after scaling to hepatic clearance [23-27]. The *in vitro-in vivo* predictions suggest that 14,15-EET-EA and 20-HETE-EA are primarily formed by CYP3A4 and CYP4F2. Therefore the partial clearance of AEA to either of these metabolites is unlikely to be a suitable *in vivo* CYP2D6 biomarker. However, plasma metabolite-to-parent ratios of 8,9-EET-EA, 11,12-EET-EA, or 14,15-EET-EA to AEA, may be useful *in vivo* biomarkers of CYP3A4. Additionally, plasma 20-HETE-EA/AEA might be an *in vivo* endogenous marker of CYP4F2. The contribution of CYP4X1 to the formation of 14,15-EET-EA could not be accounted for due to the lack of a scaling factor. As the *in vitro* intrinsic clearance estimate for CYP4X1 is relatively small, the contribution of CYP4X1 *in vivo* is likely to be insignificant. A major limitation of these *in vivo* predictions is that they only account for hepatic cytochrome P450 metabolism. Extraheptic metabolism of AEA may occur in organs such as the brain and kidneys. Microsomes from these tissues have been shown to metabolize AEA [23]. In addition, AEA is extensively hydrolyzed by fatty acid amide hydrolase [48] and also undergoes oxidation mediated by certain cyclooxygenases [49, 50] and lipoxygenases [51].

The method described herein provides a basis for simultaneous analytical quantitation of AEA, 14,15-EET-EA and 20-HETE-EA in plasma. Although 14,15-EET-EA and 20-HETE-EA were undetectable using this methodology, plasma AEA levels could be quantified. Further work is needed to demonstrate whether AEA and its metabolites are endogenous human biomarkers of cytochrome P450 enzymes, other than for CYP2D6, and whether alterations in anandamide levels were an artifact of transgenic mouse studies reported previously [28]. In addition, clinical studies should be performed to ascertain if AEA is sensitive to CYP3A induction or inhibition. The search for endogenous compounds for use as a CYP2D6 biomarker is still ongoing.

2.5 Acknowledgements

We thank Theresa Aliwarga for technical assistance. This work was supported in part by the NIH R01 HD058556 (to YSL), and CTSA TL1 TR000422 (to JT-S). The authors declare no conflict of interest.

2.6 References

1. Zhou SF: Polymorphism of human cytochrome P450 2D6 and its clinical significance: Part I. *Clinical pharmacokinetics* 48(11), 689-723 (2009).

2. Zhou SF: Polymorphism of human cytochrome P450 2D6 and its clinical significance: part II. *Clinical pharmacokinetics* 48(12), 761-804 (2009).

3. Michalets EL: Update: clinically significant cytochrome P-450 drug interactions. *Pharmacotherapy* 18(1), 84-112 (1998).

4. Ingelman-Sundberg M: Genetic polymorphisms of cytochrome P450 2D6 (CYP2D6): clinical consequences, evolutionary aspects and functional diversity. *The pharmacogenomics journal* 5(1), 6-13 (2005).

5. Kirchheiner J, Nickchen K, Bauer M *et al.*: Pharmacogenetics of antidepressants and antipsychotics: the contribution of allelic variations to the phenotype of drug response. *Molecular psychiatry* 9(5), 442-473 (2004).

6. Dalen P, Dahl ML, Bernal Ruiz ML, Nordin J, Bertilsson L: 10-Hydroxylation of nortriptyline in white persons with 0, 1, 2, 3, and 13 functional CYP2D6 genes. *Clinical pharmacology and therapeutics* 63(4), 444-452 (1998).

7. Yu AM, Idle JR, Byrd LG, Krausz KW, Kupfer A, Gonzalez FJ: Regeneration of serotonin from 5-methoxytryptamine by polymorphic human CYP2D6. *Pharmacogenetics* 13(3), 173-181 (2003).

8. Yu AM, Idle JR, Herraiz T, Kupfer A, Gonzalez FJ: Screening for endogenous substrates reveals that CYP2D6 is a 5-methoxyindolethylamine O-demethylase. *Pharmacogenetics* 13(6), 307-319 (2003).

9. Hiroi T, Imaoka S, Funae Y: Dopamine formation from tyramine by CYP2D6. *Biochemical and biophysical research communications* 249(3), 838-843 (1998).

10. Martinez C, Agundez JA, Gervasini G, Martin R, Benitez J: Tryptamine: a possible endogenous substrate for CYP2D6. *Pharmacogenetics* 7(2), 85-93 (1997).

11. Hiroi T, Kishimoto W, Chow T, Imaoka S, Igarashi T, Funae Y: Progesterone oxidation by cytochrome P450 2D isoforms in the brain. *Endocrinology* 142(9), 3901-3908 (2001).

12. Niwa T, Yabusaki Y, Honma K *et al.*: Contribution of human hepatic cytochrome P450 isoforms to regioselective hydroxylation of steroid hormones. *Xenobiotica; the fate of foreign compounds in biological systems* 28(6), 539-547 (1998).

13. Lee AJ, Cai MX, Thomas PE, Conney AH, Zhu BT: Characterization of the oxidative metabolites of 17beta-estradiol and estrone formed by 15 selectively expressed human cytochrome p450 isoforms. *Endocrinology* 144(8), 3382-3398 (2003).

14. Siegle I, Fritz P, Eckhardt K, Zanger UM, Eichelbaum M: Cellular localization and regional distribution of CYP2D6 mRNA and protein expression in human brain. *Pharmacogenetics* 11(3), 237-245 (2001).

15. Miksys S, Rao Y, Hoffmann E, Mash DC, Tyndale RF: Regional and cellular expression of CYP2D6 in human brain: higher levels in alcoholics. *Journal of neurochemistry* 82(6), 1376-1387 (2002).

16. Dutheil F, Dauchy S, Diry M *et al.*: Xenobiotic-metabolizing enzymes and transporters in the normal human brain: regional and cellular mapping as a basis for putative roles in cerebral function. *Drug metabolism and disposition: the biological fate of chemicals* 37(7), 1528-1538 (2009).

17. Zoerner AA, Gutzki FM, Suchy MT *et al.*: Targeted stable-isotope dilution GC-MS/MS analysis of the endocannabinoid anandamide and other fatty acid ethanol amides in human plasma. *Journal of chromatography. B, Analytical technologies in the biomedical and life sciences* 877(26), 2909-2923 (2009).

18. Bojesen IN, Hansen HS: Binding of anandamide to bovine serum albumin. *Journal of lipid research* 44(9), 1790-1794 (2003).

19. Eljaschewitsch E, Witting A, Mawrin C *et al.*: The endocannabinoid anandamide protects neurons during CNS inflammation by induction of MKP-1 in microglial cells. *Neuron* 49(1), 67-79 (2006).

20. Pacher P, Batkai S, Kunos G: The endocannabinoid system as an emerging target of pharmacotherapy. *Pharmacological reviews* 58(3), 389-462 (2006).

21. Wang PF, Jiang LS, Bu J *et al.*: Cannabinoid-2 receptor activation protects against infarct and ischemia-reperfusion heart injury. *Journal of cardiovascular pharmacology* 59(4), 301-307 (2012).

22. Ozdemir B, Shi B, Bantleon HP, Moritz A, Rausch-Fan X, Andrukhov O: Endocannabinoids and inflammatory response in periodontal ligament cells. *PloS one* 9(9), e107407 (2014).

23. Snider NT, Kornilov AM, Kent UM, Hollenberg PF: Anandamide metabolism by human liver and kidney microsomal cytochrome p450 enzymes to form hydroxyeicosatetraenoic and epoxyeicosatrienoic acid ethanolamides. *The Journal of pharmacology and experimental therapeutics* 321(2), 590-597 (2007).

24. Snider NT, Sikora MJ, Sridar C, Feuerstein TJ, Rae JM, Hollenberg PF: The endocannabinoid anandamide is a substrate for the human polymorphic cytochrome P450 2D6. *The Journal of pharmacology and experimental therapeutics* 327(2), 538-545 (2008).

25. Sridar C, Snider NT, Hollenberg PF: Anandamide oxidation by wild-type and polymorphically expressed CYP2B6 and CYP2D6. *Drug metabolism and disposition: the biological fate of chemicals* 39(5), 782-788 (2011).

26. Stark K, Dostalek M, Guengerich FP: Expression and purification of orphan cytochrome P450 4X1 and oxidation of anandamide. *The FEBS journal* 275(14), 3706-3717 (2008).

27. Snider NT, Walker VJ, Hollenberg PF: Oxidation of the endogenous cannabinoid arachidonoyl ethanolamide by the cytochrome P450 monooxygenases: physiological and pharmacological implications. *Pharmacological reviews* 62(1), 136-154 (2010).

28. Cheng J, Zhen Y, Miksys S *et al.*: Potential role of CYP2D6 in the central nervous system. *Xenobiotica; the fate of foreign compounds in biological systems*, (2013).

29. Marczylo TH, Lam PM, Nallendran V, Taylor AH, Konje JC: A solid-phase method for the extraction and measurement of anandamide from multiple human biomatrices. *Analytical biochemistry* 384(1), 106-113 (2009).

30. Zoerner AA, Batkai S, Suchy MT *et al.*: Simultaneous UPLC-MS/MS quantification of the endocannabinoids 2-arachidonoyl glycerol (2AG), 1-arachidonoyl glycerol (1AG), and anandamide in human plasma: minimization of matrix-effects, 2AG/1AG isomerization and degradation by toluene solvent extraction. *Journal of chromatography. B, Analytical technologies in the biomedical and life sciences* 883-884, 161-171 (2012).

31. Sager JE, Lutz JD, Foti RS, Davis C, Kunze KL, Isoherranen N: Fluoxetine and norfluoxetine mediated complex drug-drug interactions: in vitro to in vivo correlation of effects on CYP2D6, CYP2C19 and CYP3A4. *Clinical pharmacology and therapeutics*, (2014).

32. Rostami-Hodjegan A, Tucker GT: Simulation and prediction of in vivo drug metabolism in human populations from in vitro data. *Nature reviews. Drug discovery* 6(2), 140-148 (2007).

33. Hirani V, Yarovoy A, Kozeska A, Magnusson RP, Lasker JM: Expression of CYP4F2 in human liver and kidney: assessment using targeted peptide antibodies. *Archives of biochemistry and biophysics* 478(1), 59-68 (2008).

34. Vogeser M, Hauer D, Christina Azad S, Huber E, Storr M, Schelling G: Release of anandamide from blood cells. *Clinical chemistry and laboratory medicine : CCLM / FESCC* 44(4), 488-491 (2006).

35. Thomas A, Hopfgartner G, Giroud C, Staub C: Quantitative and qualitative profiling of endocannabinoids in human plasma using a triple quadrupole linear ion trap mass spectrometer with liquid chromatography. *Rapid communications in mass spectrometry : RCM* 23(5), 629-638 (2009).

36. Schreiber D, Harlfinger S, Nolden BM *et al.*: Determination of anandamide and other fatty acyl ethanolamides in human serum by electrospray tandem mass spectrometry. *Analytical biochemistry* 361(2), 162-168 (2007).

37. Lam PM, Marczylo TH, El-Talatini M *et al.*: Ultra performance liquid chromatography tandem mass spectrometry method for the measurement of anandamide in human plasma. *Analytical biochemistry* 380(2), 195-201 (2008).

38. Ozalp A, Barroso B: Simultaneous quantitative analysis of N-acylethanolamides in clinical samples. *Analytical biochemistry* 395(1), 68-76 (2009).

39. Fernandez-Rodriguez CM, Romero J, Petros TJ *et al.*: Circulating endogenous cannabinoid anandamide and portal, systemic and renal hemodynamics in cirrhosis. *Liver international : official journal of the International Association for the Study of the Liver* 24(5), 477-483 (2004).

40. Bradshaw HB, Rimmerman N, Krey JF, Walker JM: Sex and hormonal cycle differences in rat brain levels of pain-related cannabimimetic lipid mediators. *American journal of physiology. Regulatory, integrative and comparative physiology* 291(2), R349-358 (2006).

41. Felder CC, Nielsen A, Briley EM *et al.*: Isolation and measurement of the endogenous cannabinoid receptor agonist, anandamide, in brain and peripheral tissues of human and rat. *FEBS letters* 393(2-3), 231-235 (1996).

42. Kingsley PJ, Marnett LJ: Analysis of endocannabinoids by Ag+ coordination tandem mass spectrometry. *Analytical biochemistry* 314(1), 8-15 (2003).

43. Ottria R, Ravelli A, Gigli F, Ciuffreda P: Simultaneous ultra-high performance liquid chromathograpy-electrospray ionization-quadrupole-time of flight mass spectrometry quantification of endogenous anandamide and related N-acylethanolamides in bio-matrices. *Journal of chromatography. B, Analytical technologies in the biomedical and life sciences* 958, 83-89 (2014).

44. Di Marzo V, Verrijken A, Hakkarainen A *et al.*: Role of insulin as a negative regulator of plasma endocannabinoid levels in obese and nonobese subjects. *European journal of endocrinology / European Federation of Endocrine Societies* 161(5), 715-722 (2009).

45. Mcpartland JM, Giuffrida A, King J, Skinner E, Scotter J, Musty RE: Cannabimimetic effects of osteopathic manipulative treatment. *The Journal of the American Osteopathic Association* 105(6), 283-291 (2005).

46. Psychogios N, Hau DD, Peng J *et al.*: The human serum metabolome. *PloS one* 6(2), e16957 (2011).

47. Oddi S, Fezza F, Catanzaro G *et al.*: Pitfalls and solutions in assaying anandamide transport in cells. *Journal of lipid research* 51(8), 2435-2444 (2010).

48. Maccarrone M, Van Der Stelt M, Rossi A, Veldink GA, Vliegenthart JF, Agro AF: Anandamide hydrolysis by human cells in culture and brain. *The Journal of biological chemistry* 273(48), 32332-32339 (1998).

49. Yu M, Ives D, Ramesha CS: Synthesis of prostaglandin E2 ethanolamide from anandamide by cyclooxygenase-2. *The Journal of biological chemistry* 272(34), 21181-21186 (1997).

50. Kozak KR, Crews BC, Morrow JD *et al.*: Metabolism of the endocannabinoids, 2-arachidonylglycerol and anandamide, into prostaglandin, thromboxane, and prostacyclin glycerol esters and ethanolamides. *The Journal of biological chemistry* 277(47), 44877-44885 (2002).

51. Hampson AJ, Hill WA, Zan-Phillips M *et al.*: Anandamide hydroxylation by brain lipoxygenase:metabolite structures and potencies at the cannabinoid receptor. *Biochimica et biophysica acta* 1259(2), 173-179 (1995).

52. Pratt-Hyatt M, Zhang H, Snider NT, Hollenberg PF: Effects of a commonly occurring genetic polymorphism of human CYP3A4 (I118V) on the metabolism of anandamide. *Drug metabolism and disposition: the biological fate of chemicals* 38(11), 2075-2082 (2010).

2.7 Tables and Figures

Table 2.1 Multiple reaction monitoring ion transitions and voltages for ethanolamide analytes

Analyte	Q1 (*m/z*)	Q3 *(m/z)*	CE (V)	CV (V)
AEA	348.3	287.3*	14	18
	348.3	203.2	12	18
	348.3	91.0	38	18
	348.3	62.1	16	18
14,15-EET-EA	364.3	346.3*	10	18
	364.3	91.0	38	18
	364.3	62.1	14	18
20-HETE-EA	364.3	346.3	10	58
	364.3	91.0*	44	58
	364.3	62.1	12	58
d_8-AEA	356.2	62.2*	38	18
	356.2	63.2	38	18

Q1, quadrupole 1; m/z, mass-to-charge ratio; Q3, quadrupole 3; CE, collision energy; CV, cone voltage; AEA, anandamide; 14,15-EET-EA, 14,15-epoxyeicosatrienoic acid ethanolamide; 20-HETE-EA, 20-hydroxyeicosatetraenoic acid ethanolamide; * transition monitored for quantification

Table 2.2 Intraday accuracy and precision

		AEA/ d_8-AEA	14,15-EET-EA/ d_8-AEA	20-HETE-EA/ d_8-AEA
day 1	mean	-	-	-
	SD	-	-	-
	%RSD	**-**	**-**	**-**
	%Bias	**-4.79**	**+10.7**	**+14.5**
day 2	mean	11.2	29.0	26.0
	SD	0.846	2.95	1.75
	%RSD	**7.55**	**10.2**	**6.74**
	%Bias	**-3.69**	**-***	**-5.25**
day3	mean	12.0	27.7	20.4
	SD	1.48	3.69	2.50
	%RSD	**12.3**	**13.3**	**12.2**
	%Bias	**-2.86**	**+6.47**	**+9.51**

* Accuracy for 14,15-EET-EA was not determined due to inadvertent failure to include the calibration curve during analysis.
AEA, anandamide; 14,15-EET-EA, 14,15-epoxyeicosatrienoic acid ethanolamide; 20-HETE-EA, 20-hydroxyeicosatetraenoic acid ethanolamide

Table 2.3 Stability of ethanolamides after 5 hours in extracted human plasma at 4° C

	AEA	14,15-EET-EA	20-HETE-EA	d_8-AEA
Percent of initial injection	103%	157%	96.9%	116%
Percent loss	-	-	3.14%	-

AEA, anandamide; 14,15-EET-EA, 14,15-epoxyeicosatrienoic acid ethanolamide; 20-HETE-EA, 20-hydroxyeicosatetraenoic acid ethanolamide

Table 2.4 Anandamide concentrations in subjects at baseline and after treatment with a CYP2D6 inhibitor (fluoxetine)

Subject	Anandamide concentration during baseline phase (nM)	Anandamide concentration during treatment phase (nM)	Fold change comparing treatment/baseline
1	1.25	0.92	0.74
2	0.98	2.14	2.18
3	1.26	1.21	0.96
4	1.93	1.18	0.61
5	1.23	1.37	1.12
6	1.75	1.12	0.64
7	1.08	1.03	0.96
8	1.57	1.00	0.64
9	1.11	1.23	1.10
10	1.31	1.34	1.02
Mean	1.35 ± 0.31	1.25 ± 0.34	1.00 ± 0.46
%RSD	22.8	27.3	46.0

Table 2.5 Predicted intrinsic and hepatic clearance of anandamide to various metabolites in human liver microsomes based on literature values

Metabolite [a]	V_{max} [b] (pmol/min/mg protein)	K_m [b] (μM)	$CL_{int, in vitro}$ (mL/min/mg protein)	$CL_{int, in vivo}$ (L/min)	CL_H [c] (L/min)
5,6-EET-EA	184 ± 24	5.1 ± 1.9	0.0361	3.8	0.04
8,9-EET-EA	480 ± 56	4.4 ± 1.4	0.109	11.5	0.11
11,12-EET-EA	44 ± 4	4.2 ± 1.6	0.0105	1.1	0.01
14,15-EET-EA	48 ± 6	5.6 ± 2.3	0.00857	0.9	0.01
20-HETE-EA	266 ± 26	2.4 ± 0.6	0.111	11.6	0.11
					0.27

[a] AEA, anandamide; 5,6-EET-EA, 5,6-epoxyeicosatrienoic acid ethanolamide; 8,9-EET-EA, 8,9-epoxyeicosatrienoic acid ethanolamide; 11,12-EET-EA, 11,12-epoxyeicosatrienoic acid ethanolamide;14,15-EET-EA, 14,15-epoxyeicosatrienoic acid ethanolamide; 20-HETE-EA, 20-hydroxyeicosatetraenoic acid ethanolamide
[b] Values obtained from Snider et al. (2007) [23]
[c] Bolded value is the sum of estimated CL_H

Table 2.6 Predicted intrinsic and hepatic clearance of anandamide (AEA) to various AEA metabolites by recombinant enzymes

Metabolite[a]	V_{max}[b] (pmol/min/pmol)	K_m[b] (μM)	$CL_{int, in vitro}$ (mL/min/nmol)	$CL_{int, in vivo}$[c] (mL/min)	CL_H[d] (L/min)	f_m
5,6-EET-EA						
CYP3A4	41.4	118	0.35	4089	0.04	0.50
CYP2D6	--[e]	--	--	--	--	--
CYP2B6	4.6	1.32	3.48	4025	0.04	0.50
CYP4F2	--	--	--	--	--	--
CYP4X1	--	--	--	--	--	--
8,9-EET-EA						
CYP3A4	51	48	1.06	12383	0.11	0.76
CYP2D6	1.6	2.1	0.76	640	0.01	0.04
CYP2B6	3.12	1.21	2.58	2978	0.03	0.19
CYP4F2	--	--	--	--	--	--
CYP4X1	--	--	--	--	--	--
11,12-EET-EA						
CYP3A4	154	118	1.31	15211	0.14	0.67
CYP2D6	1.1	2.6	0.42	355	0.00	0.02
CYP2B6	7.56	1.32	5.73	6615	0.06	0.31
CYP4F2	--	--	--	--	--	--
CYP4X1	--	--	--	--	--	--
14,15-EET-EA						
CYP3A4	128	80	1.60	18648	0.17	0.94
CYP2D6	1.3	2.8	0.46	390	0.00	0.02
CYP2B6	2.04	3.6	0.57	655	0.01	0.04
CYP4F2	--	--	--	--	--	--
CYP4X1	0.065	65	--	--	--	--
20-HETE-EA						
CYP3A4	--	--	--	--	--	--
CYP2D6	3.7	1.3	2.85	2391	0.02	0.08
CYP2B6	--	--	--	--	--	--
CYP4F2	11.5	0.7	16.43	31050	0.26	0.92
CYP4X1	--	--	--	--	--	--

[a] AEA, anandamide; 5,6-EET-EA, 5,6-epoxyeicosatrienoic acid ethanolamide; 8,9-EET-EA, 8,9-epoxyeicosatrienoic acid ethanolamide; 11,12-EET-EA, 11,12-epoxyeicosatrienoic acid ethanolamide;14,15-EET-EA, 14,15-epoxyeicosatrienoic acid ethanolamide; 20-HETE-EA, 20-hydroxyeicosatetraenoic acid ethanolamide

[b] Reference for kinetic parameters: CYP3A4 [52], CYP2D6 [24], CYP2B6 [25], CYP4F2 [23], CYP4X1 [26]
[c] Mean liver P450 abundance for scaling: 111 pmol of CYP3A4 per mg protein [32], 8 pmol of CYP2D6 per mg protein [32], 11 pmol of CYP2B6 per mg protein [32], 18 pmol of CYP4F2 per mg protein [33], no values of CYP4X1 abundance in the literature
[d] Bolded value is the sum of estimated CL_H for each AEA metabolite
[e] Not reported

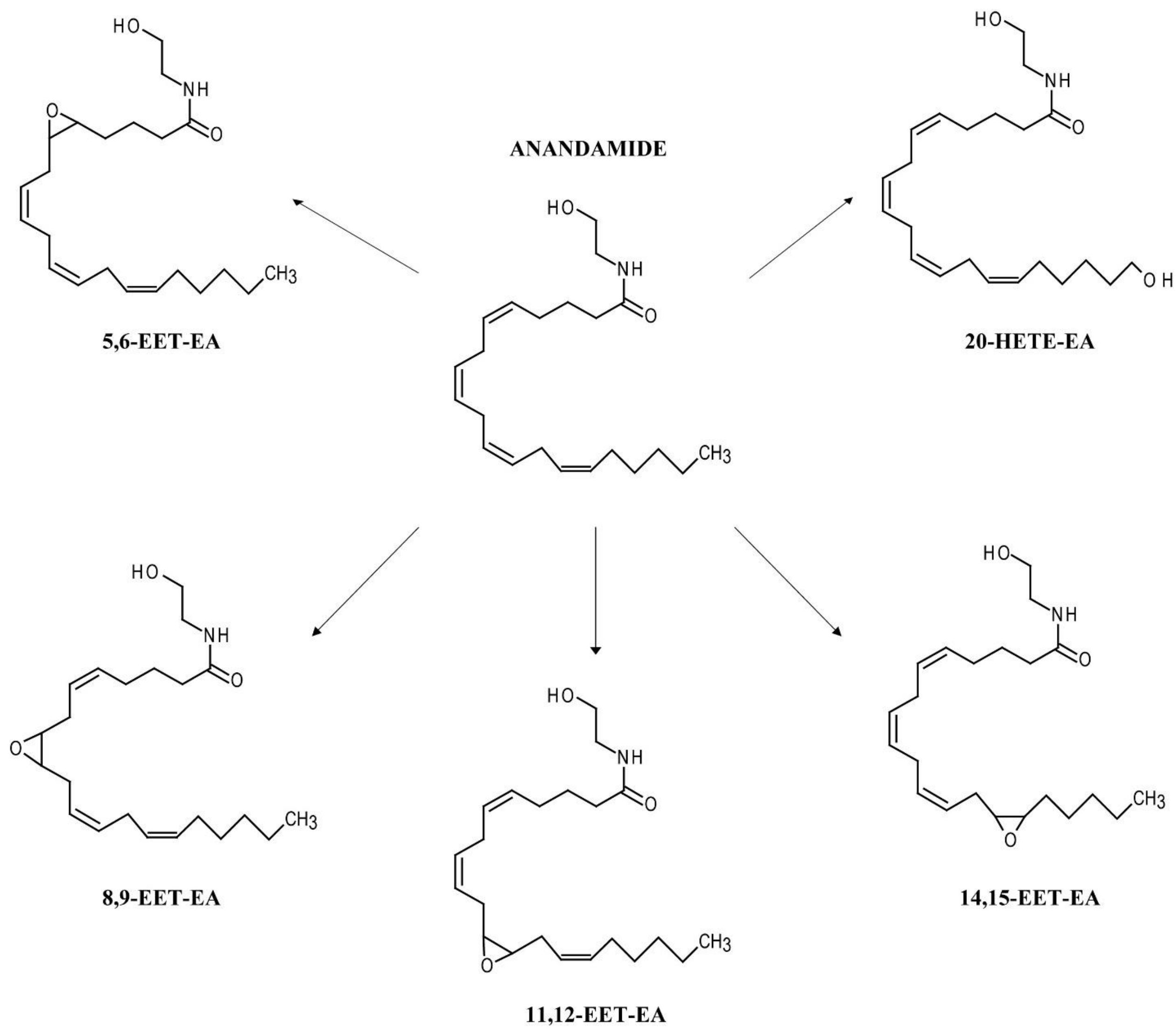

Figure 2.1 Chemical structures of anandamide (AEA) and its primary cytochrome P450 mediated metabolites observed *in vitro* [23-26].

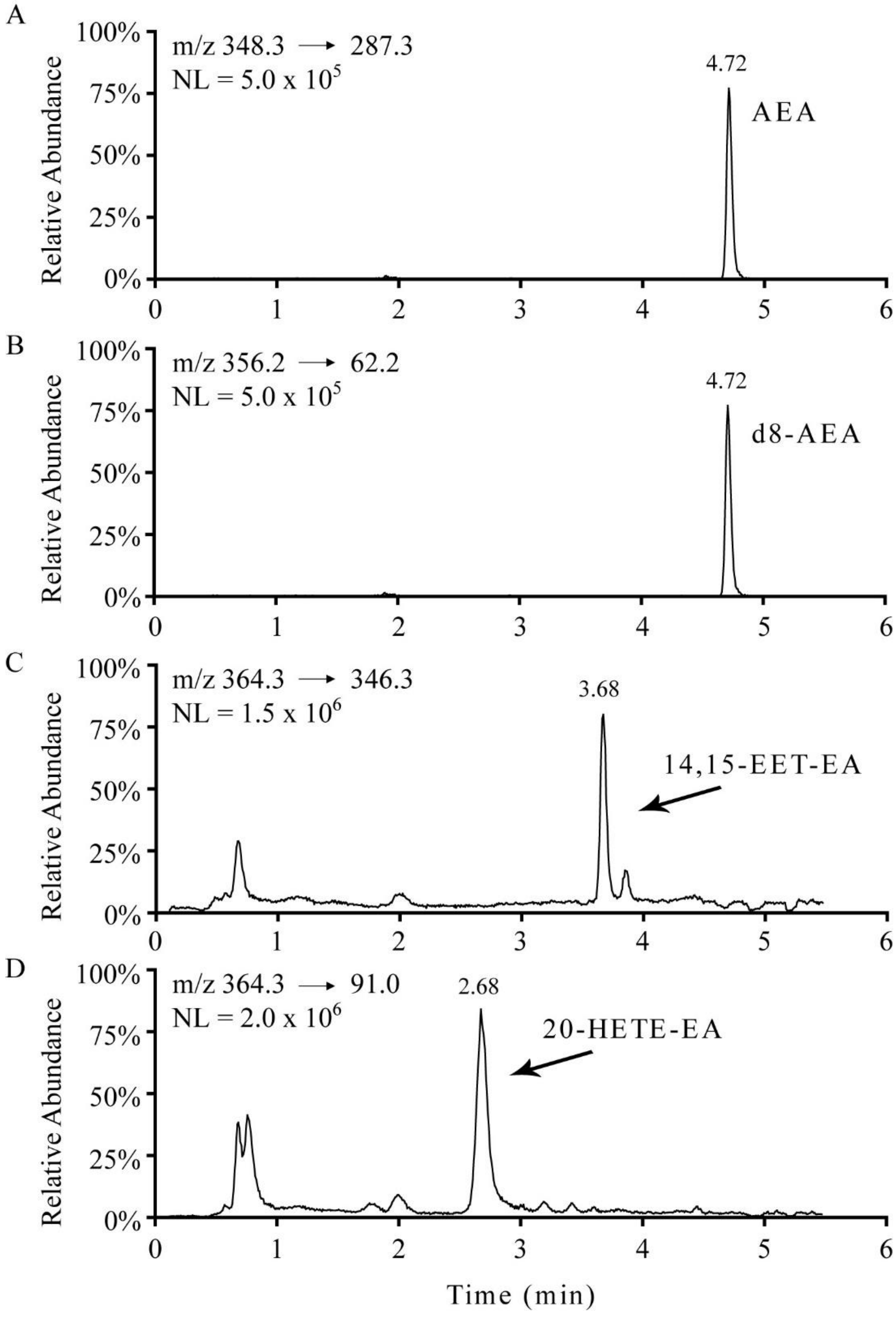

Figure 2.2 Representative LC-MS/MS chromatograms of a spiked plasma sample after liquid-liquid extraction. MRM transitions are shown for A) anandamide (AEA), B) d_8-anandamide (d_8-AEA), C) 14,15-epoxyeicosatrienoic acid ethanolamide (14,15-EET-EA) and D) 20-hydroxyeicosatetraenoic acid ethanolamide (20-HETE-EA).

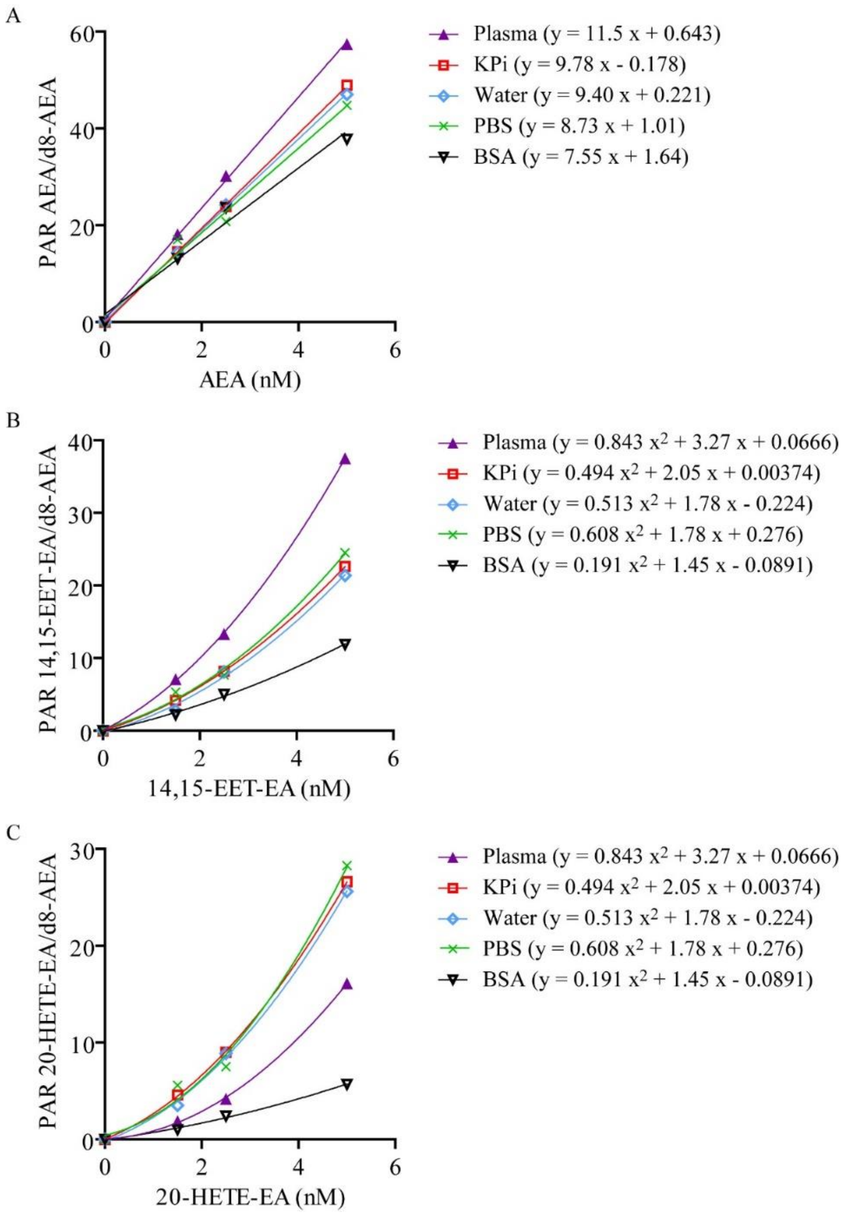

Figure 2.3 The effect of plasma, potassium phosphate buffer (KPi, 0.1 M, pH 7.4), water, phosphate-buffered saline (PBS), and bovine serum albumin (BSA, 30 mg/ml) matrices on ethanolamide analytes. Peak area ratio (PAR) of A) anandamide (AEA), B) 14,15-epoxyeicosatrienoic acid ethanolamide (14,15-EET-EA) and C) 20-hydroxyeicosatetraenoic acid ethanolamide (20-HETE-EA) to the internal standard d_8-anandamide (d_8-AEA) were A) linearly or B and C) quadratically regressed against the concentration of each analyte.

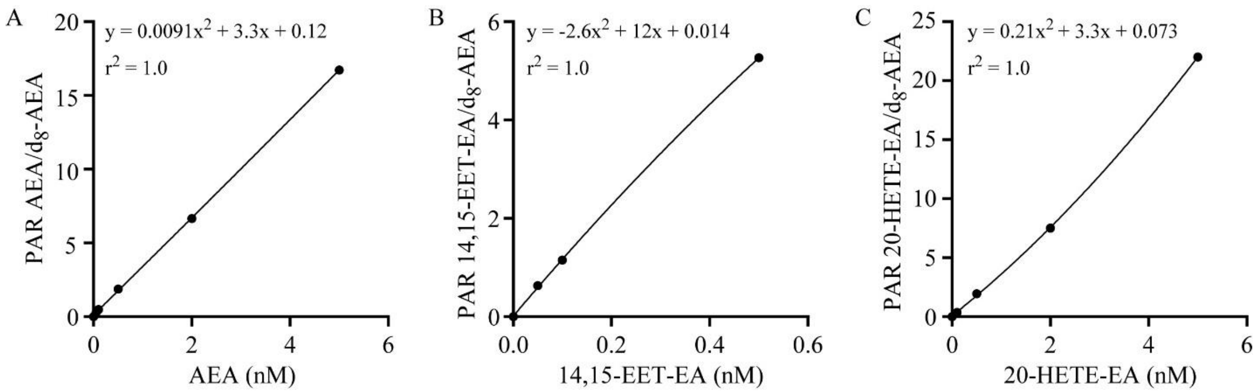

Figure 2.4 Ethanolamide calibration curves prepared in the plasma matrix. Peak area ratios (PAR) of A) anandamide (AEA), B) 14,15-epoxyeicosatrienoic acid ethanolamide (14,15-EET-EA) and C) 20-hydroxyeicosatetraenoic acid ethanolamide (20-HETE-EA) to the internal standard, d_8-anandamide are shown. The AEA calibration curve was corrected for endogenous AEA presence in the matrix. Calibration curves were calculated using a quadratic equation.

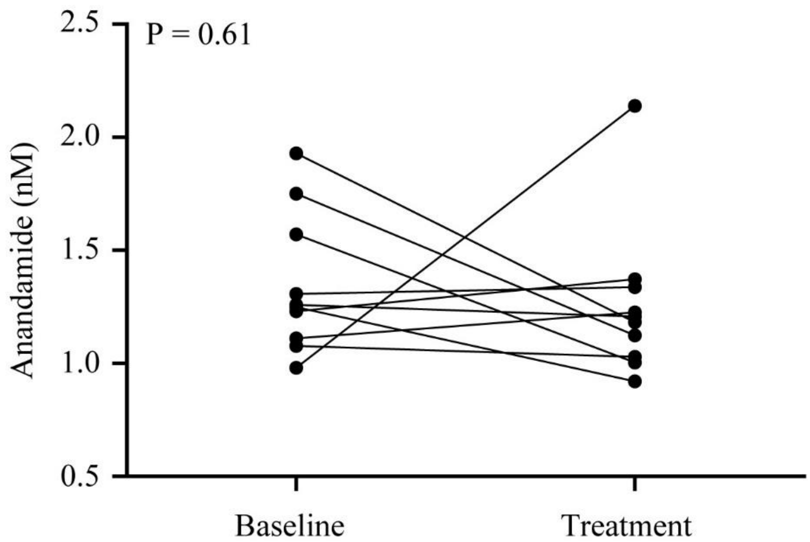

Figure 2.5 The effect of CYP2D6 inhibition on anandamide in plasma. Each subject is represented as a closed circle for anandamide concentration at baseline and after multiple dose fluoxetine treatment. Statistical analyses were performed using paired, two-tailed t-tests.

Chapter 3. Bioanalytical method development for the detection of urinary indolethylamines, potential biomarkers of CYP2D6 activity

3.1 Introduction

Unlike some other drug metabolizing enzymes, the population distribution of cytochrome P450 2D6 (CYP2D6) phenotype is typically bimodal or trimodal [1-3]. CYP2D6 phenotypes are assigned based on the plasma clearance of a probe drug or a urinary parent-to-metabolite metabolic ratio. Examples of widely used probe drugs include: debrisoquine, metoprolol, dextromethorphan, desipramine and atomoxetine [4, 5]. Individuals with little to no CYP2D6 activity are categorized as poor metabolizers (PM), whereas individuals with extremely rapid CYP2D6 activity are assigned to the ultra-rapid metabolizer (UM) group [2, 6-9]. Individuals with activities between these two extremes are classified as intermediate metabolizers (IM) or extensive metabolizers (EM), having reduced or normal activities, respectively [2, 6-9]. Genetic differences among individuals [10], in combination with environmental influences such as concomitant drugs or comorbidities [11], result in a range of catalytic activities within the population [6]. Even among people with the same genotype, CYP2D6 activity can range over two orders of magnitude [12]. Given the diversity of *CYP2D6* genetics and resulting activity, it is clear that variation in *CYP2D6* was not selected against during human evolution. Thus, the function of CYP2D6 in human health and disease is still under investigation.

CYP2D6 protein is found in the liver, but also in other tissues such as the brain [11, 13-15]. A number of studies suggest that CYP2D6 may be involved in neurological function. Personality differences between CYP2D6 EM and PM subjects have been proposed [16-18]. Investigators found a positive association between *CYP2D6* genotype and neural activity during cognitive tests [19]. Zackrisson et al. found that a higher number of individuals who committed suicide had multiple copy numbers of *CYP2D6* as compared to those who died of natural causes (7% and 3%, respectively; P = 0.007) [20]. In addition *CYP2D6* genotype may affect the prevalence of diseases which affect the brain. Lower frequencies of CYP2D6 PMs have been found among schizophrenic patients as compared to controls [21]. Finally, a small, but significantly higher proportion of individuals with *CYP2D6* poor metabolizer genotypes was observed among patients with Parkinson's Disease as compared to healthy controls in a meta-analysis of 13 studies (odds ratio of 1.47) [22]. Since CYP2D6 is expressed in the brain and may influence neurological function and/or disease progression, research has focused on identifying endogenous compounds in the brain which are CYP2D6 substrates. Yu et al. investigated a number of trace indolethylamine compounds as possible endogenous substrates of CYP2D6 [23, 24]. These investigators showed that 5-methoxytryptamine (5-MT), 5-methoxy-*N*,*N*-dimethyl-tryptamine (5-MeO-DMT) and pinoline were metabolized to their O-demethylated products, serotonin, bufotenine and 6-hydroxy-1,2,3,4-tertahydro-β-carboline (6-OH-THBC), respectively, only by recombinant CYP2D6 in a panel of 15 cytochrome P450s. In addition, they found 16-, 35- and 11-fold higher O-demethylation of 5-MT, 5-MeO-DMT and pinoline, respectively, in liver microsomes from humanized CYP2D6 mice as compared to the wild-type mice [23, 24]. More recently, *in vitro* experiments demonstrated that human liver microsomes with wild-type *CYP2D6* genotypes were able to form serotonin from 5-MT more efficiently than *CYP2D6*4/*4* variants (greater than 40-fold increase in V_{max}/K_m) [25]. In addition to CYP2D6's involvement in the biotransformation of endogenous compounds in the brain [26], hepatic CYP2D6 may play a role in the metabolism of endogenous compounds, such as those described above, and this activity may be detectable in blood or urine samples.

Parent-to-metabolite ratios of endogenous compounds may serve as surrogate phenotypic indicators, functioning much like probe drugs. The use of endogenous metabolite ratios, such as 5-MT/serotonin, 5-MeO-DMT/bufotenine and pinoline/6-OH-THBC, would avoid the administration of an exogenous substance to determine phenotype. Estimating these urinary indolethylamine metabolic ratios might provide a novel and non-invasive means of phenotyping for CYP2D6 activity. To our knowledge, there have been no reported assays for the simultaneous quantification of these compounds in biological samples. We sought to develop a bioanalytical assay to simultaneously measure these compounds (except for 6-OH-THBC, which is not commercially available) in urine.

3.2 **Materials and Methods**

3.2.1 *Chemicals and reagents*

Chemicals. Bufotenine (1 mg/mL) was purchased from Cerilliant (Round Rock, TX). HPLC-grade ethyl acetate, methyl tert-butyl ether (MTBE), hexane, methanol, acetonitrile, water, and sodium hydroxide were purchased through Fisher Scientific (Pittsburg, PA). Pinoline and serotonin were purchased in powder form as 6-methoxy-1,2,3,4-tetrahydro-9*H*-pyrido[3,4-*b*]indole hydrochloride and serotonin hydrochloride, respectively from Sigma-Aldrich (St. Louis, MO). 5-MeO-DMT and 5-MT were also purchased from Sigma-Aldrich. 5-methoxytryptamine-$\alpha,\alpha,\beta,\beta$-$d_4$ and serotonin-$\alpha,\alpha,\beta,\beta$-$d_4$ creatinine sulfate were purchased from C/D/N Isotopes (Pointe-Claire, Quebec, Canada).

Synthetic urine. Artificial synthetic urine was prepared as previously described [27]. Urea, sodium chloride, potassium chloride, sodium phosphate (monobasic), creatinine and bovine serum albumin were purchased from Sigma-Aldrich.

3.2.2 *Sample preparation method selection*

Stock solutions of 0.1 mg/mL 5-MeO-DMT, 1 mg/mL 5-MT, 0.25 mg/ml pinoline, 0.1 mg/mL bufotenine, 1 mg/mL serotonin and 1 mg/mL d_4-5-MT were prepared in methanol. d_4-serotonin was not tested. Spiked samples in urine and synthetic urine were prepared with 1% of the stock solutions. 1% methanol in urine and synthetic urine were used as blank controls samples. Neat solutions in water were prepared with 1% of the stock solutions for the assessment of compound extraction and recovery.

Filter method. A Millipore Amicon (Billerica, MA) ultra 3 kDa centrifugal filter device was used to remove proteins from 500 µL of sample (urine, synthetic urine or water). The device was centrifuged for 10 min at 14,000 x G at 25°C to recover filtrate.

Protein precipitation. 400 µL of ice-cold acetonitrile was added to 200 µL sample (urine, synthetic urine or water) in order to precipitate proteins. The sample was centrifuged at 20,000 x G for 10 min at 4°C. The supernatant was transferred to plastic culture tubes and evaporated to dryness under a gentle stream of nitrogen. The sample was reconstituted in 200 µL water. Sample was reconstituted in the starting sample volume in order to compare relative analyte concentrations across preparation methods.

Liquid-liquid extraction. A 3:1 organic-to-aqueous ratio was used to extract compounds out of the sample (urine, synthetic urine or water). Three different organics: MTBE, hexane and ethyl acetate, were tested. In a borosilicate tube, 3000 µL of organic was added to 1000 µL of sample. Samples were agitated for 15 min on a horizontal shaker and subsequently centrifuged at 3000 x G for 20 min at 4°C. The supernatant was transferred to plastic culture tubes and evaporated to dryness under a gentle stream of nitrogen. Samples were reconstituted in 1000 µL of water.

Solid phase extraction. Solid phase extraction (SPE) was performed as previously described by Karkkainen et al. with slight variations [28]. Briefly, 5 mL of 4% ammonium hydroxide was added to 5 mL of sample and centrifuged at 3500 x G for 10 min at 4°C. The supernatants were added to Oasis HLB SPE cartridges (3 cc, 60 mg, 30 µm, Waters, Milford, MA) which were conditioned with 2 mL of methanol and then 2 mL of water. After sample was allowed to flow through, columns were washed twice with 2 mL of 5% methanol and 2% ammonium hydroxide, and washed once with 2 mL 50% methanol and 2% ammonium hydroxide. Sample was eluted twice with 1.5 mL of methanol. The sample flow rate was approximately 1 mL/min. The resulting eluents were evaporated to dryness with nitrogen at room temperature and subsequently reconstituted with 5 mL water.

3.2.3 *LC-MS/MS analysis*

All analyses were performed using a Waters (Milford, MA) Xevo Tq-S QqQ MS. A Waters Acquity UPLC HS T3, 2.1 x 100 mm x 1.8 µm analytical column with in-line filter unit (0.2 µm stainless steel filter) was used to separate the samples. The injection volume was 10 µL and the autosampler was maintained at 4°C. The mobile phase consisted of A: 0.1% formic acid in water and B: 0.1% formic acid in methanol. The LC gradient was 0% B for 1 min; linear increase to 25% B by 6 min; rapid increase to 100% B by 7 min which was held until 8.5 min; re-equilibration at 0% between 8.6 – 12.5 min. The flow rate was 0.6 mL/min and the total run-time was 12.5 min.

Positive electrospray ionization (ESI+) mode and multiple reaction monitoring (MRM) was used to quantitate the analytes. Individual MRM transitions, cone voltages and collision energies along with the approximate retention times are listed in Table 3-1. MS acquisition parameters were set as follows: capillary voltage 3.5 kV, source offset 50 V, source temperature 150°C, desolvation temperature: 500°C, cone gas flow 150 L/hr, desolvation gas flow 1000 L/hr, collision gas flow: 0.15 mL/min, nebulizer gas flow: 7 bar, and dwell time: 27 msec.

3.2.4 *Solid phase extraction method development*

Selection of sample volume and Oasis HLB barrel cartridge capacity. Absolute LC-MS/MS signal and variability were compared between 2.5 mL and 5 mL urine volumes for use with Oasis HLB 3 cc (60 mg, 30 µm) sample extraction cartridges and also between the Oasis HLB 3cc and 6 cc (150 mg, 30 µm) cartridges.

A stock analyte solution of 0.03 µg/mL 5-MeO-DMT, 8 µg/mL 5-MT, 0.002 µg/mL pinoline, 0.01 µg/mL bufotenine and 25 µg/mL serotonin was prepared in a solution of 50:50 water:methanol. Separately, a stock internal standard solution of 0.08 µg/mL d_4-5-MT and 15 µg/mL d_4-serotonin was prepared in a solution of 50:50 water:methanol. We prepared 45 mL of a spiked synthetic urine sample of 1% analyte solution and 0.4% internal standard. To test the limit of detection in real urine samples, 45 mL of a blank urine sample of 1% 50:50 water:methanol and 0.4% internal standard was prepared. 2.5 mL or 5 mL of sample were tested using the 3 cc cartridges, and 5 mL of sample was tested using the 6 cc cartridges. Samples were prepared in triplicate by the addition of an equal volume 2% ammonium hydroxide to the sample. Samples were centrifuged and extracted as described previously, except that the 6 cc cartridges were equilibrated with 3 mL methanol, and then 3 mL of water, and the sample was eluted twice with 2 mL of methanol. Samples were dried for one hour at room temperature under a gentle stream of nitrogen and then vortexed in order to pull down any residue on the upper sides of the tubes. The remaining sample was evaporated to dryness and then reconstituted in 50 or 100 µL of 50:50 water:methanol for starting volumes of 2.5 mL and 5 mL, respectively.

Variability. Variability in sample preparation and analytical reproducibility was determined. Five replicates of spiked synthetic urine and spiked urine samples were prepared. Each set of five samples was injected four or five times and analyzed by LC-MS/MS. For one of the spiked synthetic urine samples, there were no detectable peaks in the bufotenine MRM channels, whereas other analytes had detectable peaks in this sample. We could not explain this discrepancy and this sample was excluded from the analysis. Variability was expressed as percent relative standard deviation ($\%\mathrm{RSD} = \frac{\text{standard deviation}*100}{\text{mean}}$). The mean %RSD for each analyte was obtained by averaging %RSD for the LC-MS/MS run. Five replicates were compared to determine the variability in sample preparation. For each sample, the results from multiple injections were compared to determine the analytical reproducibility.

Sample solvent selection. A neat sample of 0.011 µg/mL 5-MeO-DMT, 2.9 µg/mL 5-MT, 0.00071 µg/mL pinoline, 0.0036 µg/mL bufotenine, 8.9 µg/mL serotonin, 0.14 µg/mL d_4-5-MT and 2.1 µg/mL d_4-serotonin was prepared in a 50:50 water:methanol solution or a 75:25 water:methanol solution. Further dilutions were prepared as needed during the analysis. In order to obtain a sample with a 87:13 water:methanol proportion, a 2-fold dilution of the neat sample was prepared by combining 20 µL of the sample in 75:25 water:methanol with 20 µL of nanopure water. In order to obtain a sample with a 99:1 water:methanol proportion, a 100-fold dilution of the neat sample was prepared by combining 10 µL of the sample in 75:25 water:methanol with 990 µL of nanopure water. Unless otherwise stated, 10 µL of these neat solutions were analyzed by LC-MS/MS.

3.2.5 *Preparation of calibration curve and quality control (QC) samples*

Stock concentrations of 1 mg/mL 5-MeO-DMT, 1 mg/mL 5-MT, 1 mg/mL pinoline, 5 mg/mL serotonin, 1 mg/mL d_4-5-MT and 0.5 mg/mL d_4-serotonin and intermediate stock solutions of 0.25, 2.5 and 25 µg/mL 5-MeO-DMT, 1 and 10 µg/mL pinoline, and 1 and 10 µg/mL bufotenine were prepared in methanol. These stock solutions were used to create the highest stock standard of 0.03 µg/mL 5-MeO-DMT, 40 µg/mL 5-MT, 0.02 µg/mL pinoline, 0.05 µg/mL bufotenine, and 250 µg/mL serotonin in a solution of 50:50 water:methanol. As shown in Table 3-2, eight sequential stock standards, were made by a serial dilution with 50:50 water:methanol. A stock low and high QC were prepared at concentrations shown in Table 3-2. These stock calibration points and QCs were stored at -80°C. A stock internal standard solution of 1 µg/mL d_4-5-MT and 15 µg/mL d_4-serotonin was prepared in 50:50 water:methanol. Urine samples from two healthy adult donors were pooled (total volume 400 mL). Pooled urine was aliquoted and stored at -20°C for use as the matrix for the calibration curve and QC samples.

3.2.6 *Preparation and extraction of samples*

Pilot urine samples. Urine samples from one healthy adult female and one healthy male child were obtained. Urine samples were extracted as previously described, except that 20 µL of stock internal standard was added to 2.5 mL of urine and then combined with 2.5 mL of 4% sodium hydroxide. Samples were extracted using the Waters Oasis HLB 3 cc cartridges. Following extraction and evaporation, including vortexing half way through the drying process, samples were reconstituted in 50 µL of water.

Calibration standards and QCs. Calibration standard and QC samples were prepared in the same manner as the pilot urine samples except that 25 µL of working standard and 20 µL of stock internal standard were added to 2.475 mL of pooled urine and prepared with 2.5 mL of 4% ammonium hydroxide. Carry-over was analyzed by injecting a blank water sample after each of the three highest standards and the high QC. Carry-over was calculated as the percentage of the peak area in the blank divided by the peak area in the preceding sample.

3.2.7 *Data analysis*

Peak integrations were performed using Waters MassLynx with QuanLynx (version 4.1). Peak areas or peak area ratios (PARs) resulting from the matrix in the 0 ng/mL calibration points were subtracted from each of the higher calibration points and QCs in order to correct for endogenous analytes present in the pooled urine matrix. Calibration curves were determined by linear regression of concentration vs. corrected peak areas of 5-MeO-DMT or bufotenine, or corrected PARs of 5-MT/d_4-5-MT, pinoline/d_4-5-MT or serotonin/d_4-serotonin. Quadratic equations were also evaluated, but these did not fit the data well. The points included in the low and high concentration curves were determined by minimization of the back calculated concentration error. Acceptable criteria were $\leq$ 15% for accuracy, and precision.

3.3 **Results**

3.3.1 *Sample preparation method selection: recovery*

After developing an appropriate LC-MS/MS protocol to monitor the indolethylamine analytes, we focused on urine sample preparation. Blank synthetic urine was used as a control to detect any interfering peaks in the LC-MS/MS method. We tested a filter, protein precipitation, three liquid-liquid extraction, and SPE methods. Using all of the extraction methods, most analytes with the exception of serotonin, were undetectable (Table 3-3). The serotonin peak area was highest in the SPE method (4% of the peak area in the neat sample) and negligible (1 to 2%) for all other extraction methods.

To determine whether blank urine would contribute a baseline signal to the analytes and as a test of the various extraction procedures, blank urine samples were prepared and analyzed. Similar to the blank synthetic urine, the peak area of most analytes were minimal compared to the neat sample (undetectable to 1% of the neat sample) using any of the extraction methods with the exception of serotonin (Table 3-3). Serotonin as a percentage of the neat sample ranged from 1 to 2% using liquid-liquid extraction methods, 6% using SPE, 13% using the protein precipitation method, and 14% using the filter method.

In spiked synthetic urine, recovery of analytes using MTBE, ethyl acetate, and hexane was poor (undetectable to 2%, Table 3-3). Recovery of the analytes from spiked synthetic urine using the filter method and protein precipitation method ranged from 50% to 106%. Recovery of the analytes from spiked synthetic urine using SPE ranged from 6% to 59%. Recovery of 5-MeO DMT and 5-MT was roughly 2-fold higher when using the filter and protein precipitation methods

(106% and 50% for 5-MeO-DMT and 5-MT, respectively) as compared to the SPE method (59% and 24% for 5-MeO-DMT and 5-MT, respectively).

Similar to extraction from spiked synthetic urine, analyte extraction from spiked urine using MTBE, ethyl acetate, or hexane was poor (undetectable to 9%, Table 3-3). Extraction of analytes in the spiked urine ranged from 3% to 43% for the filter method, 3 to 34% for the protein precipitation method, and 8% to 67% for the SPE method.

The error between the spiked synthetic urine and spiked urine (based on % of peak area of the neat) was calculated to ascertain whether there was a matrix effect on the recovery of the analytes. As shown in Table 3-3, the overall extraction of the analytes was most similar for the spiked synthetic urine and spiked urine when using the SPE method (0 to 45% error) as compared to the filter method (120 to 2361% error) or the protein precipitation method (70 to 3200% error). As a confirmation that analyte was not lost during the evaporation or reconstitution steps, neat samples were dried, reconstituted and injected. The recovery from evaporation and reconstitution alone was 96%, 93%, 99%, 96%, and 93% for 5-MeO-DMT, 5-MT, pinoline, bufotenine and serotonin, respectively. Thus, it is unlikely that the evaporation and reconstitution steps led to significant loss of analyte.

SPE was selected as the sample preparation method as it was least influenced by differences in matrix (spiked synthetic urine vs. spiked urine), had relatively comparable recovery of the analytes to the other extraction methods in spiked urine, and would be more amenable to accommodating larger volumes of urine.

3.3.2 *Selection of sample volume and SPE cartridge*

Spiked synthetic urine and blank urine were tested using two different SPE barrel capacities (3 cc and 6 cc cartridges) and using two different sample volumes (2.5 and 5 mL) for the 3 cc cartridge. Analyte peak areas were integrated and normalized to the internal standard, d_4-5-MT. Peak area ratio (PAR) results are summarized in Table 3-4. Reconstitution volumes accounted for the difference in starting volumes of sample (e.g., 2.5 mL of sample was reconstituted in 50 µL and 5 mL of sample was reconstituted in 100 µL) permitting the comparison of PAR.

Analyte PARs were slightly higher for the larger volume of the spiked synthetic urine (5 mL vs 2.5 mL) on the 3 cc cartridge. The percent difference between the PAR of the two volumes ranged from 8% for pinoline to 45% for bufotenine. On the 3cc cartridge, variability in analyte PARs ranged from 10% to 44% for the 2.5 mL spiked synthetic urine, whereas it ranged from 30% to 63% for the 5 mL spiked synthetic urine. Although the smaller sample volume of the spiked synthetic urine resulted in lower variability, %RSD was only acceptable (< 15%) for bufotenine and serotonin. The analyte PAR were substantially different when comparing 5 mL of spiked synthetic urine on the 3 cc and 6 cc cartridges (percent difference ranging 59% to 179%). The use of 5 mL of spiked synthetic urine on the 6 cc cartridge appeared to have pronounced decreased recovery of all analytes. Variability in analyte PARs ranged from 16% to 42% for 5 mL of spiked synthetic urine on the 6 cc cartridge.

The extraction of blank urine using two SPE capacities and two different sample volumes was also compared (Table 3-4). Analyte mean PARs, except for bufotenine mean PARs, were comparable within 2-fold across barrel sizes and sample volumes. For bufotenine, the percent difference was 182% comparing 2.5 and 5 mL on the 3 cc cartridge and 67% comparing 5 mL on the 3 cc and 6 cc cartridges. Variability for all analyte PARs was acceptable using 2.5 mL of blank urine on the 3 cc cartridge. Variability in analyte PARs was acceptable for most compounds, except for bufotenine (89%) and 5-MT (17%) using 5 mL of blank urine on the 3 cc cartridge. Variability in analyte PARs was acceptable for most compounds, except for bufotenine (19%) using 5 mL of blank urine on the 6 cc cartridge.

For further work, the 2.5 mL sample volume and 3 cc SPE cartridge was chosen due to increased reproducibility and unexpected greater analyte recovery of spiked synthetic urine as compared to the 5 mL sample volume on the 6 cc cartridge.

3.3.3 *Matrix effects*

Reproducibility in SPE sample preparation. Variability in the peak areas of each analyte in spiked synthetic urine (n = 4) and spiked urine (n = 5) was determined (Table 3-5). Samples were reinjected in the multiple cycles and the mean %RSD was calculated. In the spiked synthetic urine samples, mean %RSD was greater than 15% for most analytes except for 5-MeO-DMT and bufotenine (6.8% and 15%, respectively). In the spiked urine samples, mean %RSD of 5-MeO-DMT, bufotenine, serotonin and d_4-serotonin were acceptable (3.6%, 8.9%, 12% and 7.9%, respectively), whereas 5-MT, pinoline and d_4-5-MT were greater than 15% (20%, 26%, and 17%, respectively). For all analytes, mean %RSD were lower in spiked urine as compared to spiked synthetic urine.

Analytical reproducibility. Each spiked synthetic urine (n = 4) and spiked urine (n = 5) was injected five times to determine the analytical reproducibility (Table 3-6). In the spiked synthetic urine, mean %RSD was acceptable for 5-MeO-DMT, 5-MT, and d_4-5-MT (12%, 5.7%, and 6.6%, respectively). In the spiked synthetic urine, mean %RSD for pinoline, bufotenine, serotonin, d_4-serotonin was high (27%, 22%, 18%, and 18%, respectively). In the spiked urine samples, mean %RSD was less than 15% for all analytes. Overall, the variability in spiked urine samples was less than in the spiked synthetic urine samples. The %RSD to determine the analytical reproducibility for spiked synthetic urine and spiked urine samples was high. In a separate experiment, instrument variability was determined to be ≤10% for all analytes over five consecutive injections of spiked synthetic urine (data not shown). The high %RSD for both the sample preparation and analytical replicates may be a result of the difficulty in integrating the unusually shaped analyte peaks.

3.3.4 *Effect of sample reconstitution solvent on chromatography*

Based on visual inspection, the chromatography peak shape was poor for the neat sample reconstituted in 50:50 water:methanol. All analytes, except pinoline, had broad, fronting or multiple peaks (Figure 3-1). As the initial conditions for chromatography (0% organic) differed from the reconstitution solvent, we increased the aqueous component of the reconstitution solvent. An overall improvement in peak shape was observed when the neat sample was reconstituted in 75:25 water:methanol (Figure 3-2). As a result of this change, the 5-MeO-DMT, 5-MT, d_4-5-MT and d_4-serotonin peaks improved from double to single peaks, though some were still broad or tailing. The bufotenine and serotonin peaks were still broad or had double peaks. As shown in Figure 3-3, the peak shape improved further when the neat sample was reconstituted in 87:13 water:methanol, improving peak symmetry for bufotenine and reducing tailing of the d_4-serotonin peak. However, tailing, broad and double peaks were observed for d_4-5-MT, 5-MT and serotonin. It is worth noting that the concentration of analytes in this sample was half that of the concentration of analytes in 50% and 75% water. A 10-fold lower injection volume (1 μL) resulted in improved peak symmetry for d_4-5-MT, 5-MT, and serotonin by the elimination of tailing, broad and double peaks (Figure 3-4). Symmetrical peaks were observed for all analytes, except for pinoline, when the neat sample in 75:25 water:methanol was diluted to 99:1 water:methanol (Figure 3-5). Pinoline may have been below the limit of detection at this dilution. The sample preparation method was amended to reconstitute samples in 100% water to improve the peak shapes.

3.3.5 *Calibration curve, QC and pilot urine samples*

We determined whether the high analyte concentrations could result in carry-over. Carry-over was undetectable for 5-MT, d_4-5-MT, bufotenine, serotonin, and d_4-serotonin. In blank samples following injection of calibration curve samples 8, 9, 10 and the high QC, carry-over of 5-MeO-DMT was 2%, 3%, 6%, and 4% , and pinoline was 6%, 7%, 8% and 10% of the preceding sample, respectively.

Calibration curves in pooled urine matrix were created by linear regression of peak area or peak area ratio (PAR) of each analyte and the known concentration (Table 3-2 and Figure 3-6). For the analytes, the selection of either d_4-serotonin or d_4-5-MT as the internal standard was made empirically or by structural similarity to the undeuterated compound. PARs for 5-MT and pinoline were calculated with d_4-5-MT. PARs for serotonin were calculated with d_4-serotonin. Based on various comparisons, normalization of 5-MeO-DMT and bufotenine by either internal standard introduced more error in the calibration curve, thus peak area was used to construct the calibration curves for 5-MeO-DMT and bufotenine. Calibration curves were empirically split into low and high concentration ranges by minimization of the back calculated concentration error. Table 3-7 shows the back calculated accuracy error for each calibration point and QC. Overall, the calibration curves were well behaved for 5-MeO-DMT (r^2 = 1.0 for low and high curves), 5-MT (r^2 = 0.99 for low and high curves), bufotenine (r^2 = 0.98 and 1.0 for the low and high curves), pinoline (r^2 = 0.99 for the overall curve), and serotonin (r^2 = 0.99 and 1.0 for low and high curves).

The lower limit of quantification (LLOQ) was determined by error less than 15% for the back calculated accuracy (Table 3-7). The LLOQ was 3.13 and 20 ng/mL for 5-MT and serotonin, and 3.9, 4.7, and 130 pg/mL for bufotenine, 5-MeO-DMT, and pinoline, respectively. Most of the QC samples did not have an acceptable accuracy and may need to be prepared again.

The goal of developing this assay was to quantitate urinary concentrations of various indolethylamines with *in vitro* evidence supporting their use as CYP2D6 biomarkers. We prepared two urine samples (one adult and one child). In these samples, 5-MeO-DMT and pinoline were undetectable by LC-MS/MS and bufotenine was detectable, but below the lower limit of quantitation (Table 3-8). Serotonin and 5-MT were within the ranges of quantitation in both urines. 5-MT and serotonin are the substrate and product, respectively, of a CYP2D6 demethylation reaction. The urinary molar parent-to-metabolite ratio was 1.32 and 0.27 for the subjects.

3.4 **Discussion**

Our goal was to develop a LC-MS/MS assay for the simultaneous quantification of previously reported *in vitro* CYP2D6 substrates and related products, specifically, 5-MT and serotonin, 5-MeO-DMT and bufotenine, and pinoline and 6-OH-THBC. The O-demethylated product of pinoline, 6-OH-THBC, was not included in the development of the assay as it was not commercially available.

The sample extraction was tested using filter, protein precipitation, liquid-liquid extraction and SPE methods (Table 3-3). The analytes were poorly extracted when using a variety of liquid-

liquid extraction approaches. This is perhaps due to the relatively hydrophilic nature of the compounds that may result in the analytes preferentially partitioning into the aqueous phase rather than the organic phase. The overall analyte recovery from spiked synthetic urine and spiked urine samples was highest when using a filter, protein precipitation or SPE approach. Bufotenine was the most poorly extracted analyte in the spiked samples which was surprising as the SPE method was adapted from published reports measuring bufotenine in biofluids, including urine [28]. Spiked synthetic urine sample was used for much of the method development because it was assumed to be free of the analytes and thus, presumably a superior choice to a urine matrix for calibration curve and QC samples. With this in mind, we chose to go forward with the SPE method over the filter or protein precipitation methods because analyte recovery was most consistent between spiked synthetic urine and spiked urine samples using SPE. Based on the experimental results, we selected a 3 cc SPE cartridge with 2.5 mL of sample as the most reliable sample preparation method.

The sample preparation variability (Table 3-4) and analytical reproducibility (Table 3-5) was lower in spiked urine compared to spiked synthetic urine. The urine matrix could affect sample preparation due to protein binding, pH differences or buffering, however it is unclear why the urine matrix would affect analytical reproducibility. These injections to assess analytical reproducibility were performed over about 16 hours and the reinjections of a sample did not occur consecutively. In a separate experiment, instrument variability was determined to be ≤10% for all analytes over five consecutive injections of spiked synthetic urine. Thus it is possible that the poor peak shape due to samples being reconstituted in 50:50 water:methanol or degradation of analytes over time may have occurred when assessing the variability. The use of synthetic urine was abandoned as we discovered that the overall variability of analytes was reduced in urine, and blank synthetic urine contained a small interfering peak with MRM and retention time similar to serotonin. A pooled urine sample was prepared and used for subsequent construction of calibration curves and QC samples.

The chromatography was drastically improved from the poor peak shapes in the neat sample reconstituted in 50:50 water:methanol (Figure 3-1) by increasing the percentages of aqueous in the reconstitution solvent (Figure 3-2 and 3-3). To address the question of column overloading, 10 µL and 1 µL of the neat sample reconstituted in 87:13 water:methanol were injected (Figures 3-3 and 3-4). A decreased injection volume improved the peak shapes of the problematic analytes. The increased percentage of aqueous in the reconstitution solvent to match the mobile phase initial conditions, and an awareness of column overloading, was beneficial for optimal analyte peak shapes. Following this conclusion, we adjusted our sample preparation methodology to include reconstitution of the samples with 100% water.

Two urines were prepared to test whether the analytes were quantifiable with this newly developed assay. The accuracy of the calculated concentrations of the pilot urines may be questionable as only a few of the QCs had acceptable error. Nevertheless, serotonin and 5-MT were quantifiable in these urines. Serotonin concentrations in the urines were similar between the subjects (~100 ng/mL). Literature reports of serotonin concentrations vary between 7.05 -21.2 ng/mL/mM creatinine [29], 4.58 - 10.0 ng/mL [30], and 45-450 ng/mL [31] which are generally lower than what we observed.

There was greater than 4-fold difference in urinary 5-MT concentrations between the two urines studied. Haddox et al. reported the urinary excretion of 31-79 µg 5-MT over 24 hours in patients with Rheumatic heart disease, but 5-MT was not detected in healthy controls [32]. These findings are inconsistent with measured 5-MT concentrations of 29 and 135 ng/mL in the two subjects.

A detectable, but not quantifiable peak for bufotenine was observed in our urines. This was surprising because urinary bufotenine concentrations have been reported to range from less than 0.05 ng/mL, and up to 9.1 ng/mL [28]. In addition, bufotenine has been found to be higher among psychiatric patients (1.88 µg/g creatinine) compared to healthy controls (0.37 µg/g creatinine) [33]. These concentrations are at or exceed our higher calibration curve points for bufotenine.

5-MeO-DMT and pinoline were not detected in our urine samples. Previously reported urinary 5-MeO-DMT levels range between not detected to 1.90 µg excreted over 24 hrs [34]. Consistent with our findings, pinoline has not been detected in the urine [35]. However, pinoline has been reported to range from 0.202 to 3.03 ng/mL in human plasma [36]. Serum pinoline concentrations are not related to sex or age [36], but may enter the body through diet [37] and therefore may contribute to endogenous levels.

Additional studies should be conducted to confirm our results in a larger set of human urine samples and reconcile the discrepancies from the literature reports of the urinary concentrations for serotonin, 5-MT, and 5-MeO-DMT. Clearly the accuracy and lower limit of quantitation of this assay, particularly for bufotenine, needs to be improved. A sample preparation method with increased analyte recovery or a more sensitive LC-MS/MS method might suffice. Once the bioanalytical assay is optimized, clinically relevant ranges of these indolethylamines can be determined. Of the detectable analytes, urinary molar 5-MT-to-serotonin ratios were calculated as 1.23 and 0.25 for the two subjects. This may indicate that the subjects had differing CYP2D6 activities, or that the production of urinary 5-MT may differ in children and adults, despite having similar urinary serotonin levels. Testing and validation in an appropriately designed clinical study with a fully developed analytical method could determine the utility of these parent-to-metabolite indolethanolamine metabolic ratios as *in vivo* biomarkers of CYP2D6 activity.

3.5 Acknowledgements

We are grateful to Dale Whittington and Dr. Michael Volny for their consultation regarding the sample preparation and LC-MS/MS method development.

3.6 References

1. Zanger UM, Raimundo S, Eichelbaum M: Cytochrome P450 2D6: overview and update on pharmacology, genetics, biochemistry. *Naunyn-Schmiedeberg's archives of pharmacology* 369(1), 23-37 (2004).

2. Schmid B, Bircher J, Preisig R, Kupfer A: Polymorphic dextromethorphan metabolism: co-segregation of oxidative O-demethylation with debrisoquin hydroxylation. *Clinical pharmacology and therapeutics* 38(6), 618-624 (1985).

3. Gaedigk A, Simon SD, Pearce RE, Bradford LD, Kennedy MJ, Leeder JS: The CYP2D6 activity score: translating genotype information into a qualitative measure of phenotype. *Clinical pharmacology and therapeutics* 83(2), 234-242 (2008).

4. Frank D, Jaehde U, Fuhr U: Evaluation of probe drugs and pharmacokinetic metrics for CYP2D6 phenotyping. *European journal of clinical pharmacology* 63(4), 321-333 (2007).

5. U.S. Food and Drug Administration. Drug Development and Drug Interactions: Table of Substrates, Inhibitors and Inducers. *http://www.fda.gov/Drugs/DevelopmentApprovalProcess/DevelopmentResources/DrugInteractionsLabeling/ucm093664.htm#inVivo*. (Accessed 3/24/2015)

6. Sachse C, Brockmoller J, Bauer S, Roots I: Cytochrome P450 2D6 variants in a Caucasian population: allele frequencies and phenotypic consequences. *American journal of human genetics* 60(2), 284-295 (1997).

7. Mahgoub A, Idle JR, Dring LG, Lancaster R, Smith RL: Polymorphic hydroxylation of Debrisoquine in man. *Lancet* 2(8038), 584-586 (1977).

8. Johansson I, Lundqvist E, Bertilsson L, Dahl ML, Sjoqvist F, Ingelman-Sundberg M: Inherited amplification of an active gene in the cytochrome P450 CYP2D locus as a cause of ultrarapid metabolism of debrisoquine. *Proceedings of the National Academy of Sciences of the United States of America* 90(24), 11825-11829 (1993).

9. Bock KW, Schrenk D, Forster A *et al.*: The influence of environmental and genetic factors on CYP2D6, CYP1A2 and UDP-glucuronosyltransferases in man using sparteine, caffeine, and paracetamol as probes. *Pharmacogenetics* 4(4), 209-218 (1994).

10. Zanger UM, Fischer J, Raimundo S *et al.*: Comprehensive analysis of the genetic factors determining expression and function of hepatic CYP2D6. *Pharmacogenetics* 11(7), 573-585 (2001).

11. Zanger UM, Schwab M: Cytochrome P450 enzymes in drug metabolism: regulation of gene expression, enzyme activities, and impact of genetic variation. *Pharmacology & therapeutics* 138(1), 103-141 (2013).

12. Gaedigk A: Complexities of CYP2D6 gene analysis and interpretation. *Int Rev Psychiatry* 25(5), 534-553 (2013).

13. Dutheil F, Dauchy S, Diry M *et al.*: Xenobiotic-metabolizing enzymes and transporters in the normal human brain: regional and cellular mapping as a basis for putative roles in cerebral function. *Drug metabolism and disposition: the biological fate of chemicals* 37(7), 1528-1538 (2009).

14. Siegle I, Fritz P, Eckhardt K, Zanger UM, Eichelbaum M: Cellular localization and regional distribution of CYP2D6 mRNA and protein expression in human brain. *Pharmacogenetics* 11(3), 237-245 (2001).

15. Miksys S, Rao Y, Hoffmann E, Mash DC, Tyndale RF: Regional and cellular expression of CYP2D6 in human brain: higher levels in alcoholics. *Journal of neurochemistry* 82(6), 1376-1387 (2002).

16. Llerena A, Edman G, Cobaleda J, Benitez J, Schalling D, Bertilsson L: Relationship between personality and debrisoquine hydroxylation capacity. Suggestion of an endogenous neuroactive substrate or product of the cytochrome P4502D6. *Acta psychiatrica Scandinavica* 87(1), 23-28 (1993).

17. Gonzalez I, Penas-Lledo EM, Perez B, Dorado P, Alvarez M, A LL: Relation between CYP2D6 phenotype and genotype and personality in healthy volunteers. *Pharmacogenomics* 9(7), 833-840 (2008).

18. Roberts RL, Luty SE, Mulder RT, Joyce PR, Kennedy MA: Association between cytochrome P450 2D6 genotype and harm avoidance. American journal of medical genetics. Part B, Neuropsychiatric genetics : the official publication of the International Society of Psychiatric Genetics 127B(1), 90-93 (2004).

19. Stingl JC, Esslinger C, Tost H *et al.*: Genetic variation in CYP2D6 impacts neural activation during cognitive tasks in humans. *NeuroImage* 59(3), 2818-2823 (2012).

20. Zackrisson AL, Lindblom B, Ahlner J: High frequency of occurrence of CYP2D6 gene duplication/multiduplication indicating ultrarapid metabolism among suicide cases. *Clinical pharmacology and therapeutics* 88(3), 354-359 (2010).

21. Llerena A, Dorado P, Penas-Lledo EM, Caceres MC, De La Rubia A: Low frequency of CYP2D6 poor metabolizers among schizophrenia patients. *The pharmacogenomics journal* 7(6), 408-410 (2007).

22. Mccann SJ, Pond SM, James KM, Le Couteur DG: The association between polymorphisms in the cytochrome P-450 2D6 gene and Parkinson's disease: a case-control study and meta-analysis. *Journal of the neurological sciences* 153(1), 50-53 (1997).

23. Yu AM, Idle JR, Byrd LG, Krausz KW, Kupfer A, Gonzalez FJ: Regeneration of serotonin from 5-methoxytryptamine by polymorphic human CYP2D6. *Pharmacogenetics* 13(3), 173-181 (2003).

24. Yu AM, Idle JR, Herraiz T, Kupfer A, Gonzalez FJ: Screening for endogenous substrates reveals that CYP2D6 is a 5-methoxyindolethylamine O-demethylase. *Pharmacogenetics* 13(6), 307-319 (2003).

25. Haduch A, Bromek E, Sadakierska-Chudy A, Wojcikowski J, Daniel WA: The catalytic competence of cytochrome P450 in the synthesis of serotonin from 5-methoxytryptamine in the brain: an in vitro study. *Pharmacological research : the official journal of the Italian Pharmacological Society* 67(1), 53-59 (2013).

26. Yu AM, Idle JR, Gonzalez FJ: Polymorphic cytochrome P450 2D6: humanized mouse model and endogenous substrates. *Drug metabolism reviews* 36(2), 243-277 (2004).

27. Shmaefsky BR: Artificial urine for laboratory testing. *The American Biology Teacher*, 170-172 (1990).

28. Karkkainen J, Forsstrom T, Tornaeus J *et al.*: Potentially hallucinogenic 5-hydroxytryptamine receptor ligands bufotenine and dimethyltryptamine in blood and tissues. *Scandinavian journal of clinical and laboratory investigation* 65(3), 189-199 (2005).

29. Bouatra S, Aziat F, Mandal R *et al.*: The human urine metabolome. *PloS one* 8(9), e73076 (2013).

30. Kwarts E, Kwarts J, Rutgers H: A simple paired-ion liquid chromatography assay for serotonin in cerebrospinal fluid, platelet-rich plasma, serum and urine. *Annals of clinical biochemistry* 21 (Pt 5), 425-429 (1984).

31. Twarog BM, Page IH: Serotonin content of some mammalian tissues and urine and a method for its determination. *The American journal of physiology* 175(1), 157-161 (1953).

32. Haddox CH, Jr., Saslaw MS: Urinary 5-methoxytryptamine in patients with rheumatic fever. *The Journal of clinical investigation* 42, 435-441 (1963).

33. Karkkainen J, Raisanen M, Naukkarinen H, Spoov J, Rimon R: Urinary excretion of free bufotenin by psychiatric patients. *Biological psychiatry* 24(4), 441-446 (1988).

34. Riceberg LJ, Vunakis HV: Determination of N,N-dimethylindolealkylamines in plasma, blood and urine extracts by radioimmunoassay and high pressure liquid chromatography. *The Journal of pharmacology and experimental therapeutics* 206(1), 158-166 (1978).

35. Musshoff F, Daldrup T, Bonte W, Leitner A, Lesch OM: Formaldehyde-derived tetrahydroisoquinolines and tetrahydro-beta-carbolines in human urine. *Journal of chromatography. B, Biomedical applications* 683(2), 163-176 (1996).

36. Rimon R, Airaksinen MM, Kari I *et al.*: Pinoline, a beta-carboline derivative in the serum and cerebrospinal fluid of patients with schizophrenia. *Annals of clinical research* 16(3), 171-175 (1984).

37. Pähkla R, Rägo L: Pinoline: formation, distribution and effects. In: Melatonin in the promotion of health. CRC Press Florida, 165-166 (1999).

3.7 Tables and Figures

Table 3.1 Multiple reaction monitoring ion transitions and retention times for indolethylamine analytes

Compound	Retention Time (min)	Parent ion *m/z*	Product ion *m/z*	Cone (V)	CE (V)
5-MeO-DMT	7.28	219.2	174.1	6	12
			58.0	6	10
5-MT	7.26	191.0	174.1	22	10
			159.1	30	18
			130.2	30	30
Pinoline	7.42	203.0	174.1	26	10
			131.0	26	28
d_4-5-MT	7.22	195.1	178.1	20	10
Bufotenine	4.98	205.1	160.0	16	12
			58.0	18	10
Serotonin	4.61	177.1	160.1	60	8
			115.0	60	22
d_4-serotonin	4.58	181.1	164.1	60	8

5-MeO-DMT, 5-methoxy-*N*,*N*-dimethyltryptamine
5-MT, 5-methoxytryptamine
CE, collision energy

Table 3.2 Indolethylamine calibration curve and quality control final sample concentrations

Calibration Point	5-MeO-DMT (pg/mL)	5-MT (ng/mL)	Pinoline (pg/mL)	Bufotenine (pg/mL)	Serotonin (ng/mL)
Cal 1	0.0	0.0	0.0	0.0	0.0
Cal 2	1.17	1.56	0.781	1.95	9.77
Cal 3	2.34	3.13	1.56	3.91	19.5
Cal 4	4.69	6.25	3.13	7.81	39.1
Cal 5	9.38	12.5	6.25	15.6	78.1
Cal 6	18.8	25.0	12.5	31.3	156
Cal 7	37.5	50.0	25.0	62.5	313
Cal 8	75.0	100	50.0	125	625
Cal 9	150	200	100	250	1250
Cal 10	300	400	200	500	2500
Low QC	20.0	20.0	10.0	50.0	200
High QC	100	150	100	200	1000

5-MeO-DMT, 5-methoxy-*N*,*N*-dimethyltryptamine
5-MT, 5-methoxytryptamine

Table 3.3 Assessment of extraction and recovery of indolethylamines from blank and spiked matrices (synthetic urine and human urine) as compared to a neat solution of the analyte

	5-MeO-DMT	5MT	Pinoline	d_4-5-MT	Bufotenine	Serotonin
Filter						
Blank Synthetic Urine	--	--	--	--	--	1%
Blank Urine	--	--	--	--	--	14%
Spiked Synthetic Urine	106%	50%	53%	56%	73%	94%
Spiked Urine	12%	11%	9%	6%	3%	43%
Error between spiked	**800%**	**340%**	**520%**	**860%**	**2400%**	**120%**
Protein Precipitation						
Blank Synthetic Urine	--	--	--	--	--	1%
Blank Urine	--	--	--	--	--	13%
Spiked Synthetic Urine	106%	50%	61%	64%	96%	58%
Spiked Urine	14%	14%	12%	7%	3%	34%
Error between spiked	**660%**	**260%**	**390%**	**820%**	**3200%**	**70%**
MTBE LLE						
Blank Synthetic Urine	--	--	--	--	--	2%
Blank Urine	--	--	--	--	--	1%
Spiked Synthetic Urine	2%	--	--	--	--	1%
Spiked Urine	1%	--	--	--	--	1%
Error between spiked	**nc**	**nc**	**nc**	**nc**	**nc**	**nc**
Ethyl acetate LLE						
Blank Synthetic Urine	--	--	--	--	--	2%
Blank Urine	--	1%	--	--	--	2%
Spiked Synthetic Urine	--	--	--	--	--	1%
Spiked Urine	9%	8%	7%	5%	1%	2%
Error between spiked	**nc**	**nc**	**nc**	**nc**	**nc**	**nc**
Hexane LLE						
Blank Synthetic Urine	--	--	--	--	--	1%
Blank Urine	--	--	--	--	--	1%
Spiked Synthetic Urine	--	--	--	--	--	1%
Spiked Urine	--	--	--	--	--	1%
Error between spiked	**nc**	**nc**	**nc**	**nc**	**nc**	**nc**
Solid phase extraction						
Blank Synthetic Urine	--	--	--	--	--	4%
Blank Urine	--	--	--	--	--	6%
Spiked Synthetic Urine	59%	24%	64%	10%	7%	6%
Spiked Urine	58%	33%	67%	10%	8%	11%
Error between spiked	**1%**	**27%**	**4%**	**0%**	**12%**	**45%**

--, not detected
nc, not calculated
LLE, liquid-liquid extraction
MTBE, methyl tert-butyl ether

Table 3.4 Indolethylamine peak area ratios and variability using different solid phase extraction barrel capacities and sample volumes. Reported as mean ± standard deviation of triplicate measurements.

Conditions	Urine Volume	5-MeO-DMT PAR ± SD	5-MeO-DMT %RSD	5-MT PAR ± SD	5-MT %RSD	Pinoline PAR ± SD	Pinoline %RSD	Bufotenine PAR ± SD	Bufotenine %RSD	Serotonin PAR ± SD	Serotonin %RSD
Spiked synthetic urine											
3 cc	2.5 mL	35 ± 13	37	2.1 ± 0.91	44	2.3 ± 0.95	41	1.7 ± 0.25	14	6.4 ± 0.67	10
3 cc	5 mL	40 ± 25	63	3.0 ± 1.8	60	2.5 ± 1.6	62	3.1 ± 1.3	41	7.0 ± 2.1	30
6 cc	5 mL	4.6 ± 1.9	42	0.32 ± 0.07	24	0.17 ± 0.06	35	0.56 ± 0.09	16	3.8 ± 0.67	17
Blank urine											
3 cc	2.5 mL	4.4 ± 0.44	10	0.51 ± 0.01	2.9	0.13 ± 0.00	3.1	0.21 ± 0.01	6.1	2.5 ± 0.21	8.5
3 cc	5 mL	3.2 ± 0.23	7.2	0.47 ± 0.08	17	0.21 ± 0.02	8.1	0.01 ± 0.01	89	2.1 ± 0.14	6.6
6 cc	5 mL	3.1 ± 0.05	1.5	0.49 ± 0.03	5.7	0.24 ± 0.01	3.1	0.02 ± 0.00	19	2.3 ± 0.16	6.9

5-MeO-DMT, 5-methoxy-*N*,*N*-dimethyltryptamine
5-MT, 5-methoxytryptamine
PAR, mean peak area ratio (compound/d_4-5-MT)
%RSD, percent relative standard deviation

Table 3.5 Sample preparation reproducibility as determined by peak areas of analytes in spiked synthetic urine (n = 4) and spiked urine (n = 5) cycled for repeated injections

	5-MeO-DMT		**5-MT**		**Pinoline**		**d_4-5-MT**		**Bufotenine**		**Serotonin**		**d_4-Serotonin**	
Cycle	PA	%RSD	PA	%RSD	PA	%RSD	PA	%RSD	PA	%RSD	PA	%RSD	PA	%RSD
Spiked Synthetic Urine*														
1	492 ± 47	9.6	70 ± 18	25	9.1 ± 3.5	38	51 ± 14	28	25 ± 4.2	17	291 ± 57	20	57 ± 14	24
2	458 ± 39	8.6	63 ± 18	28	8.9 ± 3.9	44	49 ± 12	24	20 ± 3.3	16	286 ± 70	25	52 ± 11	22
3	431 ± 25	5.9	63 ± 16	25	8.7 ± 3.6	41	49 ± 12	24	19 ± 2.5	13	268 ± 57	21	47 ± 10	20
4	391 ± 18	4.5	62 ± 16	25	4.8 ± 0.4	8.3	45 ± 13	29	16 ± 1.8	11	228 ± 49	21	44 ± 13	29
5	362 ± 19	5.2	63 ± 15	24	5.2 ± 1	19	46 ± 11	24	14 ± 2.1	15	186 ± 48	26	36 ± 8	22
Mean %RSD		**6.8**		**26**		**30**		**26**		**15**		**23**		**24**
Spiked Urine														
1	489 ± 28	5.8	125 ± 25	20	2.2 ± 0.6	27	101 ± 21	20	29 ± 2.1	7.1	296 ± 33	11	47 ± 4.9	10
2	455 ± 13	2.9	114 ± 23	21	2.0 ± 0.5	27	98 ± 15	16	28 ± 2.8	10	284 ± 34	12	45 ± 1.8	4.1
3	449 ± 10	2.1	111 ± 23	21	2.1 ± 0.5	23	95 ± 14	15	25 ± 1.7	6.9	266 ± 32	12	44 ± 4.4	10
4	423 ± 16	3.7	110 ± 21	19	2.2 ± 0.6	28	97 ± 18	19	22 ± 2.5	12	248 ± 27	11	37 ± 2.7	7.2
Mean %RSD		**3.6**		**20**		**26**		**17**		**8.9**		**12**		**7.9**

* Only samples 1 through 4 included in each cycle; one sample was excluded.
5-MeO-DMT, 5-methoxy-*N*,*N*-dimethyltryptamine
5-MT, 5-methoxytryptamine
PA, peak areas (x 10^3) are reported as mean ± standard deviation
%RSD, percent relative standard deviation

Table 3.6 Analytical reproducibility as assessed by peak areas of analytes in spiked synthetic urine (n = 4) and spiked urine (n = 5) samples injected five times

	5-MeO-DMT		**5-MT**		**Pinoline**		**d_4-5-MT**		**Bufotenine**		**Serotonin**		**d_4-Serotonin**	
Sample	PA	%RSD	PA	%RSD	PA	%RSD	PA	%RSD	PA	%RSD	PA	%RSD	PA	%RSD
Spiked Synthetic Urine														
1	512 ± 74	14	67 ± 5.0	7.5	8.6 ± 3.8	44	50 ± 4.3	8.6	18 ± 5.5	30	197 ± 51	26	37 ± 10	26
2	569 ± 84	15	82 ± 3.8	4.7	9.8 ± 3.6	37	60 ± 3.0	5.0	22 ± 5.0	22	293 ± 52	18	54 ± 12	23
3	534 ± 62	12	67 ± 3.1	4.6	6.5 ± 1.2	18	51 ± 2.1	4.2	18 ± 3.9	21	305 ± 54	18	58 ± 9.0	15
4	519 ± 43	8.2	42 ± 2.6	6.2	4.5 ± 0.3	7.5	31 ± 2.6	8.5	17 ± 2.2	13	213 ± 24	11	39 ± 2.2	5.8
Mean %RSD		**12**		**5.7**		**27**		**6.6**		**22**		**18**		**18**
Spiked Urine														
1	461 ± 35	7.7	134 ± 9.6	7.2	3.0 ± 0.1	2.8	114 ± 7.4	6.5	25 ± 4.8	19	304 ± 26	8.4	43 ± 6.7	16
2	441 ± 32	7.4	113 ± 7.0	6.2	1.7 ± 0.1	8.1	103 ± 3.1	3.0	27 ± 3.4	13	287 ± 19	6.5	46 ± 6.5	14
3	439 ± 11	2.6	102 ± 5.7	5.6	1.7 ± 0.1	4.8	88 ± 1.8	2.1	25 ± 2.2	8.8	277 ± 10	3.8	43 ± 3.0	6.8
4	466 ± 29	6.3	86 ± 5.4	6.4	2.3 ± 0.2	10	73 ± 2.8	3.8	29 ± 4.0	14	229 ± 13	5.5	39 ± 2.8	7.0
5	463 ± 35	7.6	142 ± 7.4	5.2	2.0 ± 0.3	16	110 ± 5.6	5.0	23 ± 3.5	15	270 ± 46	17	44 ± 4.7	11
Mean %RSD		**6.3**		**6.1**		**8.4**		**4.1**		**14**		**8.3**		**11**

5-MeO-DMT, 5-methoxy-*N*,*N*-dimethyltryptamine
5-MT, 5-methoxytryptamine
PA, peak areas (x 10^3) are reported as mean ± standard deviation
%RSD, percent relative standard deviation

Table 3.7 Low and high calibration curve ranges, lower quantitation limits and percent error for each calibration curve point and low and high QC samples

Calibration Curve	5-MeO-DMT	5-MT	Pinoline	Bufotenine	Serotonin
Lower range (ng/mL)	0 - 0.075	0 - 6.25	--	0 - 0.016	0 - 625
Higher range (ng/mL)	0.075 - 0.30	6.25 - 400	0 - 0.20	0.016 - 0.50	625 - 2500
LLOQ (ng/mL)	0.0047	3.13	0.013	0.0039	20
Percent error calculations					
Cal 1	--	--	--	--	--
Cal 2	61	24	820	60	58
Cal 3	28	1.6	560	2.8	4.6
Cal 4	8.3	1.9	240	14	9.8
Cal 5	15	14	140	2.5	3.3
Cal 6	5.0	25	4.0	18	12
Cal 7	1.0	7.3	8.0	2.8	16
Cal 8	0.8	12	3.3	0.68	3.5
Cal 9	4.7	17	17	0.14	2.6
Cal 10	0.78	3.6	3.8	0.07	0.4
Low QC	20	9	150	4.1	17
High QC	66	20	17	12	14

5-MeO-DMT, 5-methoxy-*N*,*N*-dimethyltryptamine
5-MT, 5-methoxytryptamine
QC, quality control
LLOQ, lower limit of quantitation

Table 3.8 Indolethylamine concentrations in two urine samples

Urine Sample	5-MeO-DMT (ng/mL)	5-MT (ng/mL)	Pinoline (ng/mL)	Bufotenine (ng/mL)	Serotonin (ng/mL)
1	< LLOD	135	< LLOD	< LLOQ	102
2	< LLOD	29.1	< LLOD	< LLOQ	106

5-MeO-DMT, 5-methoxy-*N*,*N*-dimethyltryptamine
5-MT, 5-methoxytryptamine
LLOD, lower limit of detection
LLOQ, lower limit of quantification

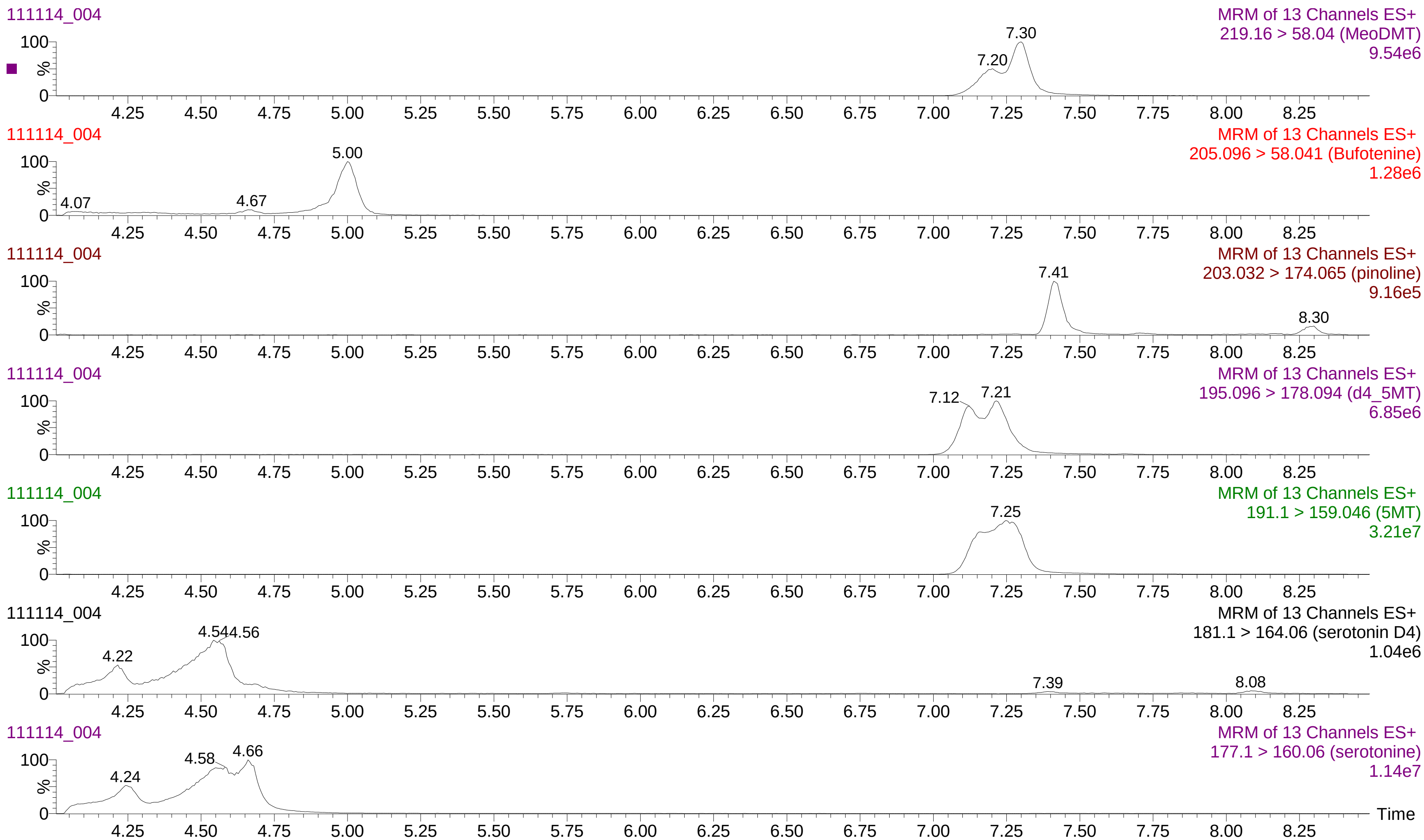

Figure 3.1 Representative chromatograms of a neat sample reconstituted in 50:50 water:methanol (10 µL injection). Analyte concentrations are listed in the Materials and Methods. Abbreviations: 5-MeO-DMT, 5-methoxy-*N*,*N*-dimethyltryptamine; 5-MT, 5-methoxytryptamine

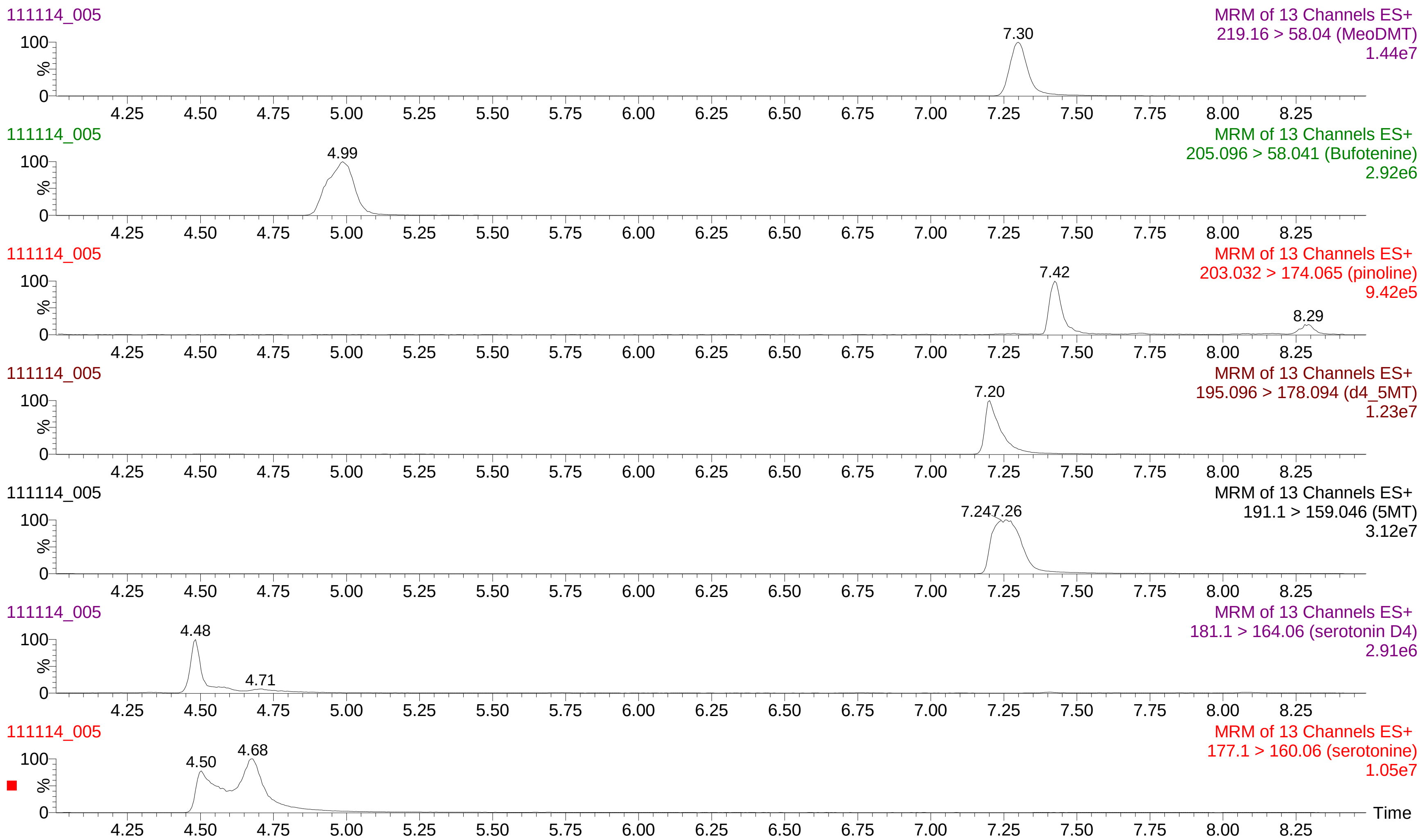

Figure 3.2 Representative chromatograms of a neat sample reconstituted in 75:25 water:methanol (10 µL injection). Analyte concentrations are listed in the Materials and Methods. Abbreviations: 5-MeO-DMT, 5-methoxy-*N*,*N*-dimethyltryptamine; 5-MT, 5-methoxytryptamine

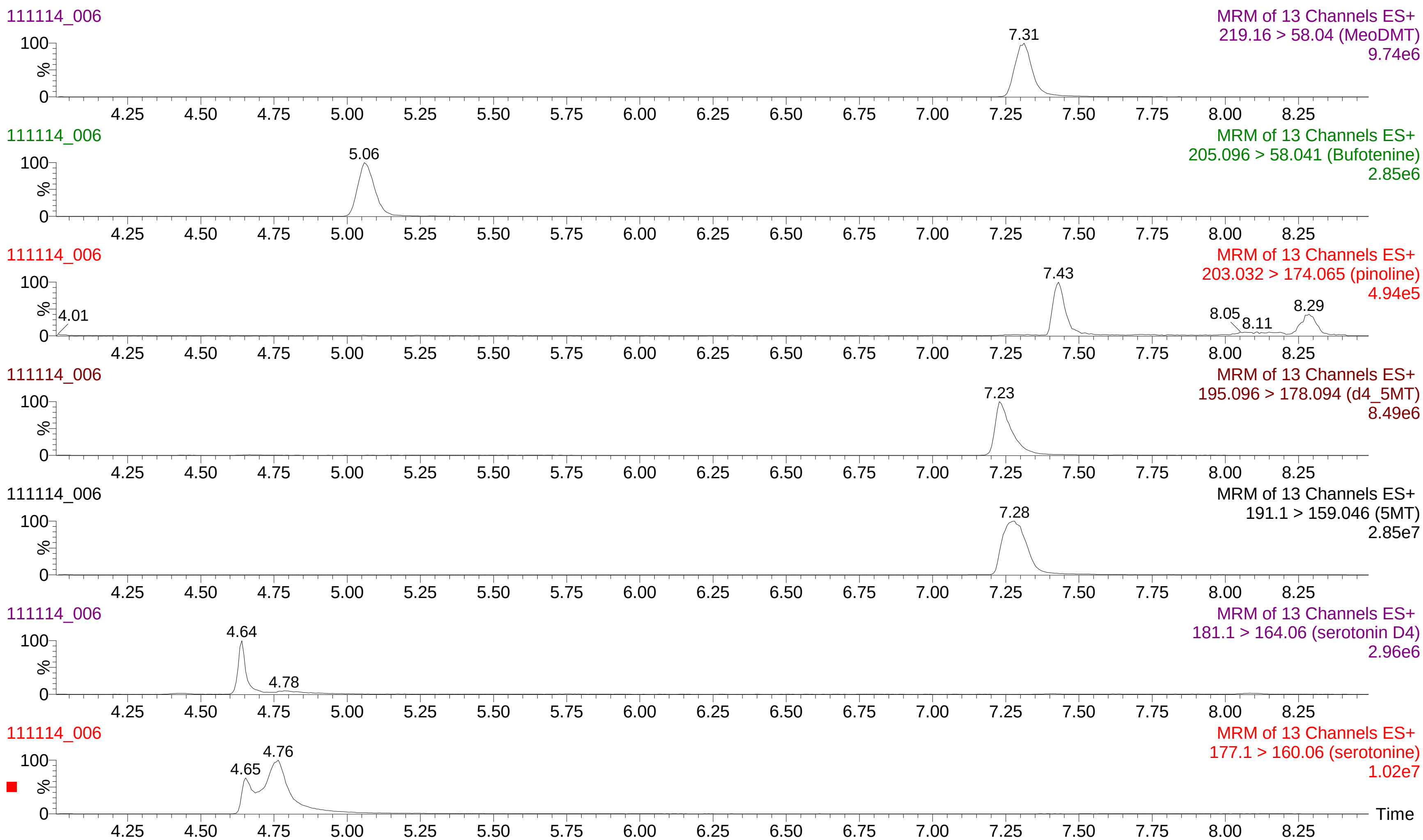

Figure 3.3 Representative chromatograms of a neat sample reconstituted in 87:13 water:methanol (2-fold dilution injected at 10 µL). Analyte concentrations are listed in the Materials and Methods. Abbreviations: 5-MeO-DMT, 5-methoxy-*N*,*N*-dimethyltryptamine; 5-MT, 5-methoxytryptamine

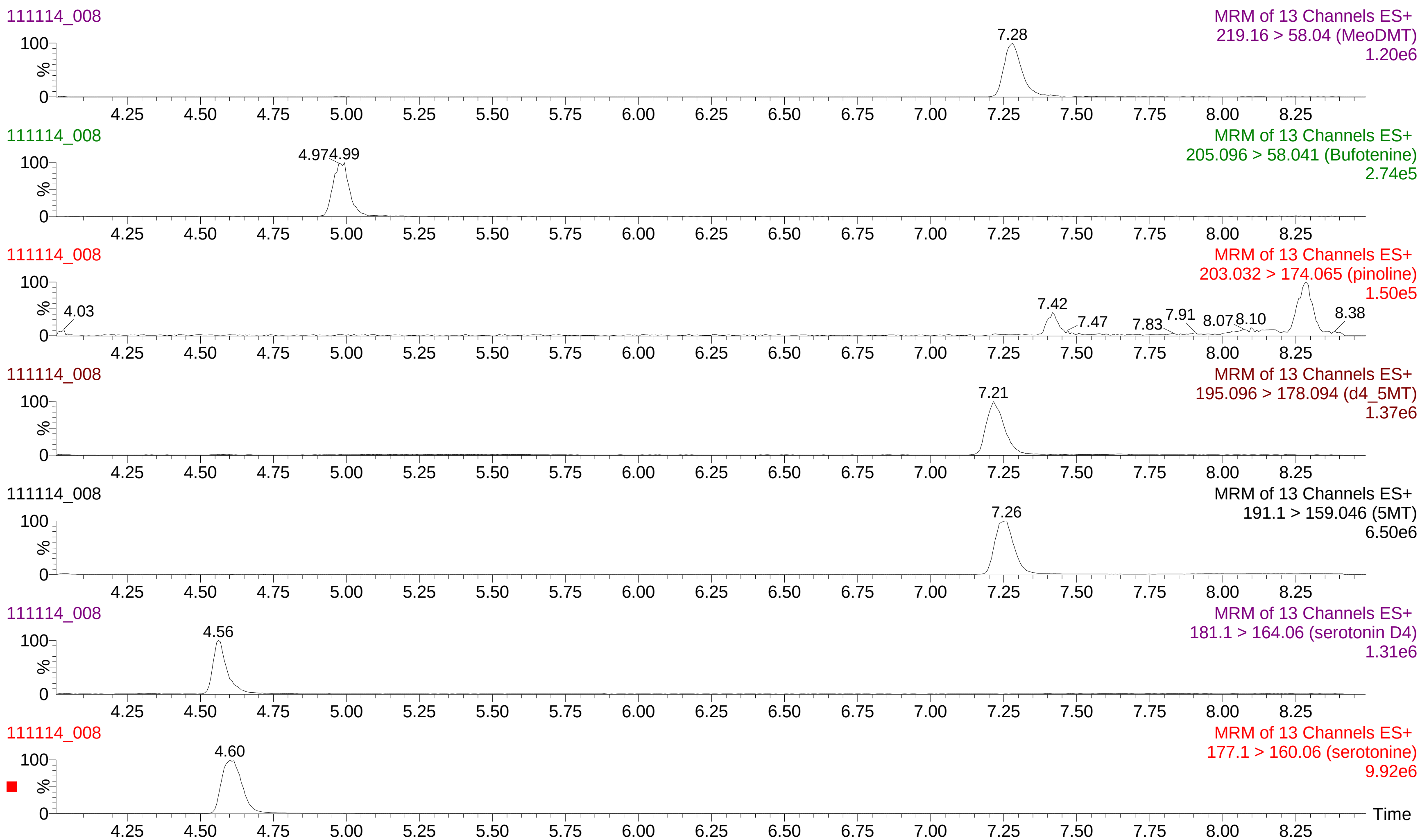

Figure 3.4 Representative chromatograms of a neat sample reconstituted in 75:25 water:methanol (2-fold dilution injected at 1 µL). Analyte concentrations are listed in the Materials and Methods. Abbreviations: 5-MeO-DMT, 5-methoxy-*N*,*N*-dimethyltryptamine; 5-MT, 5-methoxytryptamine

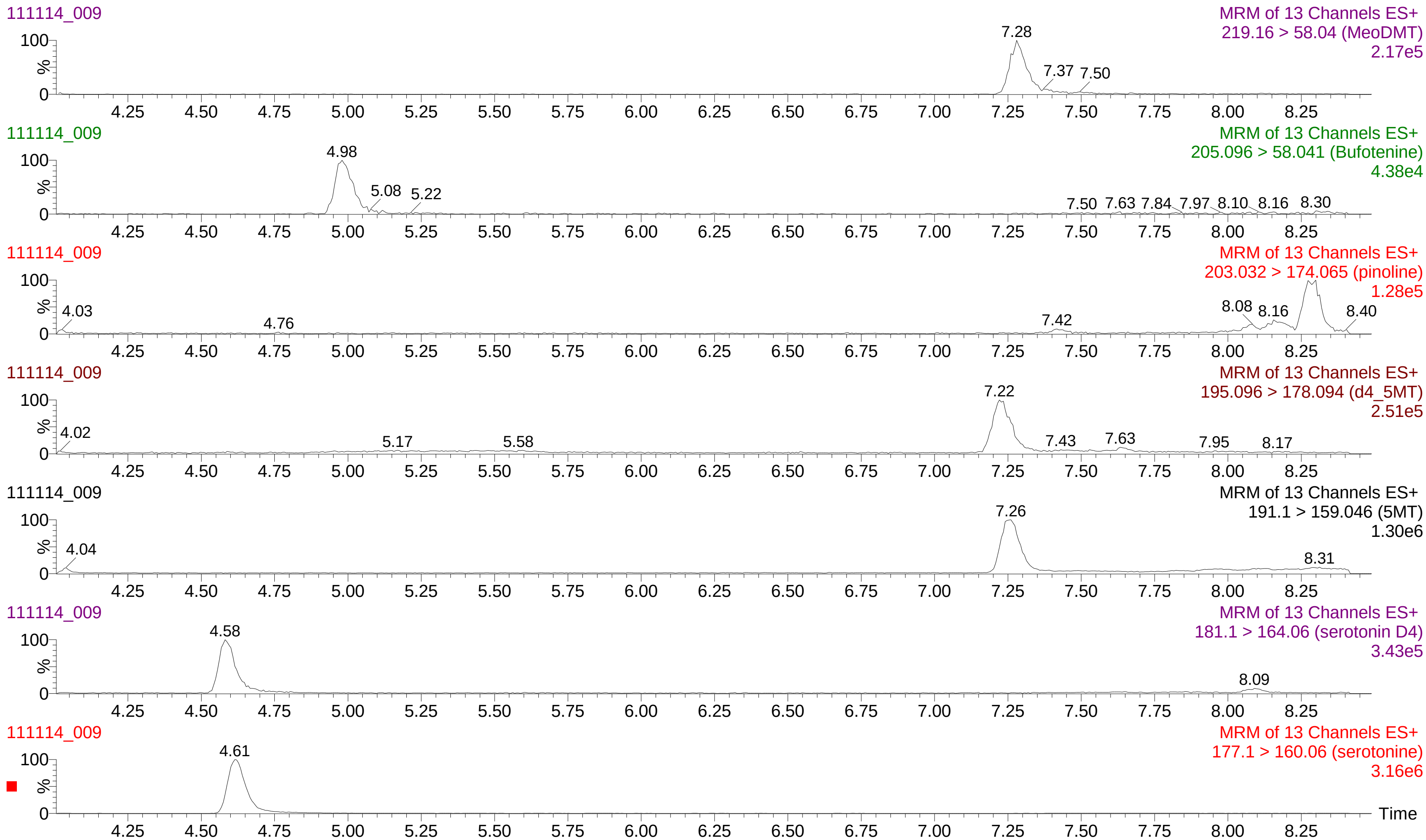

Figure 3.5 Representative chromatograms of a neat sample reconstituted in 99:1 water:methanol (100-fold dilution injected at 10 μL). Analyte concentrations are listed in the Materials and Methods. Abbreviations: 5-MeO-DMT, 5-methoxy-*N*,*N*-dimethyltryptamine; 5-MT, 5-methoxytryptamine

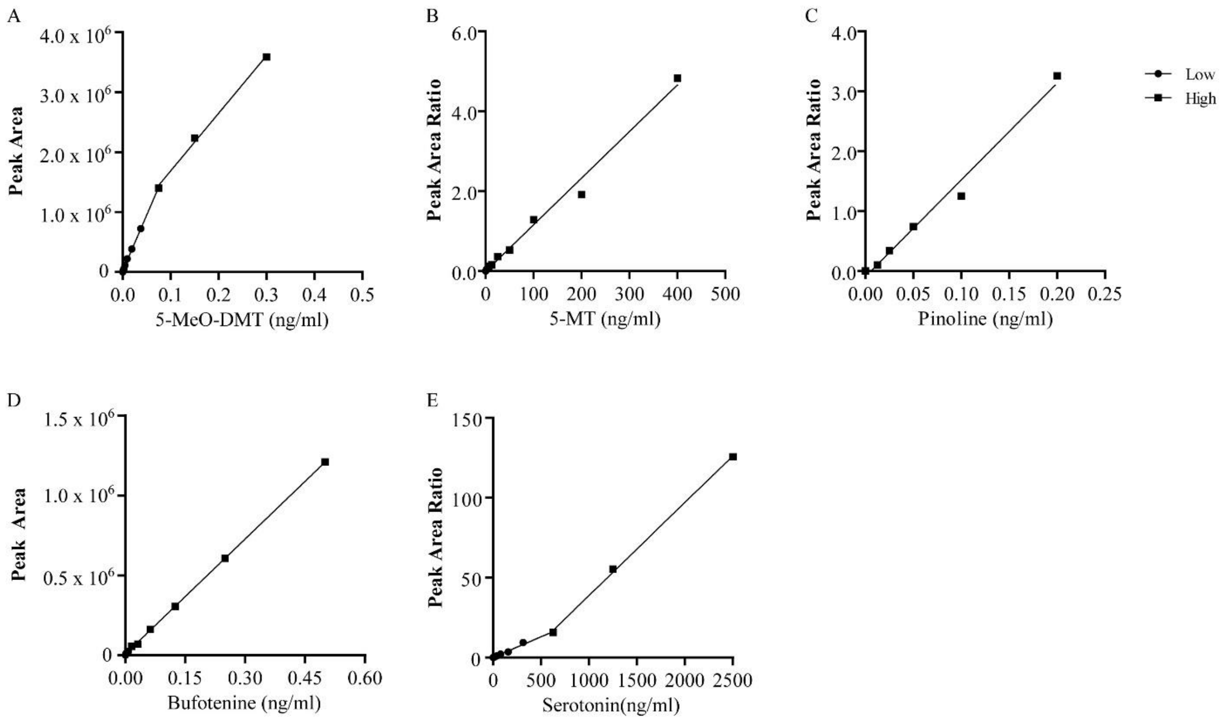

Figure 3.6 Low and high calibration curves for A) 5-methoxy-*N*,*N*-dimethyltryptamine (5-MeO-DMT) , B) 5-methoxytryptamine (5-MT), C) pinoline, D) bufotenine and E) serotonin.

Chapter 4. Detection of an Endogenous Urinary Biomarker Associated with CYP2D6 Activity Using Global Metabolomics

Jessica Tay-Sontheimer[1], Laura M. Shireman[1], Richard P. Beyer[2], Taurence Senn[1], Daniela Witten[3], Robin E. Pearce[4], Andrea Gaedigk[4,5], Cletus Lesia Gana Fomban[1], Justin D. Lutz[1], Nina Isoherranen[1], Kenneth E. Thummel[1], Oliver Fiehn[6], J. Steven Leeder[4,5] and Yvonne S. Lin[1]

[1]Department of Pharmaceutics, [2]Center for Ecogenetics and Environmental Health, and [3]Department of Biostatistics, University of Washington, Seattle, WA, USA; [4]Division of Clinical Pharmacology, Toxicology & Therapeutic Innovation, Children's Mercy Hospitals and Clinics, Kansas City, MO, USA; [5]Department of Pediatrics, University of Missouri-Kansas City, Kansas City, MO, USA and [6]UC Davis Genome Center, University of California Davis, Davis, CA, USA

This chapter has been published in its entirety in Pharmacogenetics 15 (16), 1947-1962, (2014).

4.1 Introduction

In various pediatric populations, a substantial percentage (10 to 65%) [1] of drugs are prescribed off-label, primarily because of lack of study information in this age group [2]. Although the number of drugs with *some* pediatric dosing information doubled from 22% in 1975 to 41% in 2009 [3], available information remains inadequate to provide effective safety and dosing guidances for all pediatric age groups. Studies conducted in the past two decades show major deficiencies with pediatric dosing methods built on allometry [4-8]. Optimal drug safety and efficacy in this vulnerable population requires an increased understanding of the impacts of physiological maturation and genetic variation on drug-metabolizing enzymes [9-11]. One such enzyme, cytochrome P450 2D6 (CYP2D6), participates in the elimination of approximately 15% of clinically used drugs metabolized by cytochrome P450s [12], including antipsychotics and antidepressants, beta-blockers, opioid analgesics [13, 14], and the antitussive dextromethorphan (DM) [15].

CYP2D6 activity is determined, in significant part, by genetic variation. More than 100 allelic variants and sub-variants of this highly polymorphic enzyme are defined (http://www.cypalleles.ki.se/cyp2d6.htm), including gene deletions and, non-functional, reduced-function, and multiple-copy-number alleles [16, 17]. The various allele combinations result in a continuum from little or no activity and poor metabolizer (PM) phenotype, reduced function and intermediate metabolizer phenotype, “wild-type” activity and extensive metabolizer phenotype, and, in the case of gene duplications, increased CYP2D6 expression and ultra-rapid metabolizer phenotype [17-19]. Gaedigk et al. proposed using these genetic factors to predict individual *CYP2D6* activity scores [18, 20].

Substantial interindividual variation in CYP2D6 activity exists within each category of CYP2D6 phenotype [20-22]. Factors such as ontogeny, drug-drug interactions (DDIs), diet and disease may contribute to patient variation in drug disposition. Thus, phenotyping may be necessary to determine CYP2D6 activity when personalizing drug therapy [23] or evaluating DDIs [24]. Traditional phenotyping studies involve the administration of a probe drug or drug cocktail. The administration of such drugs to children, pregnant women and the elderly may be a concern.

Phenotyping using endogenous biomarkers is an alternative method of assessing CYP2D6 activity that may eliminate risks of exogenous drug administration in CYP2D6 DDI studies or when evaluating altered activity in special patient populations. Additionally, retrospective analyses of banked samples may be conducted without prior knowledge of an individual's CYP2D6 phenotype. If biomarker measurements from a spot urine sample could be used, that could eliminate the need for prolonged clinical visits in which the patient must provide timed sample collections. For example, CYP2D6 activity can be measured using a four-hour urine collection following dextromethorphan administration. Several endogenous substrates have been proposed as CYP2D6 substrates. They include 5-methoxy-*N*,*N*-dimethyltryptamine [25], pinoline [26], progesterone [27], anandamide [28, 29], and a number of compounds up- or down-regulated in CYP2D6-transgenic mice [30]. However, the identification and validation of endogenous biomarkers for CYP2D6 phenotyping, particularly in humans, is immature.

The goal of this study was to discover endogenous biomarkers of CYP2D6 activity. Children were phenotyped for CYP2D6 activity using a urinary dextromethorphan-to-dextrorphan metabolic ratio (DM/DX) [20, 31], and a global metabolomics approach was used to detect endogenous, urinary metabolites capable of predicting DM/DX in a pediatric training set group. A targeted analytical approach was used to further analyze the relationship between a candidate biomarker and CYP2D6 activity, and these results were validated in urine from a second group of children. Furthermore, the change in metabolite levels and CYP2D6 activity was assessed in adults during CYP2D6 inhibition.

4.2 Patients & Methods

4.2.1 *Subjects*

Healthy pediatric subjects (N = 189) between 6 to 15 years of age on the date of study enrollment were recruited at Children's Mercy Hospitals and Clinics (CMH), Kansas City, MO for a longitudinal study of CYP2D6 activity. Results from the first study visit are presented. Following an overnight fast, subjects received a single oral 0.5 mg/kg dose of DM (Robitussin® Pediatric). Urine was collected predose (spot sample) and throughout the next 4 hours following DM administration (timed sample). Samples were stored at -80°C until analysis. Subjects were randomized into training and validation sets based on their CYP2D6 phenotype (PM or non-PM) so there was equal representation between the two sets.

Studies were approved by the Institutional Review Boards at CMH and the University of Washington, Seattle, WA. The study population was slightly skewed towards males due to an additional study aim to recruit children diagnosed with attention deficit hyperactivity disorder (ADHD), an aim not explored here. Exclusion criteria included: i) current therapy with medications metabolized by or known to inhibit CYP2D6 (although atomoxetine was permitted for the ADHD component of the overall study); ii) inability or unwillingness to fast 4 hours prior to the study session; iii) existence of diagnoses that may influence absorption and gastric emptying, such as reflux, inflammatory bowel disease, or Crohn’s disease; iv) a demonstrated adverse reaction to previous dextromethorphan exposure; v) impaired hepatic or renal activity, or physical examination as determined by pediatrician sub-investigator's discretion; vi) pregnancy; vii) body-mass index (BMI) <5th or > 95th percentile. Subjects were given a complete medical examination including assessment of Tanner stage and blood samples were taken for liver function testing and DNA testing at the screening visit.

Ten healthy adults (5 females and 5 males) were enrolled in a study to evaluate the complex DDI of fluoxetine on CYP2D6, CYP3A4, and CYP2C19 activities. A detailed description of the study design, demographics, and results has been reported elsewhere [24]. All subjects included in the study were genotypic *CYP2D6* extensive metabolizers. Each subject was given an oral probe drug cocktail, which included 30 mg DM, at baseline (day 1) and during a two-week multiple-dose fluoxetine treatment (day 16). Urine was collected 0-12 and 12-24 hours on days 1-4 and 16-19. Secondary use of the samples in this study was approved by the University of Washington Human Subjects Review Board.

4.2.2 *Genotype analysis and assignment of activity score of pediatric subjects*

CYP2D6 genotype analysis of greater than 20 allelic variants was performed at Children's Mercy Hospitals and Clinics. Genomic DNA was isolated from whole blood with a QIAamp DNA Blood Mini kit (Qiagen, Valencia, CA). Genotype analysis was performed using long-range (XL) PCR coupled with commercially available TaqMan (Life Technologies, Carlsbad, CA) and restriction fragment length polymorphism (RFLP) assays. The following allelic variants were assessed: *CYP2D6*2, *3, *4, *5* (gene deletion), **6, *7, *9, *10, *11, *12, *13* (*2D7/6* hybrid genes), **15, *17, *29, *31, *35, *36, *41, *42, *45* or **46* and **59*. Analysis included XL-PCR-based detection of gene deletions, duplications/multiplications and *CYP2D7/6* hybrid gene arrangements. Gene duplications were characterized for their allelic variation (**1xN, *2xN, *4xN*, etc.) and gene copy number assessed at four gene loci by quantitative multiplex PCR. Additional XL-PCR testing in conjunction with DNA sequencing was applied to resolve complex cases or cases with ambiguous results.

Genotyping procedures and assignment of CYP2D6 activity scores have been described previously [20, 32-35]. Non-functional, reduced function, fully functional and gain-of-function *CYP2D6* alleles were given values of 0, 0.5, 1 and 1.5, respectively; alleles with duplications received double the value assigned to the single counterparts. The CYP2D6 activity score was obtained by summing the two alleles for each individual.

4.2.3 *Analysis of dextromethorphan (DM) and metabolites*

Pediatric urine samples were analyzed for dextromethorphan and its metabolites at Children's Mercy Hospitals and Clinics [36]. Briefly, urine samples were adjusted to a pH of 4.5 to 5.0 and subsequently incubated with β-glucuronidase at 37°C overnight prior to analysis. Concentrations of dextromethorphan (DM) and total deconjugated dextrorphan (DX) were determined using reverse-phase high-performance liquid chromatography (HPLC) with fluorescence detection. The urinary dextromethorphan metabolic ratio was calculated as the molar ratio of DM/DX. Urine samples were analyzed for DM and total dextrorphan concentrations. Based on the DM metabolic ratio (DM/DX), subjects were assigned to PM (DM/DX $\geq$ 0.3) or non-PM phenotypes (DM/DX < 0.3) as described previously [20, 31]. Analytical details for the urinary analysis of DM and its metabolites in the adult study are described by Sager et al. [24].

4.2.4 *Determination of creatinine concentrations*

Creatinine was quantified on an Agilent 1100 series HPLC in line with an Agilent 1050 series UV detector set to monitor absorbance at 234 nm. Urine was diluted 100-fold with 10 mM potassium phosphate buffer, pH 6.5, and 10 μL were injected onto a Waters Symmetry C18 5 μm, 4.6 x 1.5 mm, 300 Å analytical column using 10 mM potassium phosphate buffer, pH 6.5, with 0.1% acetonitrile for mobile phase A and 100% acetonitrile for mobile phase B. The flow rate was 0.5 mL/min with a linear gradient consisting of 0% B until 5 min, a linear increase to 100% B from 5.0 min until 5.5 min, 100% B until 6.5 min, a linear decrease to 0% B from 6.5 to 7 min, and re-equilibration with 0% B for 8 min.

4.2.5 *Global metabolomics analysis of pediatric training set by LC-QTOF*

Samples were prepared for metabolomics analysis by adding 800 μL of ice-cold acetonitrile to 200 μL of urine to precipitate proteins. Following centrifugation (20,000 x G for 10 min, 4°C), the supernatant was evaporated under nitrogen gas. The resulting residue was reconstituted in 40 μL of methanol followed by 40 μL of 0.4% (v/v) acetic acid.

Global metabolomic analyses of samples were performed using an Agilent (Santa Clara, CA) 1200 HPLC coupled to an Agilent 6520 LC-QTOF mass spectrometer. Samples (2 μL injection) were separated chromatographically using a 3.5 μm, 2.1 x 30 mm Agilent Zorbax SB-C8 guard column and a 1.8 μm, 2.1 x 50 mm Agilent Zorbax SB-Aq analytical column heated to 60°C. The flow rate was 0.6 mL/min, and the mobile phase consisted of A: 0.2% acetic acid in water and B: 0.2% acetic acid in methanol utilizing the following gradient profile: 2% to 98% B in 13 min, 98% B until 19 min followed by re-equilibration for 6.5 min. The source temperature was maintained at 350°C with a nitrogen gas flow rate of 12 L/min and a capillary voltage of 3500 V. Scans were obtained between *m/z* 100 and 1000 at an acquisition rate of 3 spectra/sec. Data were collected in centroid mode for ESI+ and ESI- modes.

4.2.6 *Global metabolomics data processing and statistical analysis*

For the pediatric training set, raw LC-QTOF mass spectral data from each ionization mode were aligned using the Bioconductor R-package XCMS [37, 38]. Raw data files were exported to mzData format using MassHunter Qualitative Analysis (Agilent, B.05.00) with a minimum peak height of 1000 counts. Feature detection was performed using the Bioconductor R-package XCMS [37, 38]. Peak picking was performed using the centWave algorithm, requiring within-peak m/z deviations of less than 15 ppm, 5 consecutive scans above 500 counts, and peak widths between 4 and 12 seconds. The default peak integration method was used, and the peaks were fit to a Gaussian shape with a Mexican-hat wavelet for integration. The peaks were grouped using the “density” method with a mass accuracy requirement of 0.007 m/z and a peak width at half height of 4 (before retention time correction) or 2 (after retention time correction) seconds. A retention time correction was performed using the method “obiwarp”, and peaks were recursively filled. Subsequently, ion signals were normalized to the sum of all mass feature abundances in that sample as a surrogate marker for urine concentration, and finally log-transformed.

Statistical analyses were performed on each spot and timed dataset and ionization mode independently. Log-transformed DM/DX was regressed on each ion with no additional covariates. To account for possible dependencies among siblings and to avoid assuming homoscedasticity, we used a generalized estimating equation approach implemented in the R package “gee” (http://cran.r-project.org/web/packages/gee/index.html). P values were adjusted for multiple-hypothesis testing using the Benjamini-Hochberg method as implemented in the R stats package's p.adjust function. This methodology addresses the multiple hypothesis testing problem without using excessively conservative approaches to control the family-wise error, such as a Bonferroni correction. Adjusted *P*-values < 0.01 were considered to be significant.

4.2.7 *LC-QTOF spectral fragmentation*

Ions of interest were analyzed as described for global metabolomics except that the quadrupole selected the precursor ion and the TOF mass analyzer scanned product ions. Selected precursor ions (1.3 amu isolation width, 0.5 min allowable retention time shift) were fragmented at fixed collision energies of 10, 20, 40 and 80 V in ESI+ mode. The MS/MS scan rate was 4 spectra/sec.

4.2.8 *Database Queries*

For significant ions, we attempted to determine identities by querying major metabolomics databases using the accurate mass (within 20 ppm), and MS/MS fragmentation spectra or retention time, when available. Databases queried included the Scripps METLIN Metabolite Database [39] (http://metlin.scripps.edu), the Human Metabolome Database [40] (version 3.6, http://www.hmdb.ca) and in-house databases.

4.2.9 *Relative quantification of M1 by LC-QqQ*

MRM MS was performed on an Agilent 1290 Infinity HPLC coupled to an Agilent 6460 Triple Quadrupole (QqQ) to quantify the relative abundance of M1 in urine samples. A similar method as described for LC-QTOF was employed but with a shortened total run time of 6 min and a fixed collision energy of 40 V in ESI+ mode. We injected 5 μL and up to 15 μL for pediatric non-PM and PM samples, respectively. Two non-PM samples from the pediatric timed urine set were not analyzed due to insufficient sample volume. Peak areas for the mass transition of *m/z* 444.3 → 98.1 were divided by creatinine concentration (mM) to account for urine concentration differences. A value of 5, approximately the value of noise, was assigned to missing values. For the adult samples, creatinine normalized signals (*m/z* 444.3 → 98.1) for 0-12 and 12-24 hr urine samples from days 3-4 (without fluoxetine) and days 18-19 (with fluoxetine) were summed to obtain a composite 0-24 hr value.

4.2.10 *General statistical analyses*

GraphPad Prism (version 5.04, GraphPad Software, San Diego, CA) was used for general statistical analyses. Univariate regression was used to compare log (creatinine/M1) and log (DM/DX). Univariate regression was also used to model log M1 given creatinine, age, or urinary pH; and creatinine given age or urinary pH. A two-tailed t-test was used to determine whether log (DM/DX), log M1 or creatinine differed between genders. One-way analysis of variance (ANOVA) was used to determine the relationship between log (DM/DX) and Tanner stage or activity score, and to determine the relationship between log (creatinine/M1) and activity score. Spearman rank correlation was used to determine the relationship between log (DM/DX) and log (creatinine/M1) in adult subjects. $P < 0.05$ was considered significant.

4.3 **Results**

4.3.1 *Demographic characteristics of pediatric subjects*

Healthy pediatric volunteers (N=189), some of whom were related, were recruited for a longitudinal study of CYP2D6 activity. A spot urine sample was collected predose and a timed urine sample was collected from 0-4 hours after DM administration for determination of DM/DX. Based on DM/DX, 10 subjects were phenotypic CYP2D6 PMs and the remaining 179 were classified as non-PMs (intermediate, extensive or ultra-rapid metabolizers). PMs and non-PMs were randomly assigned to training or validation sets. Demographics for the training (n = 94, 5 PMs) and validation sets (n = 95, 5 PMs) are presented in Table 4-1. The subjects ranged from 7 to 16 years of age. Pubertal development was determined by the assignment of Tanner stage scores on a scale of 1 (pre-pubertal) to 5 or 6 (full maturation) for breast size and pubic hair, respectively. Log (DM/DX) did not differ by gender, age or measures of pubertal development (data not shown, manuscript in preparation). However, there was a negative correlation between log (DM/DX) and urinary pH ($P < 0.0001$, N=189).

4.3.2 *Selection of CYP2D6 endogenous biomarkers in pediatric subjects*

Identification of CYP2D6 biomarker candidates by global metabolomics in the pediatric training set. Spot and timed urine collection samples in the pediatric training set were analyzed by global metabolomic profiling using liquid chromatography quadrupole-time of flight (LC-QTOF) mass spectrometry (MS) in electrospray ionization positive (ESI+) and negative (ESI-) modes. Ions were aligned, normalized and log-transformed as described in Patients & Methods.

The LC-QTOF data contained 3839 and 2883 ions in ESI+ and ESI- modes, respectively. For selecting ions associated with CYP2D6 phenotype, a generalized-estimating equation approach was used to linearly regress log ion intensities against log (DM/DX). An independent correlation structure was used in this approach to account for subject relatedness. As summarized in Figure 4-1 and Table 4-2, in ESI+ data, one and six ions (Benjamini-Hochberg (BH) corrected P-value < 0.01) were found in the spot and timed urine samples, respectively; in ESI- data, eight ions (BH corrected $P < 0.01$) were observed in the timed urine samples. As listed in Table 4-2, some significant ions found only in timed urine samples are likely dextromethorphan metabolites, such as dextrorphan glucuronide and oxo-dextrorphan-glucuronide [41]. Significant ions found in both urine-collection time points would likely result in fewer false positives and would exclude DM metabolites. For these reasons, only significant ions found both before and after DM administration (spot and timed urine samples, respectively) were further investigated. One ESI+ ion with a *m/z* of 444.3102 and eluting at 6.5 min, which we will refer to as M1, was found to be significant in both spot and timed urine samples. We focused on this candidate biomarker in subsequent experiments. A negative correlation existed between M1 abundance and log (DM/DX) (Table 4-2) suggesting that it may be the product of a reaction catalyzed by CYP2D6.

Fragmentation of M1. Fragmentation of M1 in a representative urine sample at 20 V by LC-QTOF yielded the MS/MS spectrum shown in Figure 4-2a. The most abundant product ions were, in order of decreasing abundance, *m/z* 98.0964 > 370.2732 > 206.1883 > 56.0494 > 55.0550 > 150.1259 > 81.0692. Major metabolomics databases were queried for the potential identity of M1 based on the parent mass and product ions, but no matches were found.

4.3.3 *Association and validation of endogenous biomarkers with CYP2D6 activity in pediatric subjects*

Semi-quantitative analysis of M1 in pediatric training set samples. To improve sensitivity compared to the LC-QTOF method, we developed a targeted semi-quantitative LC-QqQ based assay. Using multiple-reaction monitoring (MRM), we monitored the mass transitions (precursor to product ions) of *m/z* 444.3 → 370.3, 444.3 → 206.2, 444.3 → 150.1, 444.3 → 98.1 and 444.3 → 56.1 (Figure 4-2b). The mass transition of *m/z* 444.3 → 98.1, the most abundant product ion, was selected to determine the relative abundance of M1 in the urine samples. All training set non-PM subjects analyzed had quantifiable levels of M1 in both spot and timed urine samples (Figure 4-2d). In contrast, M1 levels were undetectable in all but one timed PM sample, even with an injection volume 3-fold higher than that used for non-PM samples (Figure 4-2c). For reference, when urine with approximately the mean M1 abundance was diluted 264-fold, a peak was still visually observable (data not shown). In samples with undetectable M1 signals, a low value was assigned as the M1 abundance. M1 peak intensities were normalized by urinary creatinine concentration to account for differences in urine concentration for each sample. As M1 may be the product of a reaction catalyzed by CYP2D6, we expressed the ratio as creatinine/M1 to match the DM/DX, where the parent (DM) is normalized to the metabolite (DX). Compared to non-PM subjects, PM subjects had 105-fold higher DM/DX, and 123- and 147-fold higher creatinine/M1 ratios in spot and timed urine samples, respectively (Figure 4-3).

Confirmation of CYP2D6 biomarker candidate in the pediatric validation set. Similar results were found in the pediatric validation set. M1 abundance was undetectable in all PM subjects and a low value was assigned to M1 in these cases. A significant and positive relationship was observed between log (creatinine/M1) and log (DM/DX) in spot and timed urine samples (r^2

= 0.31 and 0.28, respectively; $P < 0.0001$ for each). Compared to non-PM subjects, PM subjects had 82-fold higher DM/DX and 167- and 120-fold higher creatinine/M1 ($P < 0.0001$) in spot and timed urine samples, respectively (Figure 4-4).

Relationship between CYP2D6 activity score and phenotypic activity as determined by DM/DX and M1 in pediatric subjects. Assigning an activity score to each child allowed us to group individuals by genotypes with comparable levels of function. In both the training and validation sets, 5% of the subjects had an activity score of 0 (PMs), 91-92% of the subjects had activity scores between 0.5 and 2 owing to the presence of partially or fully functional alleles and 3% of subjects had activity scores greater than 2. Despite the large interindividual variability observed in each activity score group, both DM/DX and creatinine/M1 differed among the activity score groups ($P < 0.0001$ for all sets, Figure 4-5).

4.3.4 *Biomarker response to CYP2D6 inhibition in adult subjects*

Effect of CYP2D6 inhibition on M1 in adult subjects. The ability of M1 to reflect alterations in CYP2D6 activity was tested in adults. As part of a DDI study, ten subjects received multiple doses of oral fluoxetine, a potent CYP2D6 inhibitor. Urine was collected before and during fluoxetine treatment. The urinary DM/DX increased 218-fold during fluoxetine treatment ($P < 0.0001$, Figure 4-6a) compared to baseline. Creatinine/M1 ratios were increased by 9.56-fold during the treatment phase ($P = 0.029$, Figure 4-6b). In addition, log (DM/DX) and log (creatinine/M1) were correlated (Spearman $r = 0.55$, $P = 0.012$; Figure 4-6c).

4.4 Discussion

To our knowledge, this is the first study using global metabolomics to identify endogenous biomarkers of CYP2D6 activity in humans. Using this approach, we obtained a list of unique ions (*m/z* and retention time) in urine samples from a cohort of pediatric subjects and selected the ion *m/z* 444.3102 (M1) from our ESI+ training set data because its abundance correlated significantly with DM/DX parent-to-metabolite ratios in both spot and timed urine samples in these subjects. We were unable to identify M1 based on the parent mass and product ion fragmentation spectra in metabolomics databases. By restricting our investigation to the ions present in both spot (predose) and timed (postdose) urine samples, DM and its metabolites were excluded as biomarker candidates. As expected, DM metabolites were significantly correlated with DM/DX in timed but not spot samples (Table 4-2). Additional significant ions that were present only in timed samples may be uncharacterized metabolites of DM.

The mass transition of M1 to the most abundant product ion (*m/z* 444.3 → 98.1) in ESI+ mode was monitored using a targeted approach on a QqQ instrument. In the pediatric training set, M1 was present in all non-PM individuals and absent in all but one PM individuals, even with increased injection volumes for PM subjects. Admittedly, the lower limit of detection of our targeted assay is unknown without a standard, but an M1 peak diluted over 250-fold below the mean training set M1 abundance was visually observable. For our statistical comparisons, we assigned a low value of M1 for samples with experimentally undetectable levels, allowing us to conservatively and semi-quantitatively compare the two phenotypic groups. The creatinine/M1 ratio clearly distinguished PMs from non-PMs.

We verified that creatinine/M1 was associated with DM/DX in both spot and timed urine samples in the validation set of urine collected from an additional 95 children. PMs have lower

M1 abundances than non-PMs ($P < 0.0001$), suggesting that M1 is likely a product of a reaction catalyzed by CYP2D6. However, much of the variance in the relationship between log-transformed DM/DX and creatinine/M1 is still unexplained ($r^2 \sim 0.3$). A stronger correlation with DM/DX would likely be observed if M1 were normalized by its unidentified precursor in a parent-to-metabolite molar ratio.

The creatinine/M1 ratio differed among activity score groups; however, there was appreciable overlap among non-PMs (activity scores between 0.5 and 3) (Figure 4-5). The differentiation between activity scores may improve if the parent-to-M1 molar ratio can be used. In addition, fine-tuning *CYP2D6* genotype by taking recently described enhancer SNPs into account [42] may alter activity score assignments. These enhancer SNPs appear to impact the regulation of *CYP2D6* expression and thereby modulate an individual's activity.

Although age-dependent increases in CYP2D6 mRNA, and microsomal protein and activity levels have been reported in human fetal and pediatric liver [43, 44], we observed no correlation between log M1 abundance and age in our study cohort (data not shown). However, *in vivo* pharmacokinetic data and longitudinal phenotyping studies indicate that genetic variation in *CYP2D6* is a more important determinant of interindividual variability in activity than ontogeny [10, 11, 36]. Moreover, neither log M1 abundance nor creatinine concentration differed by gender or urinary pH. Creatinine was used to normalize for urine concentrations in our study, and urinary creatinine concentrations were not significantly correlated with log M1 in any dataset except for the spot urine samples of the training set ($P = 0.01$). Urinary creatinine concentrations have been reported to change with age, [45] and a significant association between creatinine concentrations and age was observed in the training set ($P = 0.036$ and < 0.0001 in the spot and timed urine collections, respectively) but not in the validation set. Admittedly, creatinine concentrations may influence the interpretation of the data in the training set, but it does not appear to be an important confounder in the validation set.

In addition to distinguishing CYP2D6 phenotype in pediatric subjects, the creatinine/M1 ratio was sensitive to inhibition of CYP2D6 in adults, increasing by approximately 9-fold in adults during fluoxetine treatment as compared to control. Creatinine/M1 was less sensitive to CYP2D6 inhibition than DM/DX, once again reinforcing the need to account for the parent of M1.

M1 may join the growing list of endogenous CYP2D6 substrates and products. CYP2D6 catalyzed the *O*-demethylation of 5-methoxy-*N*,*N*-dimethyltryptamine, pinoline, and 5-methoxytryptamine to bufotenine, 6-hydroxy-1,2,3,4-tetrahydro-β-carboline and serotonin, respectively, in human recombinant CYP2D6 and CYP2D6-transgenic mouse liver microsomes [25, 46]. Additionally, CYP2D6 has been shown to hydroxylate and epoxygenate anandamide in human recombinant CYP2D6 and brain microsomal and mitochondrial preparations [28]. Recently, Cheng et al. reported that serotonin, 5-hydroxyindoleacetic acid, *L*-carnitine, acetyl-*L*-carnitine, pantothenic acid, 2'-deoxycytidine diphosphate, anandamide, *N*-acetylglucosaminylamine and stearoyl-*L*-carnitine concentrations differed significantly in brain homogenate and cerebrospinal fluid between wild-type and CYP2D6-transgenic mice [30]. Using chemical standards, many of these compounds were screened by LC-QTOF MS, but they were undetectable in our urine samples (data not shown). These urinary compound concentrations may be below our detection limit or elute with the column void volume (e.g., bufotenine). Many previously identified compounds were detected in specific tissues or biofluids, such as the brain or cerebrospinal fluid, and may not be excreted to an appreciable extent in the urine. Further investigation of these endogenous compounds as possible human CYP2D6 biomarkers may require the development of specific and sensitive targeted urinary assays or sampling of other biofluids.

In the field of metabolomics, the identification of complete unknowns from complex biological samples presents a substantial challenge. A limitation of our study is our current inability to identify M1. Unlike traditional metabolite identification, we have few clues regarding the structure of M1 since the precursor to M1 is also unknown. Preliminary efforts to obtain a high yield and pure isolate of M1 from urine for NMR analysis were unsuccessful. Despite the lack of structural information for M1, we would propose that the use of global metabolomics to identify endogenous biomarkers is akin to genome wide association studies (GWAS) to identify single nucleotide polymorphisms (SNPs) associated with a particular disease. For example, the identified SNPs associated with a particular disease can be located in the protein-coding region of genes or are in linkage disequilibrium with SNPs in those regions. However, the majority of the identified SNPs (~80%) are located in intergenic regions or noncoding introns [47]. Despite the apparent non-functional nature of these significantly associated SNPs, validation, replication, and efforts to identify the causal SNPs have resulted in continued use of GWAS approaches. Similarly, the relationship between M1 and CYP2D6 activity is still valid, even if the structure is currently unknown. Although structural identification of M1 is beyond the scope of the study at present, the identification of M1 and its parent will increase our understanding of the endogenous role of CYP2D6. The possibility that M1 or its precursor is a dietary component or a product of the microbiome cannot be excluded, but it is worth noting that the pediatric and adult studies were conducted independently and at two geographic sites, suggesting that regional or site-specific exposures can be ruled out as sources of M1.

4.5 Conclusion

In conclusion, we demonstrated that discovery of human biomarkers of CYP2D6 can be facilitated using a global metabolomics approach. We found that a positive ion with *m/z* of 444.3102 was associated with the urinary DM/DX ratio, an established method of CYP2D6 phenotyping, in two cohorts of children and was altered following CYP2D6 inhibition in adults. The ability of this ion to distinguish between CYP2D6 metabolizer phenotypes is currently limited to PM and non-PM phenotypes. Clearly, future structural identification of M1 and its parent are needed and may lead to a combined marker of CYP2D6 phenotype that may be more sensitive than the metabolite alone.

The findings of this study extend our current knowledge of CYP2D6 and demonstrate that metabolomics methods may be useful in revealing new biomarkers of drug metabolizing enzymes. In this study, the exploration of urinary metabolites led to the detection of a novel ion, M1, which may, lead to its use as an endogenous marker alone or in combination with other biomarkers of CYP2D6 activity. Future studies of M1 could include validation in different ethnic groups, additional pediatric and adult studies, and may be useful in studying CYP2D6 activity in pregnant women and patients with kidney or liver disease. Upon further *in vitro* and *in vivo* validation, the clinical implementation of a non-invasive, endogenous biomarker test predictive of CYP2D6 phenotype could advance personalized medicine by potentially replacing current phenotyping or genotyping methods. Futhermore, validated endogenous biomarkers would make retrospective analyses of clinical samples possible and may aid in first-in-man studies where there is a concern for drug-drug interactions.

4.6 Acknowledgements

We would like to thank Dr. Kathleen Kerr (University of Washington, Seattle, WA) for her statistical consultation.

4.7 References

1. Kimland E, Odlind V: Off-label drug use in pediatric patients. *Clinical pharmacology and therapeutics* 91(5), 796-801 (2012).

2. Kimland E, Nydert P, Odlind V, Bottiger Y, Lindemalm S: Paediatric drug use with focus on off-label prescriptions at Swedish hospitals - a nationwide study. *Acta Paediatr* 101(7), 772-778 (2012).

3. Sachs AN, Avant D, Lee CS, Rodriguez W, Murphy MD: Pediatric information in drug product labeling. *JAMA : the journal of the American Medical Association* 307(18), 1914-1915 (2012).

4. Rodriguez W, Selen A, Avant D *et al.*: Improving pediatric dosing through pediatric initiatives: what we have learned. *Pediatrics* 121(3), 530-539 (2008).

5. Johnson TN: The problems in scaling adult drug doses to children. *Archives of disease in childhood* 93(3), 207-211 (2008).

6. Bouzom F, Walther B: Pharmacokinetic predictions in children by using the physiologically based pharmacokinetic modelling. *Fundamental & clinical pharmacology* 22(6), 579-587 (2008).

7. Mahmood I: Prediction of drug clearance in children from adults: a comparison of several allometric methods. *British journal of clinical pharmacology* 61(5), 545-557 (2006).

8. Abernethy DR, Burckart GJ: Pediatric dose selection. *Clinical pharmacology and therapeutics* 87(3), 270-271 (2010).

9. Laer S, Barrett JS, Meibohm B: The in silico child: using simulation to guide pediatric drug development and manage pediatric pharmacotherapy. *Journal of clinical pharmacology* 49(8), 889-904 (2009).

10. Leeder JS, Kearns GL, Spielberg SP, Van Den Anker J: Understanding the relative roles of pharmacogenetics and ontogeny in pediatric drug development and regulatory science. *Journal of clinical pharmacology* 50(12), 1377-1387 (2010).

11. Allegaert K, Rochette A, Veyckemans F: Developmental pharmacology of tramadol during infancy: ontogeny, pharmacogenetics and elimination clearance. *Paediatric anaesthesia* 21(3), 266-273 (2011).

12. Zanger UM, Turpeinen M, Klein K, Schwab M: Functional pharmacogenetics/genomics of human cytochromes P450 involved in drug biotransformation. *Analytical and bioanalytical chemistry* 392(6), 1093-1108 (2008).

13. Zhou SF: Polymorphism of human cytochrome P450 2D6 and its clinical significance: Part I. *Clinical pharmacokinetics* 48(11), 689-723 (2009).

14. Zhou SF: Polymorphism of human cytochrome P450 2D6 and its clinical significance: part II. *Clinical pharmacokinetics* 48(12), 761-804 (2009).

15. Abduljalil K, Frank D, Gaedigk A *et al.*: Assessment of activity levels for CYP2D6*1, CYP2D6*2, and CYP2D6*41 genes by population pharmacokinetics of dextromethorphan. *Clinical pharmacology and therapeutics* 88(5), 643-651 (2010).

16. Gaedigk A: Complexities of CYP2D6 gene analysis and interpretation. *Int Rev Psychiatry* 25(5), 534-553 (2013).

17. Crews KR, Gaedigk A, Dunnenberger HM *et al.*: Clinical Pharmacogenetics Implementation Consortium (CPIC) guidelines for codeine therapy in the context of cytochrome P450 2D6 (CYP2D6) genotype. *Clinical pharmacology and therapeutics* 91(2), 321-326 (2012).

18. Hicks JK, Swen JJ, Gaedigk A: Challenges in CYP2D6 Phenotype Assignment from Genotype Data: A Critical Assessment and Call for Standardization. *Current drug metabolism* 15(2), 218-232 (2014).

19. Teh LK, Bertilsson L: Pharmacogenomics of CYP2D6: molecular genetics, interethnic differences and clinical importance. *Drug metabolism and pharmacokinetics* 27(1), 55-67 (2012).

20. Gaedigk A, Simon SD, Pearce RE, Bradford LD, Kennedy MJ, Leeder JS: The CYP2D6 activity score: translating genotype information into a qualitative measure of phenotype. *Clinical pharmacology and therapeutics* 83(2), 234-242 (2008).

21. Jones AE, Brown KC, Werner RE *et al.*: Variability in drug metabolizing enzyme activity in HIV-infected patients. *European journal of clinical pharmacology* 66(5), 475-485 (2010).

22. Llerena A, Dorado P, Ramirez R *et al.*: CYP2D6 genotype and debrisoquine hydroxylation phenotype in Cubans and Nicaraguans. *The pharmacogenomics journal* 12(2), 176-183 (2012).

23. Wu AH: Drug metabolizing enzyme activities versus genetic variances for drug of clinical pharmacogenomic relevance. *Clinical proteomics* 8(1), 12 (2011).

24. Sager JE, Lutz JD, Foti RS, Davis C, Kunze KL, Isoherranen N: Fluoxetine and norfluoxetine mediated complex drug-drug interactions: in vitro to in vivo correlation of effects on CYP2D6, CYP2C19 and CYP3A4. *Clinical pharmacology and therapeutics*, (2014).

25. Yu AM, Idle JR, Herraiz T, Kupfer A, Gonzalez FJ: Screening for endogenous substrates reveals that CYP2D6 is a 5-methoxyindolethylamine O-demethylase. *Pharmacogenetics* 13(6), 307-319 (2003).

26. Jiang XL, Shen HW, Yu AM: Pinoline may be used as a probe for CYP2D6 activity. *Drug metabolism and disposition: the biological fate of chemicals* 37(3), 443-446 (2009).

27. Hiroi T, Kishimoto W, Chow T, Imaoka S, Igarashi T, Funae Y: Progesterone oxidation by cytochrome P450 2D isoforms in the brain. *Endocrinology* 142(9), 3901-3908 (2001).

28. Snider NT, Sikora MJ, Sridar C, Feuerstein TJ, Rae JM, Hollenberg PF: The endocannabinoid anandamide is a substrate for the human polymorphic cytochrome P450 2D6. *The Journal of pharmacology and experimental therapeutics* 327(2), 538-545 (2008).

29. Sridar C, Snider NT, Hollenberg PF: Anandamide oxidation by wild-type and polymorphically expressed CYP2B6 and CYP2D6. *Drug metabolism and disposition: the biological fate of chemicals* 39(5), 782-788 (2011).

30. Cheng J, Zhen Y, Miksys S *et al.*: Potential role of CYP2D6 in the central nervous system. *Xenobiotica; the fate of foreign compounds in biological systems* 43(11), 973-984 (2013).

31. Schmid B, Bircher J, Preisig R, Kupfer A: Polymorphic dextromethorphan metabolism: co-segregation of oxidative O-demethylation with debrisoquin hydroxylation. *Clinical pharmacology and therapeutics* 38(6), 618-624 (1985).

32. Gaedigk A, Fuhr U, Johnson C, Berard LA, Bradford D, Leeder JS: CYP2D7-2D6 hybrid tandems: identification of novel CYP2D6 duplication arrangements and implications for phenotype prediction. *Pharmacogenomics* 11(1), 43-53 (2010).

33. Gaedigk A, Jaime LK, Bertino JS, Jr. *et al.*: Identification of Novel CYP2D7-2D6 Hybrids: Non-Functional and Functional Variants. *Frontiers in pharmacology* 1, 121 (2010).

34. Gaedigk A, Twist GP, Leeder JS: CYP2D6, SULT1A1 and UGT2B17 copy number variation: quantitative detection by multiplex PCR. *Pharmacogenomics* 13(1), 91-111 (2012).

35. Gaedigk A, Isidoro-Garcia M, Pearce RE *et al.*: Discovery of the nonfunctional CYP2D6 31 allele in Spanish, Puerto Rican, and US Hispanic populations. *European journal of clinical pharmacology* 66(9), 859-864 (2010).

36. Blake MJ, Gaedigk A, Pearce RE *et al.*: Ontogeny of dextromethorphan O- and N-demethylation in the first year of life. *Clinical pharmacology and therapeutics* 81(4), 510-516 (2007).

37. Smith CA, Want EJ, O'maille G, Abagyan R, Siuzdak G: XCMS: processing mass spectrometry data for metabolite profiling using nonlinear peak alignment, matching, and identification. *Analytical chemistry* 78(3), 779-787 (2006).

38. Tautenhahn R, Bottcher C, Neumann S: Highly sensitive feature detection for high resolution LC/MS. *BMC bioinformatics* 9, 504 (2008).

39. Tautenhahn R, Cho K, Uritboonthai W, Zhu Z, Patti GJ, Siuzdak G: An accelerated workflow for untargeted metabolomics using the METLIN database. *Nature biotechnology* 30(9), 826-828 (2012).

40. Wishart DS, Knox C, Guo AC *et al.*: HMDB: a knowledgebase for the human metabolome. *Nucleic acids research* 37(Database issue), D603-610 (2009).

41. Lutz U, Bittner N, Lutz RW, Lutz WK: Metabolite profiling in human urine by LC-MS/MS: method optimization and application for glucuronides from dextromethorphan metabolism. *Journal of chromatography. B, Analytical technologies in the biomedical and life sciences* 871(2), 349-356 (2008).

42. Wang D, Poi MJ, Sun X, Gaedigk A, Leeder JS, Sadee W: Common CYP2D6 polymorphisms affecting alternative splicing and transcription: long-range haplotypes with two regulatory variants modulate CYP2D6 activity. *Human molecular genetics* 23(1), 268-278 (2014).

43. Yokoi T: Essentials for starting a pediatric clinical study (1): Pharmacokinetics in children. *The Journal of toxicological sciences* 34 Suppl 2, SP307-312 (2009).

44. Stevens JC, Marsh SA, Zaya MJ *et al.*: Developmental changes in human liver CYP2D6 expression. *Drug metabolism and disposition: the biological fate of chemicals* 36(8), 1587-1593 (2008).

45. Gu H, Pan Z, Xi B *et al.*: 1H NMR metabolomics study of age profiling in children. *NMR in biomedicine* 22(8), 826-833 (2009).

46. Yu AM, Idle JR, Byrd LG, Krausz KW, Kupfer A, Gonzalez FJ: Regeneration of serotonin from 5-methoxytryptamine by polymorphic human CYP2D6. *Pharmacogenetics* 13(3), 173-181 (2003).

47. Manolio TA: Genomewide association studies and assessment of the risk of disease. *The New England journal of medicine* 363(2), 166-176 (2010).

4.8 **Tables and Figures**

Table 4.1 Demographics of the pediatric study population

Characteristic	All Subjects (N = 189)	Training Set (n = 94)		Validation Set (n = 95)	
		PM (n = 5)	Non-PM (n= 89)	PM (n = 5)	Non-PM (n = 90)
Age (years)	11.2 ± 2.5 (7 to 16)	11.3 ± 2.4 (9 to 14)	11.2 ± 2.4 (7 to 16)	11.0 ± 1.6 (9 to 14)	11.1 ± 2.5 (7 to 16)
Tanner Stage					
Breast Size	2.4 ± 1.5 (1 to 5)	2.4 ± 1.7 (1 to 5)	2.4 ± 1.5 (1 to 5)	1.6 ± 0.5 (1 to 2)	2.5 ± 1.5 (1 to 5)
Pubic Hair	2.4 ± 1.5 (1 to 6)	2.4 ± 1.7 (1 to 5)	2.3 ± 1.5 (1 to 6)	1.4 ± 0.5 (1 to 2)	2.5 ± 1.5 (1 to 5)
Gender					
Male (%)	61	60	66	80	56
Race (%)					
African American	43	0	43	20	47
Caucasian (Hispanic)	49 (5)	100 (0)	46 (4)	80 (0)	47 (6)
Mixed	8	0	11	0	7
Urinary DM/DX Ratio	0.078 ± 0.3 (9.0×10^{-5} to 3.3)	1.4 ± 1 (0.63 to 3.3)	0.014 ± 0.03 (9.0×10^{-5} to 0.20)	1.1 ± 0.7 (0.28 to 1.8)	0.013 ± 0.02 (3.0×10^{-4} to 0.14)

PM: CYP2D6 poor metabolizer phenotype subjects
Non-PM: CYP2D6 intermediate, extensive or ultra-rapid metabolizer phenotype subjects
Age at visit 1, Tanner stage at enrollment and DM/DX are shown as the mean ± standard deviation (range).

Table 4.2 Summary of significant (Benjamini-Hochberg (BH) corrected P-value < 0.01) m/z ions by ionization mode associated with log (DM/DX) following global metabolomics analysis of pediatric training set samples by LC-QTOF mass spectrometry. The possible identity of m/z ions was assigned based on mass.

m/z	**RT (min)** [a]	**Possible Identity** [(ref)]	**Slope**	r^2	***P*-value**	**BH corrected *P*-value**
ESI+ using spot urine samples						
444.3102	6.5	-- [b]	-0.79	0.34	1.69×10^{-7}	6.50×10^{-4}
ESI+ using timed urine samples						
421.2056	2.5	-- [b]	-1.70	0.67	1.31×10^{-44}	5.03×10^{-41}
444.3102	6.5	-- [b]	-0.79	0.27	2.33×10^{-6}	3.80×10^{-3}
464.2283	3.2	-- [b]	-0.78	0.40	2.97×10^{-6}	3.80×10^{-3}
273.1668	5.6	-- [b]	0.73	0.24	3.97×10^{-6}	3.81×10^{-3}
434.2196	2.6	Dextrorphan glucuronide (49)	-1.51	0.56	1.09×10^{-5}	7.85×10^{-3}
445.3135	6.5	-- [b]	-0.65	0.25	1.23×10^{-5}	7.85×10^{-3}
ESI- using timed urine samples [c]						
447.1866	6.3	-- [b]	-2.05	0.70	9.55×10^{-52}	2.75×10^{-48}
448.1884	6.3	Hydroxy-dextrorphan-glucuronide (41)	-2.23	0.68	1.87×10^{-44}	2.70×10^{-41}
446.1827	6.3	Oxo-dextrorphan-glucuronide (41)	-1.91	0.71	1.49×10^{-41}	1.43×10^{-38}
336.1275	3.5	Dextrorphan sulfate (49)	-1.49	0.57	1.63×10^{-29}	1.18×10^{-26}
432.1668	4.5	Oxo-hydroxymorphinan-glucuronide (41)	-1.60	0.56	5.77×10^{-23}	3.33×10^{-20}
433.1697	4.5	-- [b]	-1.73	0.51	1.47×10^{-14}	7.08×10^{-12}
418.1878	2.5	3-hydroxymorphinan-glucuronide (49)	-1.14	0.41	1.21×10^{-10}	4.97×10^{-8}
193.0358	2.6	-- [b]	1.03	0.093	2.52×10^{-5}	9.08×10^{-3}

[a] Retention time
[b] Identity unknown
[c] No ions were found to be significant in the spot urine collection samples in ESI- mode

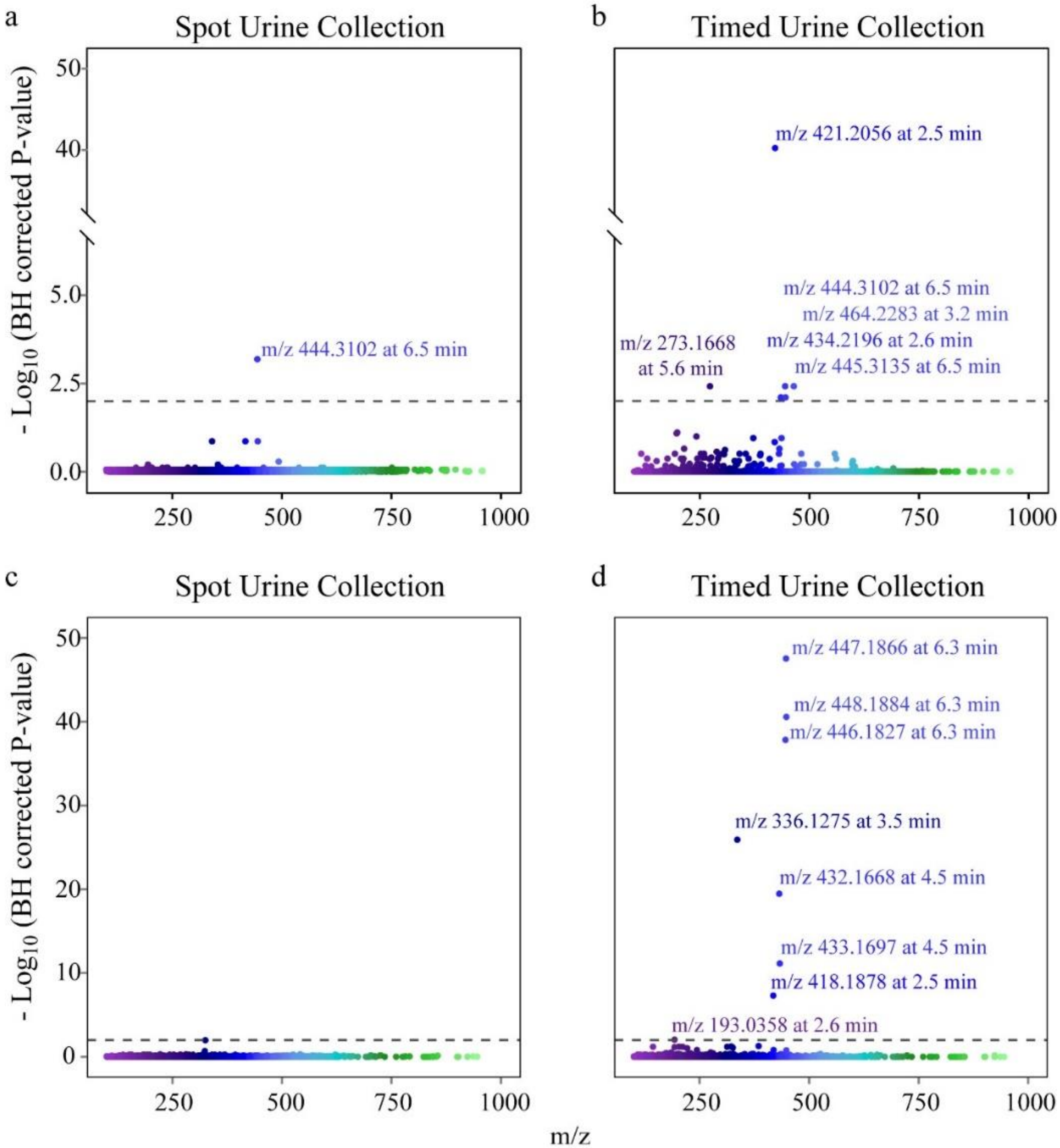

Figure 4.1 Manhattan plots of pediatric training dataset ions. The ion abundances were regressed against log (DM/DX). Corresponding *P*-values were obtained and corrected using the Benjamini-Hochberg (BH) method. The corresponding -log (BH corrected *P*-values) are shown for ESI+ mode (panels a and b) and ESI- mode (panels c and d) from LC-QTOF analysis. Results from spot and 0-4 hour timed urine samples are presented in panels a and c, and panels b and d, respectively. Ion *m/z* and retention time are explicitly shown for significant ions. The BH corrected significance threshold is indicated by the dashed line (P = 0.01).

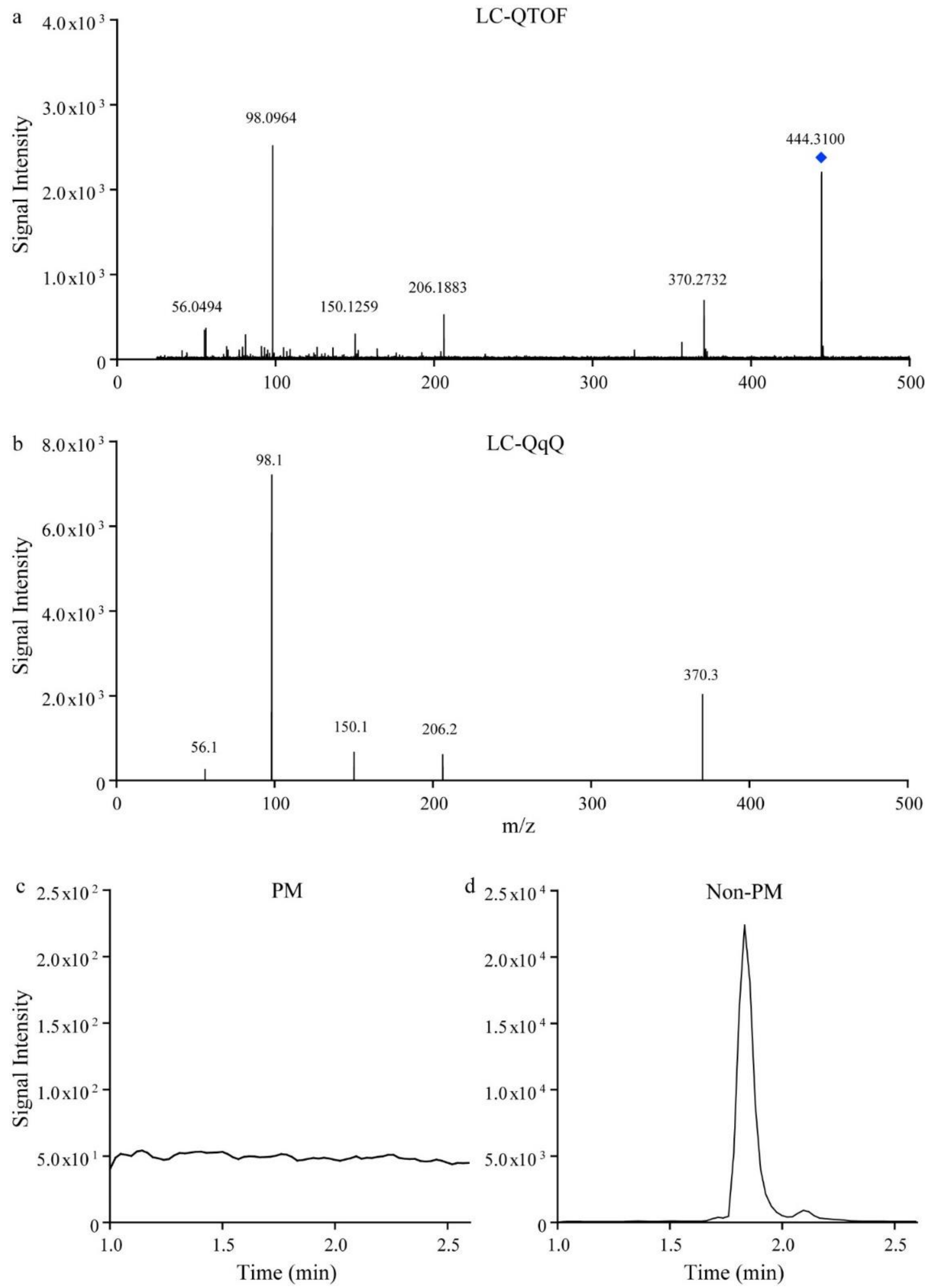

Figure 4.2 Product ion spectra of M1 (*m/z* 444.3102) from a representative pediatric spot urine sample. Spectra were obtained in ESI+ mode via (a) liquid chromatography quadrupole time-of-flight (LC-QTOF), precursor *m/z* indicated by a diamond, and (b) liquid chromatography triple-quadrupole (LC-QqQ), parent *m/z* not shown. A peak for the mass transition of *m/z* 444.3 → 98.1, the most abundant product ion, was (c) undetectable in a representative poor metabolizer (PM) subject after a 15 µl injection, and (d) clearly observable in a urine sample in a representative non-PM subject after a 5 µl injection.

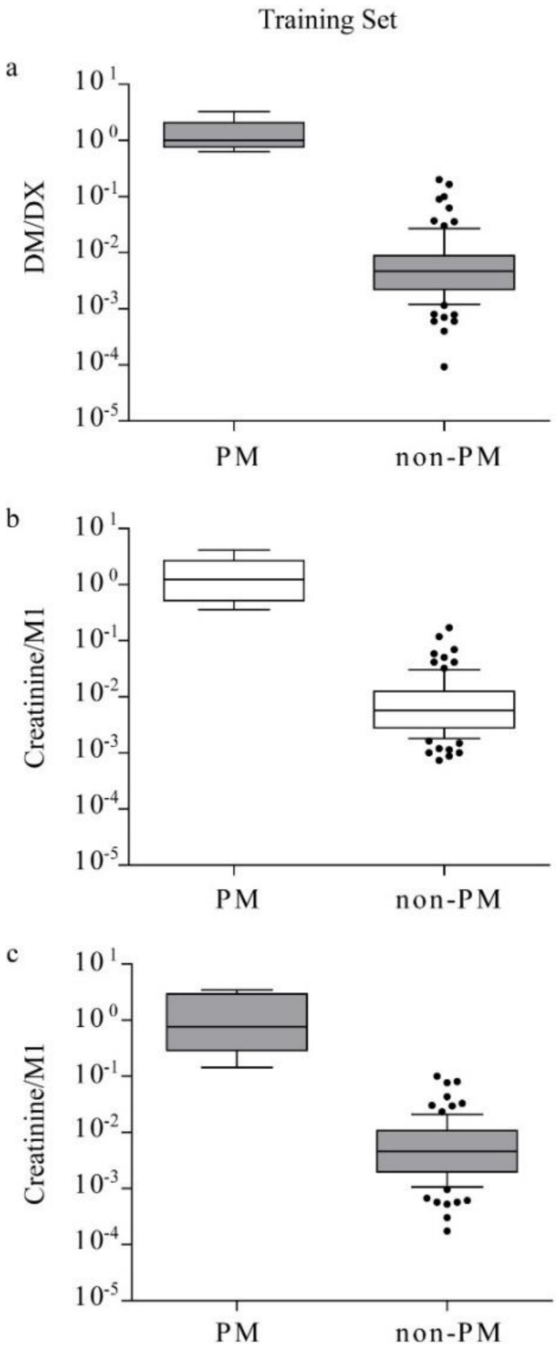

Figure 4.3 Phenotypic measures of CYP2D6 in the pediatric training set for poor metabolizer (PM) (n=5) and non-PM (n=89) groups. (A) Dextromethorphan metabolic ratio (DM/DX) was determined in timed urine samples. Creatinine/M1 was measured by LC-MS/MS in (b) spot and (c) timed urine samples. A low value was assigned for samples with undetectable M1 abundances. Lines depict the median and boxes represent the 25^{th} and 75^{th} percentiles. The 10^{th} and 90^{th} percentiles are indicated by the whiskers. As PM and non-PM status was determined by DM/DX, the *P*-value is not reported in (a). Similarly, as M1 was identified as a marker of CYP2D6 using DM/DX in this same set of urine samples, the P-values are not reported in (b) and (c).

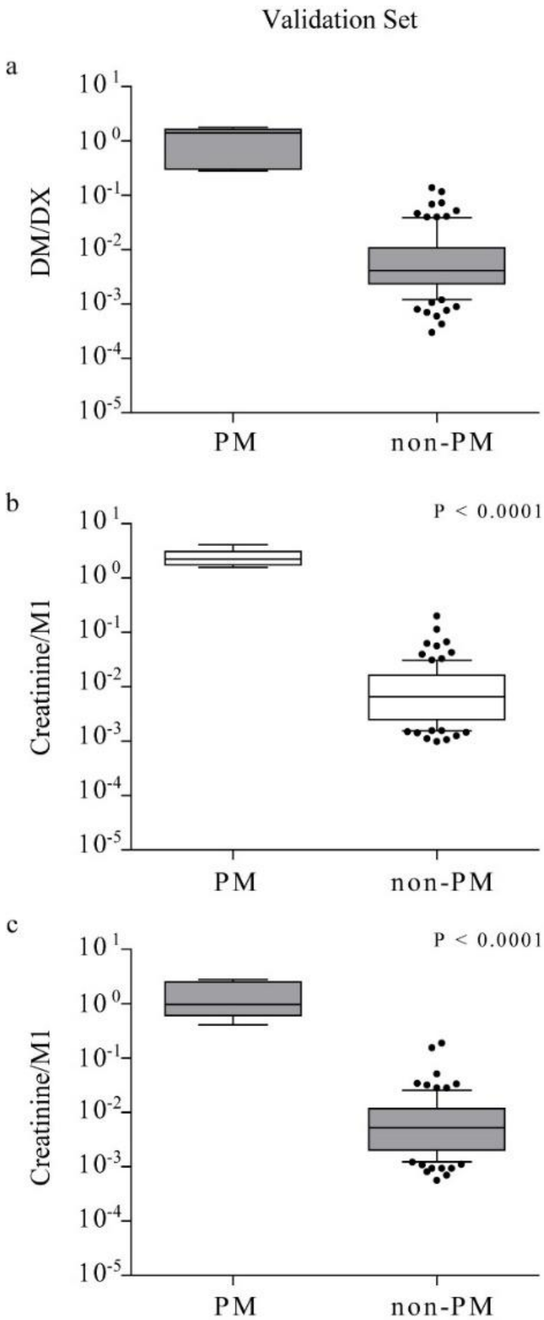

Figure 4.4 Phenotypic measures of CYP2D6 in the pediatric validation set for poor metabolizer (PM) (n=5) and non-PM (n=90) subjects. (A) Dextromethorphan metabolic ratio (DM/DX) was determined in timed urine samples. Creatinine/M1 was measured by LC-MS/MS in (b) spot and (c) timed urine samples. A low value was assigned for samples with undetectable M1 abundances. Lines depict the median and boxes represent the 25th and 75th percentiles. The 10th and 90th percentiles are indicated by the whiskers. Statistical analyses were performed using unpaired t-tests. As PM and non-PM status was determined by DM/DX, the *P*-value is not reported in (a).

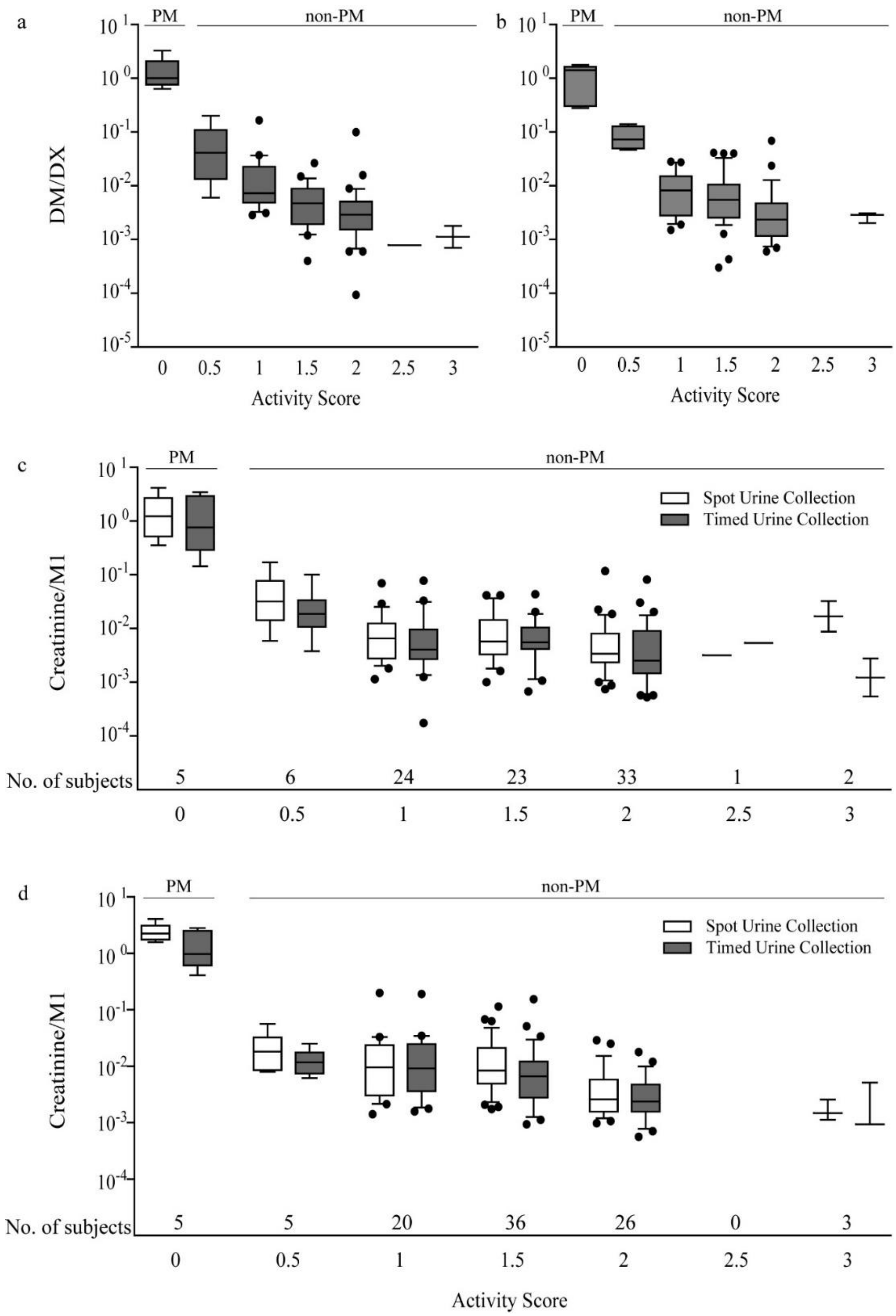

Figure 4.5 The relationship between phenotypic measures of CYP2D6 activity and CYP2D6 activity score. Dextromethorphan metabolic ratio (DM/DX) and creatinine/M1 as measured by LC-QqQ in subjects from the (a and c) training (n = 94), and (b and d) validation (n = 95) datasets are shown. Lines depict the median and boxes represent the 25th and 75th percentiles. The 10th and 90th percentiles are indicated by the whiskers. Spot and timed urine samples are indicated with open and shaded boxes, respectively. DM/DX and creatinine/M1 ratios differed by activity score ($P < 0.0001$) as determined by one-way ANOVA.

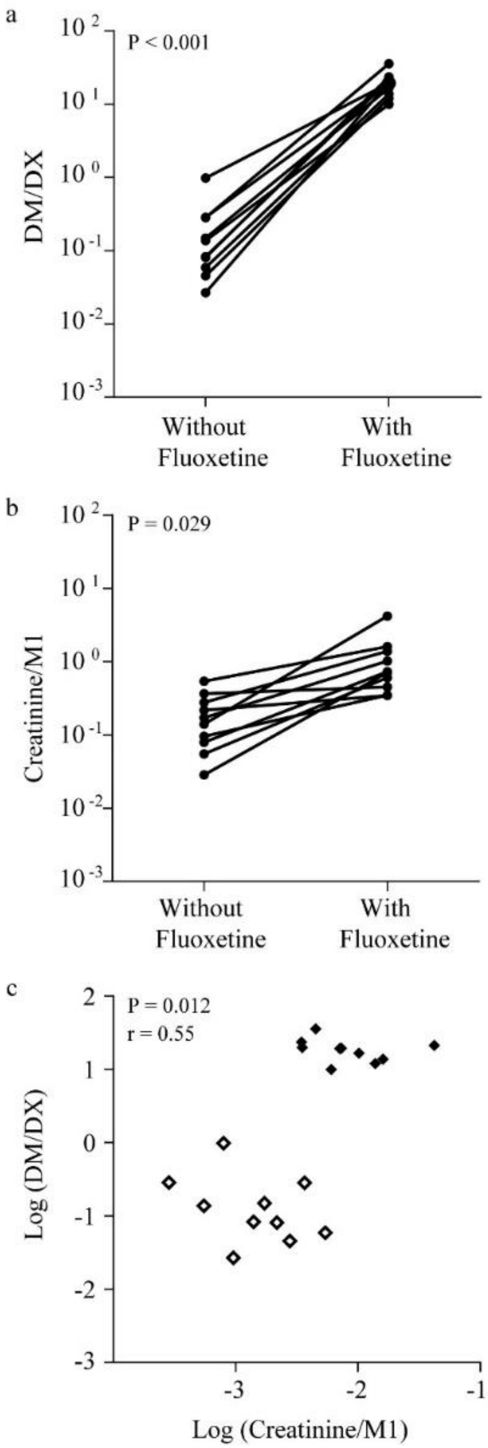

Figure 4.6 The effect of CYP2D6 inhibition on (a) dextromethorphan metabolic ratio (DM/DX) and (b) creatinine/M1 in adult subjects. (c) The relationship between log (DM/DX) and log (creatinine/M1). Open diamonds indicate subjects without fluoxetine treatment, closed diamonds show subjects with fluoxetine treatment. Statistical analyses were performed using paired t-tests or the Spearman rank correlation.

Chapter 5. Association and concordance of a novel endogenous biomarker (M1) with CYP2D6 activity as determined by probe substrates

5.1 Introduction

Cytochrome P450 2D6 (CYP2D6) activity can be partially explained by genetic variation in the highly polymorphic and complex *CYP2D6* gene locus [1-3]. An activity scoring system was developed by Gaedigk et al. [4] to simplify the interpretation of genotypes. In brief, each *CYP2D6* allele receives a numerical value that approximates its function. Null, reduced and fully functional alleles are compared to the reference *CYP2D6*1* allele, and are assigned values of 0, 0.5 and 1, respectively. For gene duplications, the score of the single counterpart is multiplied by the copy number. An individual's CYP2D6 activity score (AS) is the sum of the assigned values of the alleles.

In general, CYP2D6 phenotype can be predicted from genotype, but there can be variability in CYP2D6 activity within each genotype [3, 5]. Typically, an AS of 0 translates to a CYP2D6 poor metabolizer (PM) phenotype and those of 0.5, 1-2 and >2 translate to intermediate metabolizer (IM), extensive metabolizer (EM) and ultra-rapid metabolizer (UM) phenotypes [3, 4, 6]. However, genotype-to-phenotype predictions are less robust when individuals are taking medications that act as CYP2D6 inhibitors or are undergoing physiological changes that affect CYP2D6 activity [7-12]. Thus, directly assessing CYP2D6 activity by the use of probe drugs may be more useful than making genotype-to-phenotype predictions.

The pharmacokinetics of select drugs can reflect CYP2D6 activity. Plasma or urine samples are collected for the determination of drug clearance or metabolic ratios of the parent to CYP2D6-mediated metabolite [13]. If plasma clearance of the drug is used as the phenotyping marker, CYP2D6 should the major route of metabolism in the body (i.e., a high fraction of hepatic clearance (f_m) should be mediated by CYP2D6). Alternatively, for drugs whose elimination is dependent on several metabolic enzymes and renal excretion, the theoretical gold standard for phenotyping CYP2D6 activity is the determination of partial clearance of a drug metabolized to a primarily CYP2D6-mediated metabolite [13]. Although urine samples are less invasive for the patient to collect, the urinary metabolic ratios can be influenced by several factors. The urinary metabolic ratio is dependent on the renal clearance of each of the compounds (parent and metabolite) as well as the formation clearance of the metabolite. Moreover, the passive renal reabsorption of lipid-soluble basic drugs, such as some CYP2D6 drugs or metabolites, may be influenced by the normal physiological range of urine pH, adding variability to the measurement of enzyme activity [14]. Several drugs have been proposed and validated for use as CYP2D6 probes, including dextromethorphan (DM), metoprolol, and atomoxetine [13, 16-18].

DM has been used as a CYP2D6 probe since the 1980s. Despite results where 16.5% of healthy adult subjects experienced an adverse event after a single oral 80 mg dose of DM hydrobromide [19], doses of DM used in phenotyping studies are well below 80 mg and is generally well tolerated [20] and considered a safe probe drug for pediatric studies [21-24]. Thus, the risk of adverse events is low. The fraction of DM metabolized by CYP2D6 is about 95% [25]. The primary metabolite is the O-demethylated product, dextrorphan, which is subsequently conjugated and excreted in the urine [26]. Phenotyping using DM/DX has been used in urine, plasma, and saliva samples [27-31] using various collection intervals. Measurement of the urinary molar ratio of dextromethorphan/dextrorphan (DM/DX), typically after deconjugation by β-glucuronidase, has been demonstrated as a reliable method of assessing *in vivo* CYP2D6 activity [32-36]. However, there is some evidence that DM/DX and DM oral clearance are only weakly correlated [37]. Although the majority of DM to DX metabolism has been attributed to CYP2D6, CYP3A4 has also been implicated in DM biotransformation, leading some to question its robustness as a phenotyping probe [38]. Labbe et al. observed that variations in physiologic urine pH account for 20-80% of the intra-individual variability when using DM/DX. Although the influence of pH is unlikely to cause misidentification between PM and EM phenotypes, it may cause inconsistencies within the CYP2D6 EM group [14, 17].

Metoprolol, a beta blocker, is considered a “gold standard” CYP2D6 probe, however its use as a probe substrate is typically restricted to healthy adult volunteer studies due to its pharmacological effects. Metoprolol may cause hypotension [39], or other adverse effects [40], but is considered a sensitive substrate by the U.S. Food and Drug Administration (FDA). Metoprolol is administered as a racemic mixture (R- and S-metoprolol), and is metabolized extensively (70-90%) by CYP2D6 to α-hydroxymetoprolol [13, 41]. Interestingly, CYP2D6 expresses differential metabolism of metoprolol enantiomers. EMs preferentially metabolize the R-metoprolol enantiomer; therefore an EM might have a higher S/R-metoprolol ratio (1.37 S/R-metoprolol AUC ratio) as compared to a PM who receives the same dose of racemic metoprolol [13, 42]. Both the S/R-metoprolol and metoprolol/α-hydroxymetoprolol metabolic ratios in urine and plasma have been used to characterize CYP2D6 activity [16, 42-44]. Like DM, metoprolol, a lipid-soluble, partially ionized substrate probe, appears to be sensitive to urine pH [14], accounting for 20-80% of intraindividual variability in the urinary metoprolol:α-hydroxymetoprolol metabolic ratio [17]. In *CYP2D6* EMs, S/R-metoprolol AUC decreased after multiple doses of paroxetine, a potent inhibitor of CYP2D6 [45].

Atomoxetine is a norepinephrine reuptake inhibitor used to treat attention deficit hyperactivity disorder (ADHD) in children and adults. The FDA lists atomoxetine as an *in vivo* substrate that can be used to study CYP2D6 activity . Both *in vitro* and *in vivo* studies indicate that CYP2D6 is primarily responsible for the metabolism of atomoxetine to the major metabolite, 4-hydroxyatomoxetine [46, 47]. Based on a single 20 mg dose of ^{14}C-atomoxetine, oral clearance was over 10-fold higher in EMs compared to PMs [48]. The f_m by CYP2D6 for atomoxetine was estimated to be approximately 0.87 [49]. Atomoxetine steady-state oral clearance decreased 6.5-fold in *CYP2D6* EMs after enzyme inhibition by paroxetine [50].

Although CYP2D6 is in not inducible by xenobiotics [1], CYP2D6 activity in women appears to temporarily increase during pregnancy [51, 52]. One study found an increase in CYP2D6 activity (DM/DX decreased 53%) during late pregnancy compared to postpartum among *CYP2D6* EMs [53]. Additionally, Tracy et al. observed a 25%, 35%, and 48% increase in CYP2D6 activity as determined by the urinary DM/DX among EMs during the first, second and third trimesters of pregnancy, respectively, compared to postpartum [52]. Of the other probe substrates mentioned, only metoprolol has been studied in pregnancy. The oral clearance of metoprolol was increased greater than 4-fold during pregnancy as compared to postpartum [51]. Although the mechanism by which human CYP2D6 activity increases is unclear, recent evidence in CYP2D6-humanized mice suggest that the increase in activity may be transcriptionally regulated by the small heterodimer partner (SHP) and hepatocyte nuclear factor 4α (HNF4α) transactivation of CYP2D6 promoter [54].

The use of dextromethorphan, metoprolol or atomoxetine for CYP2D6 phenotyping can be challenging in healthy volunteer studies. In particular, children or pregnant women may be more reluctant to take unneeded medication or participate in a sample intensive pharmacokinetic study. With this in mind, we attempted to discover an endogenous biomarker that would reflect CYP2D6 activity. Recently, we reported that a novel endogenous urinary metabolite, M1, was correlated with urinary DM/DX in children and replicated our findings in a validation set (Chapter 4). M1 was absent among PM children and present in EM children, suggesting that M1 is likely a metabolite of a reaction mediated by CYP2D6. In addition, we observed that urinary DM/DX was correlated with urinary creatinine/M1 in adult subjects at baseline and after inhibition of CYP2D6 activity by fluoxetine [55].

Although the identity of M1 is still unknown, we were interested in whether M1 as a phenotyping marker would be comparable to other CYP2D6 probes. The criteria for validating CYP2D6 probes were reviewed by Frank et al. [13]. These criteria include, but are not limited to, changes in metabolism with treatment of CYP2D6 inhibitors, high contribution of CYP2D6-mediated metabolism to the overall metabolism of the parent species and correlation with other validated metrics for CYP2D6 [13]. Some of these criteria can be extended beyond drug probes to include endogenous biomarkers of CYP2D6 activity.

The goals of this study were to explore the relationship between M1 and metoprolol and atomoxetine. Metoprolol was studied in a longitudinal cohort of pregnant women, whereas atomoxetine was studied in children with differing *CYP2D6* genotypes. Although we previously observed a change in urinary M1 and the DM metabolic ratio upon fluoxetine inhibition, it is unknown if M1 is detectable in plasma and if it reflects changes in CYP2D6 activity in this biofluid. Thus, an additional aim of this study was to characterize the relationship between plasma M1 and DM clearance.

5.2 Materials and Methods

5.2.1 *Subjects*

Adult drug inhibition study with fluoxetine and dextromethorphan. Ten healthy adults (ages 30 ± 10 years; 5 men, 5 women) participated in a study evaluating the effect of two-week, multiple-dose fluoxetine treatment on CYP2D6, CYP3A4 and CYP2C19 activities. Detailed descriptions of the study design, demographics and results have been reported previously [12]. Only CYP2D6 extensive metabolizers were included in the study. Subjects were given a single 30 mg oral dose of DM as part of a probe drug cocktail at baseline (Study Day 1) and during the treatment phase (Study Day 16). Timed plasma and urine (0-12 and 12-24 hr) samples were collected during both phases. The secondary analysis of study samples was approved by the University of Washington Human Subjects Institutional Review Board. Results for plasma DM clearance and urinary DM/DX, determined on Study Days 1 and 16, were provided by Sager et al. [12]. Urinary M1 and creatinine from Study Days 1 and 18, and plasma M1 from predose samples from Study Days 3 and 18, were determined as described below.

Pregnancy study with metoprolol. Twenty-two women, receiving metoprolol for therapeutic purposes, participated in a multi-center opportunistic study investigating the pharmacokinetic changes that occur during pregnancy and postpartum. Details of the study design and patient demographics are described elsewhere (Hebert et al., manuscript in preparation). Subjects included one CYP2D6 PM, five IMs, 19 EMs and 2 subjects whose genotype was not obtained. Plasma metoprolol clearance was determined at various gestational times: early (10-14 weeks gestation), mid (22-26 weeks gestation), late (34-38 weeks gestation) pregnancy, and postpartum (12-16 weeks after delivery). Secondary analysis of patient samples was approved by the University of Washington Human Subjects Institutional Review Board. Urinary M1 and creatinine were determined as described below in samples from the various visit days.

Pediatric study with atomoxetine. Twenty-three children (aged 7-16; 20 males and 3 females) with ADHD participated in a study evaluating the effect of CYP2D6 genotype on the systemic exposure of atomoxetine, 4-hydroxyatomoxetine and N-desmethylatomoxetine. The study was approved by the Institutional Review Board at Children's Mercy Hospitals and Clinics (Kansas City, MO). These children were selected from a larger cohort participating in the longitudinal study of CYP2D6 activity presented in Chapter 4 [55]. To participate in the atomoxetine phenotyping study, children must be diagnosed with attention deficit-hyperactivity disorder. CYP2D6 genotyping analysis and AS (range: 0 to 3) were determined as described in Chapter 4 and by Gaedigk et al [4]. The children were administered a single oral dose of atomoxetine (at or near 0.5 mg/kg for children weighing less than 70 kg or 40 mg for children weighing greater than 70 kg). Plasma samples were collected and assayed for atomoxetine concentrations. Determination of atomoxetine clearance and other results are reported elsewhere [56].

5.2.2 *Analytical methods*

Determination of urinary creatinine. Urinary creatinine was determined in pediatric samples as described in Chapter 4 [55]. Urinary creatinine measurements from women during the pregnancy and postpartum visits were extracted from clinical chemistry results.

Determination of plasma and urinary M1. Urinary M1 was determined in the pediatric samples as described in Chapter 4 [55], including samples for subjects for which atomoxetine oral clearance was determined at a subsequent visit. Relative quantification of M1 in plasma (fluoxetine study) and urine (metoprolol study) was performed as described previously [55]. Briefly, following the addition of 800 µL of ice-cold acetonitrile to 200 µL of plasma or urine, samples were centrifuged to remove proteins, and the supernatant was evaporated and reconstituted for analysis. LC-MS/MS analysis was performed on an Agilent 1290 Infinity UPLC (Santa Clara, CA) coupled to an Agilent 6460 QqQ operated in positive electrospray ionization mode. Chromatographic separation of a 15 µL sample injection was achieved using an Agilent Zorbax SB-Aq analytical column fitted with a C8 guard column heated to 60°C. Using a gradient elution scheme with mobile phases consisting of 0.2% acetic acid in water and 0.2% acetic acid in methanol, M1 eluted at 1.8 min during a total run time of 6 min on the LC-QqQ system. The mass transition m/z 444.3 → 98.1 was used for quantitation. Additional details are provided in Chapter 4 [55].

5.2.3 *Data analysis*

M1 peak heights were calculated using Agilent MassHunter Quantitative Analysis (version B 04.00 for QqQ). Absolute concentrations of M1 could not be calculated due to the lack of an authentic standard for M1. Therefore, M1 peak height was determined and corrected with creatinine for urine concentrations and changes were compared semi-quantitatively within or between subjects. For subjects where M1 was undetectable (i.e., PM subjects), M1 was set to a low value of 5. The ratio is reported as M1/creatinine when compared with CYP2D6 probe clearance and creatinine/M1 when compared with urinary metabolic ratios (parent/metabolite). Pediatric subjects were grouped into *CYP2D6* AS of 0, 0.5, 1 and ≥ 2; there were no subjects in this group that had AS of 1.5 or 2.5.

Statistical analysis. GraphPad Prism (version 5.04, GraphPad Software, San Diego, CA) was used for statistical analysis. Data were log-transformed for normality. One-way ANOVA was used to compare steady-state metoprolol oral clearance, M1/creatinine and creatinine among the pregnancy and postpartum visits. One-way ANOVA was used to compare atomoxetine oral clearance and urinary M1/creatinine among children with different *CYP2D6* AS. The Pearson correlation coefficient (r) was used to assess the relationship between steady-state metoprolol oral clearance and urinary M1/creatinine, DM oral clearance and plasma M1, urinary DM/DX and urinary creatinine/M1, and atomoxetine oral clearance and urinary M1/creatinine. Linear regression was used to determine whether urinary creatinine/M1 was affected by age, weight, or Tanner score. The significance of changes in urinary DM/DX, urinary creatinine/M1 and plasma M1 between baseline and fluoxetine treatment groups were assessed using a paired t-test. $P < 0.05$ was considered significant.

5.3 **Results**

5.3.1 *Effect of pregnancy on metoprolol oral clearance and urinary M1*

Due to the opportunistic nature of the study in pregnant women taking metoprolol, urine from all three stages of pregnancy and postpartum were obtained for only one subject. For the other participants, 7 women participated in one study day, 10 women participated in two study days, and 4 women participated in three study days. One subject was excluded from the analyses of pregnancy-related CYP2D6 changes because her CYP2D6 activity was unlikely to be induced during pregnancy (PM genotype). One subject was studied twice during the postpartum visit (lactating and post-lactation) and postpartum data were averaged for this subject. In contrast to reported changes in creatinine during pregnancy [57, 58], in this study, the urinary creatinine levels during pregnancy and postpartum were comparable ($P = 0.37$), therefore we used creatinine to normalize for urine concentration. Overall, the steady-state metoprolol oral clearance differed during pregnancy and postpartum ($P = 0.028$, Figure 5-1a). In particular, steady-state metoprolol oral clearance was 3.42-fold higher during late pregnancy than during postpartum visits (591 ± 412 L/hr and 173 ± 112 L/hr, respectively; Figure 5-1a). In contrast to the changes observed in steady-state metoprolol oral clearance, urinary M1/creatinine were comparable during pregnancy and postpartum visits ($P = 0.67$, Figure 5-1b). As shown in Figure 5-2, steady-state metoprolol oral clearance and urinary M1/creatinine were weakly correlated ($P < 0.0001$).

5.3.2 *Effect of CYP2D6 inhibition on dextromethorphan metrics and M1*

As reported previously, urinary DM/DX increased 218-fold (Figure 5-3a) [12, 55] and urinary M1/creatinine increased 9.56-fold between baseline and fluoxetine treatment phases (Figure 5-3b and Chapter 4 [55]). Unlike urine, we assumed that overall dilution of plasma is tightly regulated within the same individual and did not correct plasma M1 by plasma creatinine concentrations. Compared to baseline, mean dextromethorphan oral clearance decreased by 87.5-fold following fluoxetine inhibition (Figure 5-3c) [12]. Plasma M1 decreased 4.09-fold between baseline and treatment phases, albeit with large variation (440 ± 406 and 108 ± 64.4 relative intensity, respectively; Figure 5-3d).

As shown in Figures 5-4a and b, urinary DM/DX was moderately correlated with urinary creatinine/M1 ($r^2 = 0.42$, $P = 0.019$, Chapter 4, [55]) and dextromethorphan oral clearance was weakly correlated with plasma M1 ($r^2 = 0.25$, $P = 0.024$). However, plasma M1 was strongly correlated with urinary M1/creatinine in adults studied at baseline and following fluoxetine treatment ($r^2 = 0.81$, $P < 0.0001$; Figure 5-4c).

5.3.3 *Effect of CYP2D6 genotype on atomoxetine oral clearance and urinary M1*

Pediatric subjects were assigned *CYP2D6* AS of 0, 0.5, 1 and ≥ 2. A gene-dose effect on atomoxetine oral clearance and urinary M1/creatinine was observed in the children (ANOVA P < 0.0001 for both, Figure 5-5a and b). Atomoxetine oral clearance among subjects with an AS of 0 differed from subjects with an AS of 0.5, 1, and ≥ 2 (P = 0.034, < 0.0001, < 0.0001, respectively) and the oral clearance among subjects with an AS of 0.5 differed from subjects with AS of 1 or ≥ 2 (P = 0.0018 and 0.0011, respectively). Urinary M1/creatinine among subjects with an AS of 0 differed from subjects with an AS of 0.5, 1, and ≥ 2 (P = 0.0040, < 0.0001, < 0.0001, respectively) and urinary M1/creatinine among subjects with AS of 0.5 only differed from subjects with AS of ≥ 2 (P = 0.022). Atomoxetine oral clearance was strongly correlated with urinary M1/creatinine (r^2 = 0.68, P < 0.0001, Figure 5-6). Neither creatinine/M1, nor atomoxetine oral clearance was correlated with age, weight or Tanner score in the children (data not shown).

5.4 **Discussion**

In Chapter 4 we reported the detection of M1, an endogenous biomarker of CYP2D6 activity with *m/z* of 444.30, by global and targeted metabolomics methods [55]. This chapter addresses whether M1 correlates with other CYP2D6 probes, is sensitive to CYP2D6 induction in pregnant women, and if plasma M1 can be used to ascertain CYP2D6 inhibition by fluoxetine. We found that urinary M1/creatinine was correlated with steady-state metoprolol oral clearance (Figure 5-2) and atomoxetine oral clearance (Figure 5-6), in addition to urinary DM/DX (Figure 5-4a as shown previously). We also found that M1 was detectable in plasma, reflected CYP2D6 inhibition by fluoxetine, and correlated with dextromethorphan oral clearance (Figure 5-4b). Moreover, the positive correlation of M1 with the apparent oral clearance of dextromethorphan, metoprolol and atomoxetine is consistent with our hypothesis that M1 is likely a product of a biological reaction mediated by CYP2D6 [55].

In agreement with literature reports that CYP2D6 activity transiently increases during pregnancy [51-53], a 3.4-fold increase in steady-state metoprolol oral clearance was observed during late pregnancy compared to postpartum. In contrast, M1 did not differ between the pregnancy and postpartum visits. It is possible that our sample size was too small to observe changes in CYP2D6 activity as determined by M1. Alternatively, M1 may not be a sensitive marker to CYP2D6 induction. M1 may have a limited dynamic range relative to interindividual variability in CYP2D6 activity, other enzymes may contribute to M1 formation, or transporters may be involved in the renal clearance of M1. Any of these could confound the detection of pregnancy-related changes in CYP2D6.

Similarly, the fold-change in M1 levels did not reflect the magnitude of change in dextromethorphan phenotyping metrics in the adult drug interaction study. After potent CYP2D6 inhibition by fluoxetine, a 9.56-fold increase in urinary creatinine/M1 was observed, whereas a 218-fold increase was seen in urinary DM/DX in these subjects. For plasma data, after fluoxetine treatment, an average 4.09-fold decrease in plasma M1 and 87.5-fold decrease in dextromethorphan oral clearance [12] were observed. In addition to reasons provided above, if M1 has an exceedingly long half-life, the discrepancy in dextromethorphan metrics and M1 could be explained that periods longer than two weeks are needed to observe the full effect of CYP2D6 inhibition on M1 formation. If this were the case, the utility of M1 in DDI screening may be limited. However, if in the pregnancy, CYP2D6 inhibition or atomoxetine studies, the circulating concentrations of the parent of M1 were altered, then M1 alone would not be a suitable phenotyping marker for CYP2D6 activity.

Future characterization of a parent to M1 metabolite ratio may be a superior surrogate marker of enzyme activity than the urinary or plasma M1 concentrations alone. To compare the CYP2D6 activity of two individuals, or the same individual following CYP2D6 inhibition or induction, the plasma or urinary concentration of M1 alone may not be sufficient. Higher M1 concentrations may be the result of higher parent concentrations, rather than differences in the formation clearance of M1. Thus, a plasma parent to metabolite ratio, $\frac{C_{ss,parent}}{C_{ss,M1}} = \frac{CL_{M1}}{CL_{f,M1}}$, where the C_{ss} are the steady-state concentrations of parent and M1, CL_{M1} is the clearance of the M1 and $CL_{f,M1}$ is the formation clearance of M1, may be less susceptible to misinterpretation. A similar urinary metabolic ratio could be obtained, although it would also depend on renal clearances of both the parent and metabolite, as well as the formation and elimination clearances of M1. Correcting for renal clearance may be needed, but would eliminate the non-invasive advantage of urinary M1 metabolic ratios.

There was a large portion of unexplained variability when M1 was correlated with CYP2D6 probes. Plasma M1 only explained approximately 25% of the variability in dextromethorphan oral clearance. Urinary M1/creatinine only explained approximately 30% of the variability in steady-state metoprolol oral clearance, 42% in urinary DM/DX, and 68% in atomoxetine oral clearance. Again, this could be due to the fact that the parent of M1 was not available for calculating a metabolic ratio. Alternatively, other metabolic enzymes may contribute to the formation or elimination of M1, confounding its use as a CYP2D6 endogenous probe; this possibility cannot be tested until the parent of M1 is identified. Future *in vitro* studies should be performed to determine the enzymes responsible for the formation and elimination of M1 and to correlate M1 with hepatic CYP2D6 expression or activity in human liver microsomes. Nevertheless, imperfect *in vivo* correlations have been observed between CYP2D6 probes, such as between DM and debrisoquine (r^2 = 0.52-0.86 in various ethnic groups) [34, 59, 60]. The discrepancies between probes among racial groups [59-61] might be explained by variability in urine pH [14]. The intrasubject variability between dextromethorphan and debrisoquine may be due to the influence of urinary pH on DM renal clearance, but not debrisoquine [14, 17]. More broadly, as not all probes are highly correlated with one another, factors which affect the CYP2D6 phenotyping measures include: sensitivity of some probes to urine pH, metabolism by multiple enzymes, sequential drug metabolism, and extrahepatic elimination, such as renal excretion [62]. These factors will have to be tested for M1.

The distributions of urinary M1/creatinine overlapped among children with AS of 0.5, 1 and ≥ 2 which corresponds to intermediate, extensive and ultra-rapid metabolizers. The lack of discrimination of urinary M1/creatinine among non-PM groups is not surprising given that the atomoxetine oral clearance values also overlap between these AS. Similar results were seen with urinary creatinine/M1 and urinary DM/DX in the larger cohort of children (Chapter 4 [55]). Moreover, it has been reported that the CYP2D6 activity of EM subjects, even those with the same genotype, can span 2 orders of magnitude [3]. Despite the limitations of the urinary M1/creatinine measurements, this endogenous ratio is clearly different between *CYP2D6* PM (AS of 0) and non-PM subjects. Following validation, urinary M1 could be used clinically to determine whether an individual is a PM and should be initiated on a lower starting dose of drugs predominantly metabolized by CYP2D6. Screening for M1 levels might be more rapid than obtaining *CYP2D6* genotyping results and would not be subject to misclassification due to the presence of rare inactivating or null *CYP2D6* alleles.

In this study, we demonstrated that M1 was correlated with CYP2D6 activity as measured by three probe drug oral clearances, namely that of metoprolol, dextromethorphan and atomoxetine. These studies confirmed that urinary M1 is a biomarker of CYP2D6 activity in children. In addition, plasma M1 was altered upon CYP2D6 inhibition by fluoxetine in adults. We found that the urinary M1/creatinine ratio was not sensitive enough to reflect the magnitude of induction in pregnant women, discriminate between the non-PM genotypes in children, or quantitatively match the changes noted in dextromethorphan metrics upon CYP2D6 inhibition. Carefully designed clinical studies should be performed to ascertain why M1 is less sensitive to changes in CYP2D6 activity than metoprolol, dextromethorphan and atomoxetine, and whether plasma or urinary M1 is a more robust marker of endogenous CYP2D6 activity.

Following identification and validation of M1 and its parent compound, these endogenous biomarkers might be used to non-invasively phenotype for CYP2D6 activity. This could potentially eliminate the need for exogenous phenotyping probe drugs that require timed sample collections and permit an easier way to determine of CYP2D6 activity in population studies.

5.5 Acknowledgements

We are grateful to Dr. Nina Isoherranen, Dr. Justin Lutz and Jennifer Sager for providing clinical samples and pharmacokinetic data from the multiple-dose fluoxetine study in adults. We thank Dr. Mary Hebert for providing urine samples and the pharmacokinetic and clinical chemistry data from pregnant and postpartum women. We appreciate the help of Drs. J. Steven Leeder and Jacob Brown in providing urine samples and pharmacokinetic and genotypic data from the pediatric subjects.

5.6 References

1. Zanger UM, Schwab M: Cytochrome P450 enzymes in drug metabolism: regulation of gene expression, enzyme activities, and impact of genetic variation. *Pharmacology & therapeutics* 138(1), 103-141 (2013).

2. Hicks JK, Bishop JR, Sangkuhl K *et al.*: Clinical Pharmacogenetics Implementation Consortium (CPIC) Guideline for CYP2D6 and CYP2C19 Genotypes and Dosing of Selective Serotonin Reuptake Inhibitors. *Clinical pharmacology and therapeutics*, (2015).

3. Gaedigk A: Complexities of CYP2D6 gene analysis and interpretation. *Int Rev Psychiatry* 25(5), 534-553 (2013).

4. Gaedigk A, Simon SD, Pearce RE, Bradford LD, Kennedy MJ, Leeder JS: The CYP2D6 activity score: translating genotype information into a qualitative measure of phenotype. *Clinical pharmacology and therapeutics* 83(2), 234-242 (2008).

5. Chiba K, Kato M, Ito T, Suwa T, Sugiyama Y: Inter-individual variability of in vivo CYP2D6 activity in different genotypes. *Drug metabolism and pharmacokinetics* 27(4), 405-413 (2012).

6. Hicks JK, Swen JJ, Gaedigk A: Challenges in CYP2D6 Phenotype Assignment from Genotype Data: A Critical Assessment and Call for Standardization. *Current drug metabolism* 15(2), 218-232 (2014).

7. Brosen K, Gram LF, Haghfelt T, Bertilsson L: Extensive metabolizers of debrisoquine become poor metabolizers during quinidine treatment. *Pharmacology & toxicology* 60(4), 312-314 (1987).

8. Brinn R, Brosen K, Gram LF, Haghfelt T, Otton SV: Sparteine oxidation is practically abolished in quinidine-treated patients. *British journal of clinical pharmacology* 22(2), 194-197 (1986).

9. Girardin F, Daali Y, Gex-Fabry M *et al.*: Liver kidney microsomal type 1 antibodies reduce the CYP2D6 activity in patients with chronic hepatitis C virus infection. *Journal of viral hepatitis* 19(8), 568-573 (2012).

10. Jones AE, Brown KC, Werner RE *et al.*: Variability in drug metabolizing enzyme activity in HIV-infected patients. *European journal of clinical pharmacology* 66(5), 475-485 (2010).

11. Monek O, Paintaud G, Bechtel Y, Miguet JP, Mantion G, Bechtel PR: Influence of donor and recipient genotypes on CYP2D6 phenotype after liver transplantation: a study of mutations CYP2D6*3 and CYP2D6*4. *European journal of clinical pharmacology* 54(1), 47-52 (1998).

12. Sager JE, Lutz JD, Foti RS, Davis C, Kunze KL, Isoherranen N: Fluoxetine and norfluoxetine mediated complex drug-drug interactions: in vitro to in vivo correlation of effects on CYP2D6, CYP2C19 and CYP3A4. *Clinical pharmacology and therapeutics*, (2014).

13. Frank D, Jaehde U, Fuhr U: Evaluation of probe drugs and pharmacokinetic metrics for CYP2D6 phenotyping. *European journal of clinical pharmacology* 63(4), 321-333 (2007).

14. Ozdemir M, Crewe KH, Tucker GT, Rostami-Hodjegan A: Assessment of in vivo CYP2D6 activity: differential sensitivity of commonly used probes to urine pH. *Journal of clinical pharmacology* 44(12), 1398-1404 (2004).

15. U.S. Food and Drug Administration. Drug Development and Drug Interactions: Table of Substrates, Inhibitors and Inducers. *http://www.fda.gov/Drugs/DevelopmentApprovalProcess/DevelopmentResources/DrugInteractionsLabeling/ucm093664.htm#inVivo*. (3/24/2015)

16. Bozkurt A, Basci NE, Isimer A, Sayal A, Kayaalp SO: Metabolic ratios of four probes of CYP2D6 in Turkish subjects: a cross-over study. *European journal of drug metabolism and pharmacokinetics* 21(4), 309-314 (1996).

17. Labbe L, Sirois C, Pilote S *et al.*: Effect of gender, sex hormones, time variables and physiological urinary pH on apparent CYP2D6 activity as assessed by metabolic ratios of marker substrates. *Pharmacogenetics* 10(5), 425-438 (2000).

18. Streetman DS, Bertino JS, Jr., Nafziger AN: Phenotyping of drug-metabolizing enzymes in adults: a review of in-vivo cytochrome P450 phenotyping probes. *Pharmacogenetics* 10(3), 187-216 (2000).

19. Funck-Brentano C, Boelle PY, Verstuyft C, Bornert C, Becquemont L, Poirier JM: Measurement of CYP2D6 and CYP3A4 activity in vivo with dextromethorphan: sources of variability and predictors of adverse effects in 419 healthy subjects. *European journal of clinical pharmacology* 61(11), 821-829 (2005).

20. Bem JL, Peck R: Dextromethorphan. An overview of safety issues. *Drug safety* 7(3), 190-199 (1992).

21. Blake MJ, Gaedigk A, Pearce RE *et al.*: Ontogeny of dextromethorphan O- and N-demethylation in the first year of life. *Clinical pharmacology and therapeutics* 81(4), 510-516 (2007).

22. Blake MJ, Abdel-Rahman SM, Pearce RE, Leeder JS, Kearns GL: Effect of diet on the development of drug metabolism by cytochrome P-450 enzymes in healthy infants. *Pediatric research* 60(6), 717-723 (2006).

23. Kennedy MJ, Abdel-Rahman SM, Kashuba AD, Leeder JS: Comparison of various urine collection intervals for caffeine and dextromethorphan phenotyping in children. *Journal of clinical pharmacology* 44(7), 708-714 (2004).

24. Abdel-Rahman SM, Leeder JS, Wilson JT *et al.*: Concordance between tramadol and dextromethorphan parent/metabolite ratios: the influence of CYP2D6 and non-CYP2D6 pathways on biotransformation. *Journal of clinical pharmacology* 42(1), 24-29 (2002).

25. Ke AB, Nallani SC, Zhao P, Rostami-Hodjegan A, Isoherranen N, Unadkat JD: A physiologically based pharmacokinetic model to predict disposition of CYP2D6 and CYP1A2 metabolized drugs in pregnant women. *Drug metabolism and disposition: the biological fate of chemicals* 41(4), 801-813 (2013).

26. Gorski JC, Jones DR, Wrighton SA, Hall SD: Characterization of dextromethorphan N-demethylation by human liver microsomes. Contribution of the cytochrome P450 3A (CYP3A) subfamily. *Biochemical pharmacology* 48(1), 173-182 (1994).

27. Chladek J, Zimova G, Beranek M, Martinkova J: In-vivo indices of CYP2D6 activity: comparison of dextromethorphan metabolic ratios in 4-h urine and 3-h plasma. *European journal of clinical pharmacology* 56(9-10), 651-657 (2000).

28. Kohler D, Hartter S, Fuchs K, Sieghart W, Hiemke C: CYP2D6 genotype and phenotyping by determination of dextromethorphan and metabolites in serum of healthy controls and of patients under psychotropic medication. *Pharmacogenetics* 7(6), 453-461 (1997).

29. Chladek J, Zimova G, Martinkova J, Tuma I: Intra-individual variability and influence of urine collection period on dextromethorphan metabolic ratios in healthy subjects. *Fundamental & clinical pharmacology* 13(4), 508-515 (1999).

30. Hou ZY, Pickle LW, Meyer PS, Woosley RL: Salivary analysis for determination of dextromethorphan metabolic phenotype. *Clinical pharmacology and therapeutics* 49(4), 410-419 (1991).

31. Hu OY, Tang HS, Lane HY, Chang WH, Hu TM: Novel single-point plasma or saliva dextromethorphan method for determining CYP2D6 activity. *The Journal of pharmacology and experimental therapeutics* 285(3), 955-960 (1998).

32. Jacqz-Aigrain E, Funck-Brentano C, Cresteil T: CYP2D6- and CYP3A-dependent metabolism of dextromethorphan in humans. *Pharmacogenetics* 3(4), 197-204 (1993).

33. Alvan G, Bechtel P, Iselius L, Gundert-Remy U: Hydroxylation polymorphisms of debrisoquine and mephenytoin in European populations. *European journal of clinical pharmacology* 39(6), 533-537 (1990).

34. Schmid B, Bircher J, Preisig R, Kupfer A: Polymorphic dextromethorphan metabolism: co-segregation of oxidative O-demethylation with debrisoquin hydroxylation. *Clinical pharmacology and therapeutics* 38(6), 618-624 (1985).

35. Kupfer A, Schmid B, Pfaff G: Pharmacogenetics of dextromethorphan O-demethylation in man. *Xenobiotica; the fate of foreign compounds in biological systems* 16(5), 421-433 (1986).

36. Lutz U, Volkel W, Lutz RW, Lutz WK: LC-MS/MS analysis of dextromethorphan metabolism in human saliva and urine to determine CYP2D6 phenotype and individual variability in N-demethylation and glucuronidation. *Journal of chromatography. B, Analytical technologies in the biomedical and life sciences* 813(1-2), 217-225 (2004).

37. Borges S, Li L, Hamman MA, Jones DR, Hall SD, Gorski JC: Dextromethorphan to dextrorphan urinary metabolic ratio does not reflect dextromethorphan oral clearance. *Drug metabolism and disposition: the biological fate of chemicals* 33(7), 1052-1055 (2005).

38. Rostami-Hodjegan A, Kroemer HK, Tucker GT: In-vivo indices of enzyme activity: the effect of renal impairment on the assessment of CYP2D6 activity. *Pharmacogenetics* 9(3), 277-286 (1999).

39. Chainuvati S, Nafziger AN, Leeder JS *et al.*: Combined phenotypic assessment of cytochrome p450 1A2, 2C9, 2C19, 2D6, and 3A, N-acetyltransferase-2, and xanthine oxidase activities with the "Cooperstown 5+1 cocktail". *Clinical pharmacology and therapeutics* 74(5), 437-447 (2003).

40. Fux R, Morike K, Prohmer AM *et al.*: Impact of CYP2D6 genotype on adverse effects during treatment with metoprolol: a prospective clinical study. *Clinical pharmacology and therapeutics* 78(4), 378-387 (2005).

41. Anderson GD, Carr DB: Effect of pregnancy on the pharmacokinetics of antihypertensive drugs. *Clinical pharmacokinetics* 48(3), 159-168 (2009).

42. Lennard MS, Tucker GT, Silas JH, Freestone S, Ramsay LE, Woods HF: Differential stereoselective metabolism of metoprolol in extensive and poor debrisoquin metabolizers. *Clinical pharmacology and therapeutics* 34(6), 732-737 (1983).

43. Sohn DR, Kusaka M, Shin SG, Jang IJ, Chiba K, Ishizaki T: Utility of a one-point (3-hour postdose) plasma metabolic ratio as a phenotyping test using metoprolol in two east Asian populations. *Therapeutic drug monitoring* 14(3), 184-189 (1992).

44. Lennard MS, Iyun AO, Jackson PR, Tucker GT, Woods HF: Evidence for a dissociation in the control of sparteine, debrisoquine and metoprolol metabolism in Nigerians. *Pharmacogenetics* 2(2), 89-92 (1992).

45. Hemeryck A, Lefebvre RA, De Vriendt C, Belpaire FM: Paroxetine affects metoprolol pharmacokinetics and pharmacodynamics in healthy volunteers. *Clinical pharmacology and therapeutics* 67(3), 283-291 (2000).

46. Ring BJ, Gillespie JS, Eckstein JA, Wrighton SA: Identification of the human cytochromes P450 responsible for atomoxetine metabolism. *Drug metabolism and disposition: the biological fate of chemicals* 30(3), 319-323 (2002).

47. Farid NA, Bergstrom RF, Ziege EA, Parli CJ, Lemberger L: Single-dose and steady-state pharmacokinetics of tomoxetine in normal subjects. *Journal of clinical pharmacology* 25(4), 296-301 (1985).

48. Sauer JM, Ponsler GD, Mattiuz EL *et al.*: Disposition and metabolic fate of atomoxetine hydrochloride: the role of CYP2D6 in human disposition and metabolism. *Drug metabolism and disposition: the biological fate of chemicals* 31(1), 98-107 (2003).

49. Gibbs JP, Hyland R, Youdim K: Minimizing polymorphic metabolism in drug discovery: evaluation of the utility of in vitro methods for predicting pharmacokinetic consequences associated with CYP2D6 metabolism. *Drug metabolism and disposition: the biological fate of chemicals* 34(9), 1516-1522 (2006).

50. Belle DJ, Ernest CS, Sauer JM, Smith BP, Thomasson HR, Witcher JW: Effect of potent CYP2D6 inhibition by paroxetine on atomoxetine pharmacokinetics. *Journal of clinical pharmacology* 42(11), 1219-1227 (2002).

51. Hogstedt S, Lindberg B, Peng DR, Regardh CG, Rane A: Pregnancy-induced increase in metoprolol metabolism. *Clinical pharmacology and therapeutics* 37(6), 688-692 (1985).

52. Tracy TS, Venkataramanan R, Glover DD, Caritis SN: Temporal changes in drug metabolism (CYP1A2, CYP2D6 and CYP3A Activity) during pregnancy. *American journal of obstetrics and gynecology* 192(2), 633-639 (2005).

53. Wadelius M, Darj E, Frenne G, Rane A: Induction of CYP2D6 in pregnancy. *Clinical pharmacology and therapeutics* 62(4), 400-407 (1997).

54. Koh KH, Pan X, Shen HW *et al.*: Altered expression of small heterodimer partner governs cytochrome P450 (CYP) 2D6 induction during pregnancy in CYP2D6-humanized mice. *The Journal of biological chemistry* 289(6), 3105-3113 (2014).

55. Tay-Sontheimer J, Shireman LM, Beyer RP *et al.*: Detection of an endogenous urinary biomarker associated with CYP2D6 activity using global metabolomics. *Pharmacogenomics* 15(16), 1947-1962 (2014).

56. Brown J, Abdel-Rahman S, Van Haandel L, Gaedigk A, Leeder J: Single dose pharmacokinetics of atomoxetine in children with attention deficit hyperactivity disorder (ADHD) stratified by their CYP2D6 activity score (AS). *Clinical pharmacology and therapeutics* (97(Suppl 1):S97 (abstract PW-07)), (2015).

57. Pinto J, Barros AS, Domingues MR *et al.*: Following healthy pregnancy by NMR metabolomics of plasma and correlation to urine. *Journal of proteome research* 14(2), 1263-1274 (2015).

58. Chapman AB, Abraham WT, Zamudio S *et al.*: Temporal relationships between hormonal and hemodynamic changes in early human pregnancy. *Kidney international* 54(6), 2056-2063 (1998).

59. Droll K, Bruce-Mensah K, Otton SV, Gaedigk A, Sellers EM, Tyndale RF: Comparison of three CYP2D6 probe substrates and genotype in Ghanaians, Chinese and Caucasians. *Pharmacogenetics* 8(4), 325-333 (1998).

60. Irshaid YM, Al-Hadidi HF, Latif A, Awwadi F, Al-Zoubi M, Rawashdeh NM: Dextromethorphan metabolism in Jordanians: dissociation of dextromethorphan O-demethylation from debrisoquine 4-hydroxylation. *European journal of drug metabolism and pharmacokinetics* 21(4), 301-307 (1996).

61. Wennerholm A, Dandara C, Sayi J *et al.*: The African-specific CYP2D617 allele encodes an enzyme with changed substrate specificity. *Clinical pharmacology and therapeutics* 71(1), 77-88 (2002).

62. Kivisto KT, Kroemer HK: Use of probe drugs as predictors of drug metabolism in humans. *Journal of clinical pharmacology* 37(1 Suppl), 40S-48S (1997).

5.7 Tables and Figures

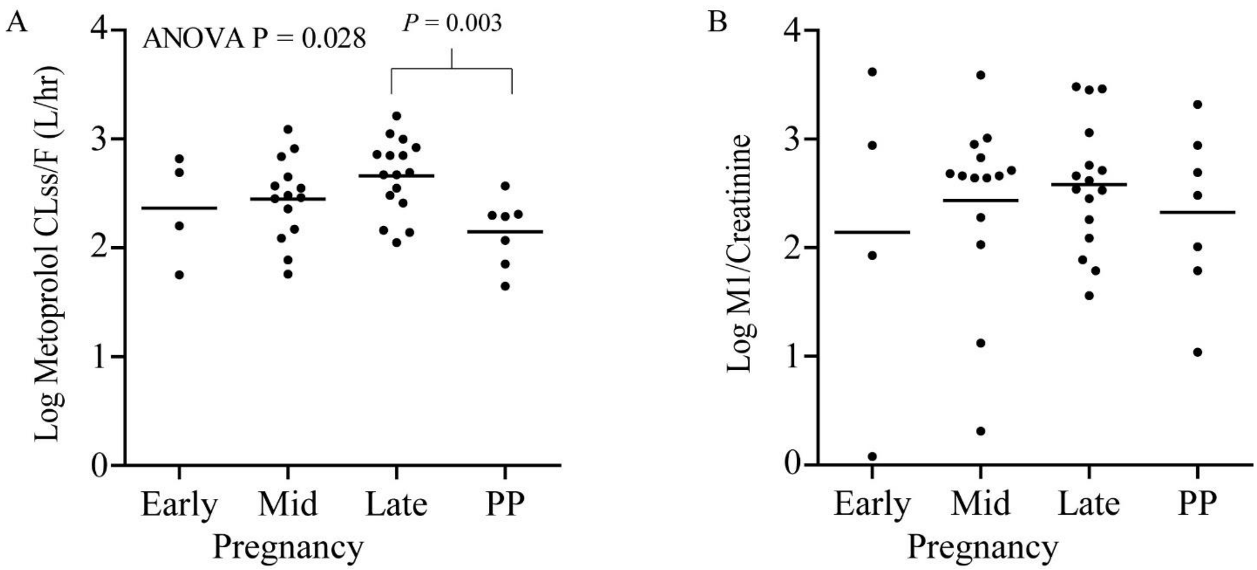

Figure 5.1 A) Steady-state metoprolol oral clearance (CL_{ss}/F) and B) M1/creatinine ratio during early, mid and late pregnancy and postpartum (PP) visits. The bars represent the mean for early (n = 4), mid (n = 14), late (n = 16) pregnancy and postpartum (n = 7). A poor metabolizer subject (n = 1) was excluded from these analyses.

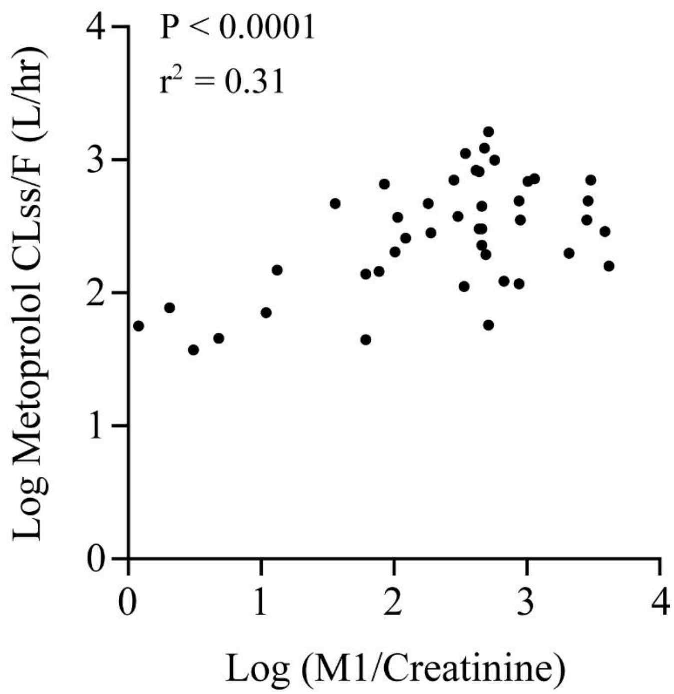

Figure 5.2 Correlation of steady-state metoprolol oral clearance and urinary M1/creatinine in women studied during pregnancy and postpartum (N = 22).

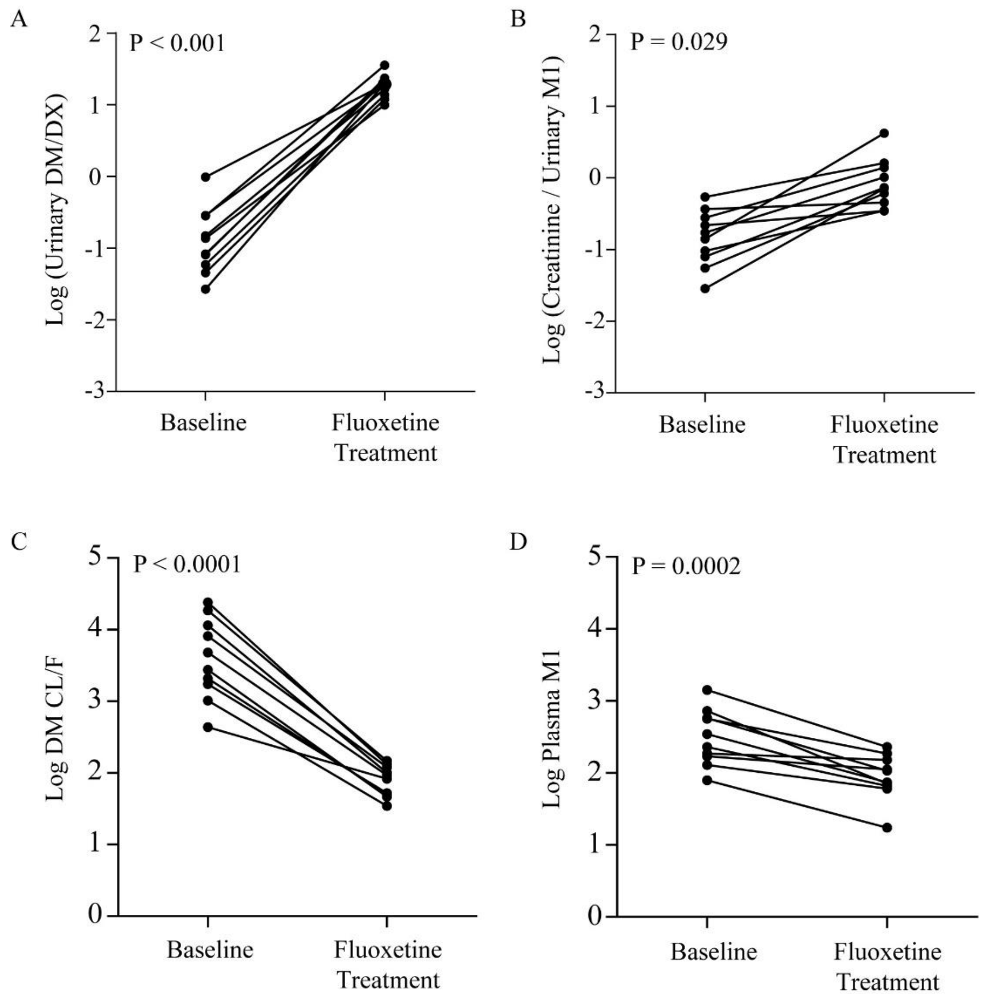

Figure 5.3 Effect of CYP2D6 inhibition by fluoxetine treatment in 10 CYP2D6 extensive metabolizers on A) urinary dextromethorphan metabolic ratio, B) urinary creatinine/M1 ratio, C) dextromethorphan oral clearance and D) plasma M1 concentrations. A) and B) are reproduced with permission from Pharmacogenomics [55].

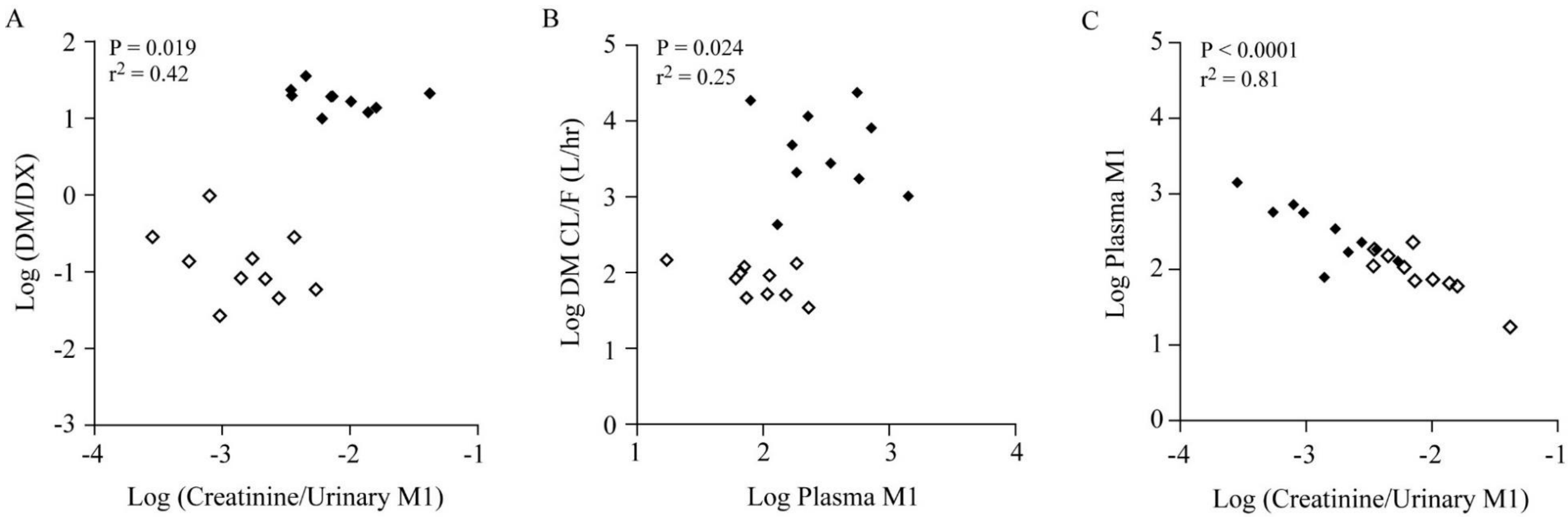

Figure 5.4 Correlations of A) dextromethorphan (DM) metabolic ratio and urinary creatinine/M1 ratio, B) dextromethorphan oral clearance (DM CL/F) and plasma M1, and C) plasma M1 and urinary creatinine/M1. Observations from baseline and fluoxetine treatment are indicated by the closed and open diamonds, respectively.

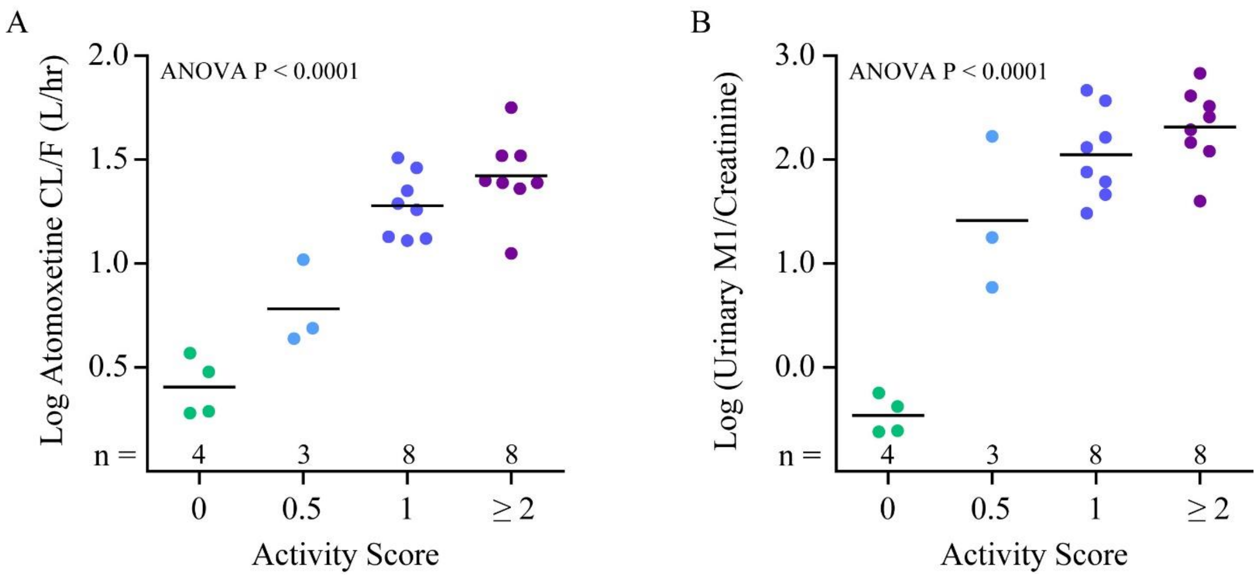

Figure 5.5 Effect of *CYP2D6* activity score in pediatric subjects (N = 23) on A) atomoxetine oral clearance and B) urinary M1/creatinine ratios. Lines depict the mean and activity score is shown by color for each individual.

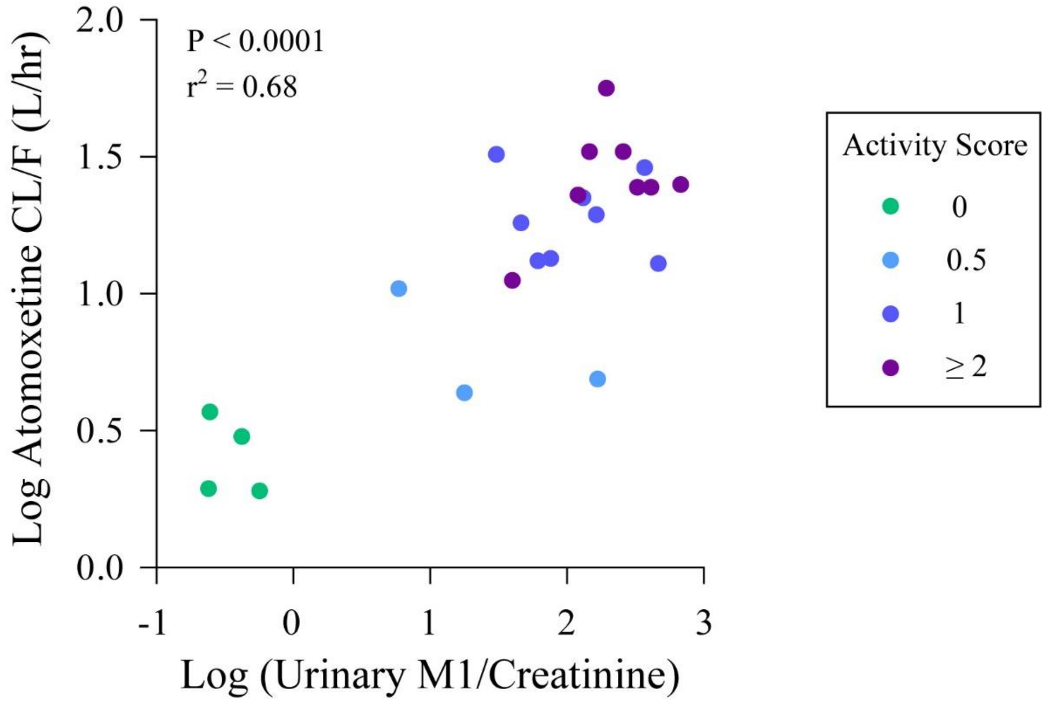

Figure 5.6 Correlation between atomoxetine oral clearance and urinary M1/creatinine. *CYP2D6* activity scores are shown by color for each individual (N = 23).

Chapter 6. Semi-purification and attempted structural identification of M1, a novel endogenous CYP2D6 biomarker

6.1 Introduction

Identification of an unknown metabolite is a central challenge in the field of metabolomics given the nature of metabolomics data and complex nature of biological fluids from which a metabolome is analyzed [1]. Nearly two thirds of the metabolites captured by mass spectrometry (MS)-based metabolomics remain unidentified [2]. MS-based metabolomics data typically consist of *m/z*, retention time and analyte intensity data for each ion. Databases, such as the METLIN (metlin.scripps.edu) or the Human Metabolome Database (www.hmdb.ca), can be used to predict identities based on *m/z*. Ions of interest can be fragmented and compared with fragmentation information if it is available in the databases, or under ideal conditions, with *m/z*, retention time and fragmentation information of an authentic standard if it is available commercially. For ions not found in databases, metabolite identification is challenging and necessitates isolation or enrichment of the ion of interest for further analysis by nuclear magnetic resonance (NMR) or MS. [3, 4]

NMR techniques are robust, non-destructive and provide rich structural content for molecular structure elucidation [4]. Compared to MS approaches, NMR sensitivity is quite low [5, 6], requiring up to milligram amounts of pure analyte. In particular, enrichment of the sample is critical as the transfer or accumulation of contaminants during extraction and chromatographic purification of dilute solutions may affect the quality of NMR data [7]. Using “virgin”, pre-rinsed glassware, avoiding plastics, and minimizing dilution and excessive solvent transfers may help to limit the introduction of impurities [7]. NMR instruments with low volume cryoprobes used to maintain high sample concentration, and high field magnets to increase the resolution of the ^{1}H NMR spectra, should be used for detailed spectra needed for structural elucidation [6, 7]. In practice, when complex mixtures are analyzed by NMR, metabolite signals overlap and may be difficult to differentiate [6]. Detection of specific metabolites in complex mixtures can be enhanced by correlating MS and NMR results of the sample [2, 6, 8]. Often, the use of both MS and NMR techniques are required for structural elucidation. Functional groups such as carboxylic acid, phenol, amino groups and sulfate conjugates may be silent using NMR approaches, but detectable using MS; whereas NMR gives structural information that is not obtainable from *m/z*, fragmentation data and molecular formula gathered or inferred by MS techniques [4].

In contrast to NMR, MS techniques can be applied to more complex mixtures, however the enrichment of the sample is still preferred. Examples of MS instruments used for traditional metabolite identification include quadrupole time-of-flight (Q-TOF), linear ion traps, triple quadrupole (QqQ), Orbitrap and Fourier transform ion cyclotron resonance systems (reviewed in [5]). High-resolution MS instruments such as Orbitrap analyzers allow for accurate mass determination at resolutions up to 100,000 and can be useful even in complex biological matrices with co-eluting, interfering compounds (reviewed in [9]). The Orbitrap has a high mass accuracy, often < 1 ppm [9, 10]. Based on the accurate mass obtained on this instrument, predicted elemental composition for the analyte can be calculated; however the number of possible elemental formulas exponentially increases with higher *m/z* values [5, 9]. Due to the high resolution nature of accurate mass data, isobaric molecular ions can be distinguished and calculations of accurate mass shifts of related species such as a parent and metabolites are permitted [5]. Inspection of high resolution analyte MS spectra may qualify or eliminate the possibility of halides, such as compounds containing chlorine or bromine, as they exhibit a characteristic isotopic pattern corresponding to their natural abundance [9]. Disadvantages to using this system are the relatively slow rate of data acquisition and low sensitivity for full scans [9, 11].

A major strength of linear ion trap (or Linear Trap Quadrupole, LTQ) systems are their multiple-stage mass spectrometry (MS^n) capabilities, which allows for collision induced dissociation (CID) of a parent ion and consecutive fragment ions [5]. Additionally, ion traps may be an order of magnitude more sensitive than QqQ systems in full scan mode, but less selective and sensitive in MRM mode and have poor mass accuracy (> 50 ppm) [5].These analytical techniques were used to attempt to identify a novel endogenous biomarker detected using global metabolomics approaches. In Chapter 4, we reported the detection of urinary biomarker of cytochrome P450 2D6 (CYP2D6) activity, M1, an ion with a *m/z* of 444.30 [12]. We determined that M1 was absent in poor metabolizers and present in non-poor metabolizers (intermediate, extensive and ultra-rapid metabolizers) in healthy pediatric subjects, and was reduced upon CYP2D6 inhibition in adult volunteers. In Chapter 5, plasma and/or urinary M1 was correlated with the oral clearances of CYP2D6 probes, dextromethorphan, metoprolol and atomoxetine in adults, pregnant women, and children with attention deficit hyperactivity disorder, respectively. We hypothesize that M1 is a product of a reaction mediated by CYP2D6. To further develop M1 as an endogenous biomarker, the identity and chemical structure of M1 needs to be established. Here we report our efforts to semi-purify M1 from human urine in a pilot study and develop liquid-liquid extraction and HPLC fraction collection methods suitable for large scale studies as outlined in Figure 6-1. We obtained clues to the structural identity of M1 using high-resolution mass spectrometry (MS^n) and nuclear magnetic resonance (NMR) by analyzing fractions containing M1.

6.2 Materials and Methods

6.2.1 *Chemicals*

Ammonium acetate, glacial acetic acid, and HPLC grade water, methanol, acetonitrile and methyl tert-butyl ether were purchased from Fisher Scientific (Waltham, MA). Midazolam was purchased from Cerilliant (Round Rock, TX).

6.2.2 *Subjects*

Collection of urine for the purposes of concentration and semi-purification of M1 was approved by the Institutional Review Board at the University of Washington (UW), Seattle, WA. Urine from a male adult volunteer was collected and stored at 4° C. A total of approximately 5.5 L of urine was collected over four separate collection intervals.

6.2.3 *Pilot sample preparation and fraction collection*

Five aliquots of 200 µL of urine were prepared by adding 800 µl ice-cold acetonitrile to each sample in order to precipitate proteins. The samples were centrifuged at 20,000 x g for 10 min at 4 °C. The supernatant was transferred to glass culture tubes and evaporated under a gentle stream of nitrogen at 25 °C. The samples were reconstituted in 25 µL methanol followed by 25 µL 0.4% acetic acid. The five reconstituted samples were pooled for fraction collection.

Fraction collection was performed using an Agilent 1200 Infinity HPLC. The pooled sample was separated using an Agilent Zorbax SB-Aq (2.1 x 50 mm x 1.8 µm) analytical column coupled to a Grace Davison Discovery Sciences (Deerfield, IL) 5 µm, 316 stainless steel and PTFE pre-column filter. The columns were maintained at 60 °C. The mobile phases consisted of A: 0.2% acetic acid in water and B: 0.2% acetic acid in methanol. The flow rate was 0.6 mL/min throughout. The elution gradient was: starting at 30% B; a linear increase to 52.5% B by 3 min, a rapid increase to 100% by 3.1 min, held until 4.1 min, followed by a rapid decrease to 30% by 4.2 min and re-equilibration to initial starting conditions. The total run time was 6.2 min. 250 µl of sample was injected repeatedly at 15 µL until expended. Fractions were collected using an Agilent 1260 fraction collector every 18 seconds for the first 3 min for a total of ten fractions, referred to as fractions A through J. Due to the dilute nature of the fractions (about 3 mL each), each fraction was evaporated to dryness under nitrogen and reconstituted in 20 µL methanol followed by 20 µL 0.4% acetic acid.

Fractions A through J were analyzed for the abundance of M1 by LC-MS/MS as described below. To ascertain the contribution of interfering compounds (ions) in selected fractions, we performed additional MS scans. The fraction with the highest abundance of M1 was selected for a second semi-purification step using fraction collection. This second fraction collection method used the same columns and mobile phases described for the first fraction collection method. The selected fraction was diluted by adding 30 µl 0.2% acetic acid in 1:1 methanol:water. In this second fraction collection step, 2 µL was injected and an isocratic elution method (35% B) was used. Fractions were collected every 24 seconds for the first four minutes for a total of 10 fractions; these were referred to as sub-fractions 1 through 10. The abundance of M1 in these fractions was confirmed by LC-MS/MS. The sub-fraction with the highest abundance of M1 was used for initial MS^n experiments conducted using a liquid chromatography-linear trap quadrupole-orbitrap (LTQ-OT) at UW as described below.

6.2.4 *Scale-Up Method Development*

Selection of chemical extraction solvent. To extract large volumes of urine, a liquid-liquid extraction procedure was deemed to be more appropriate than an acetonitrile protein precipitation procedure. Hexane, methyl tert-butyl ether (MTBE), 7:3 toluene:methylene chloride, and ethyl acetate were selected as potential organic solvents for M1 urine extraction. Since the structure of M1 is unknown, midazolam (MDZ) was arbitrarily chosen as a pseudo-internal standard. Each sample contained 50 µL of MDZ (0.6 µM) and 1 mL of urine to which 3 mL of organic solvent was added. Samples were placed in a horizontal shaker for 20 min at high speed and then centrifuged at 664 x g for 20 min. The organic layer was transferred to a glass culture tube and evaporated under a gentle stream of nitrogen. Samples were reconstituted using 100 µl methanol and 100 µl of 0.4% acetic acid in water. Samples were transferred to a microcentrifuge tube and centrifuged at 20,000 x g for 5 min. in order to remove debris. The supernatant was transferred to LC vials containing glass inserts and stored at 4 °C until LC-MS/MS analysis for M1 abundance.

Acidification or basification of urine prior to organic extraction. In order to test the effect of acids and bases on removing impurities in the urine, 1 M hydrochloric acid (pH 0), 1 M acetic acid (pH 2.4), 1 M sodium hydroxide (pH 14) and saturated sodium borate (pH 10) were used. Two milliliters of these solutions or deionized water were added to glass culture tubes and the urine samples were prepared as stated above with MTBE as the organic solvent. Prepared samples were stored at 4 °C until LC-MS/MS analysis for M1 abundance.

6.2.5 *Large scale extraction of M1*

Liquid-liquid extraction of M1 in urine. Liquid-liquid extraction was performed by combining 200 mL of urine and 200 mL MTBE in a separatory funnel. Contents of the separatory funnel were shaken gently by hand for 15 min with occasional venting. The mixture was then allowed to rest until the two phases were clearly separated. The organic phase was transferred to a round bottom flask and concentrated under partial vacuum using a rotary evaporator until the volume was reduced to less than 5 mL. The remaining organic phase was transferred to a single glass culture tube and was evaporated to dryness under a gentle stream of nitrogen. The resulting residue was reconstituted in methanol followed by an equal volume of 0.4% acetic acid in water.

Large scale urine extractions were performed on four different days. Over all of the extraction days, a total of about 5 L of urine was extracted and resulted in a final volume of about 12 mL. After 2 L of urine were extracted, resulting in final volume of about 2 mL, the sample was semi-purified by C-18 HPLC, subject to NMR analysis as described below and then semi-purified again by C-18 HPLC before being combined with the remaining urine extract (from 3 L of urine) that had already undergone extraction by MTBE and semi-purification by C-18 HPLC (Figure 6-1). This pooled urine extract was subject to an additional semi-purification step by pentylfluorophenyl HPLC described below.

Semi-purification of M1 in urine by C-18 HPLC. The first semi-purification step was performed using a Hewlett Packard (HP) (Palo Alto, CA) series 1100 LC. Separation of 20 µL injections was achieved using a 5 µm, 4.6 x 250 mm Phenomenex (Torrance, CA) Luna C-18(2) column coupled to a C-18 guard column. Both columns were heated to 30° C. The mobile phases consisted of 10 mM ammonium acetate, pH 4 (mobile phase A) and methanol (mobile phase B) at a flow rate of 1.5 mL/min. The mobile phase gradient was: 50% B from 0 to 8 min, increasing to

90% B by 9 min and held until 13 min, returning to initial conditions of 50% B by 14 min, and finally re-equilibration at 50% B for a total run time of 17.5 min. A T-splitter divided the flow between a HP series 1100 single quadrupole mass spectrometer (MS) operated in positive electrospray ionization mode, and a HP diode array detector (DAD) coupled to a Gilson 203B fraction collector. The majority of the flow was directed toward the DAD and fraction collector. UV wavelengths of 254.4 nm, 260.4 nm and 210.8 nm were monitored throughout the sample separation. M1 was monitored by selective ion monitoring MS of *m/z* 444.3 with a dwell time of 580 msec. The MS fragmentor was set to 135 V.

The elution time of M1 was around 6.9 min. For each collection day, ten fractions were collected with equal retention times over the elution period of the M1 peak (about 1.1 min range) as monitored by MS. The abundance of M1 in each fraction was verified by LC-MS/MS as described below. Fractions from the extract starting from 2 L of urine were prepared for NMR analysis as stated below. Eventually, both these fractions and fractions containing M1 from the remaining 3 L of urine were pooled, evaporated and concentrated by rotary evaporator. When the volume was reduced (< 5 mL), the fraction was transferred to a tube and evaporated under nitrogen gas. The resulting residue was reconstituted in 500 µl methanol and 500 µl 0.4% acetic acid.

Semi-purification of M1 by Penytlfluorophenyl HPLC. Following semi-purification using the Luna C-18(2) column, an orthogonal pentylfluorophenyl (PFP) column was used to further separate M1 from other compounds in the pooled sample. This was accomplished using a HP series 1100 LC with a HP series 1100 single quadrupole MS, and a HP DAD coupled to a Gilson 203B fraction collector as described above. Separation of 20 µL injections was achieved using a 3 µm, 4.6 x 150 mm Supelco (Bellefonte, PA) Discovery HS F5 (PFP) column preceded by a

Phenomenex phenyl guard column. Both columns were heated to 30˚ C. The flow rate was 1.5 mL/min, and the mobile phase consisted of A: 10 mM ammonium acetate, pH 4 and B: acetonitrile. The following gradient profile was used: 57% B held for 2 min, a gradual increase to 68% B by 9.5 min, a ramp up to 90% B by 11.5 min and held until 14 min, a decrease to 57% B by 16 min and re-equilibration until 18.5 min. As before, a T-splitter divided flow between the MS and the UV detector coupled to the fraction collector.

The retention time of M1 was approximately 7.9 min. Over the course of six days, 8 to 9 fractions with equal retention times were collected over the elution time of M1 (roughly 1.8 min total). The presence of M1 in each fraction was verified by LC-MS/MS as described below. As the elution time of fractions with similar M1 abundances shifted slightly from day-to-day, daily fractions were assigned to one of 10 sections, referred to as fractions α – κ, spanning the distribution of the M1 peak abundances. Fractions from the same section of the M1 abundance distribution were pooled across days and stored at -80˚ C. The final volume of each pooled fraction was between 15-20 mL.

6.2.6 *Detection of M1 abundance using liquid chromatography-mass spectrometry.*

The abundance of M1 was determined using an Agilent 1290 Infinity HPLC coupled to an Agilent 6460 Triple Quadrupole (QqQ) MS operated in positive electrospray ionization mode. As described in the first semi-purification step, samples were separated using an Agilent Zorbax SB-Aq (2.1 x 50 mm x 1.8 µm) analytical column coupled to a Grace Davison Discovery Sciences (Deerfield, IL) 5 µm, 316 stainless steel and PTFE pre-column filter following a 2 µL injection. The columns were heated to 60 °C. The mobile phases consisted of A: 0.2% acetic acid in water and B: 0.2% acetic acid in methanol. The elution gradient was: starting at 30% B; a linear increase to 52.5% B by 3 min, a rapid increase to 100% by 3.1 min, held until 4.1 min, followed by a rapid decrease to 30% by 4.2 min and re-equilibration to initial starting conditions. The total run time was 6.2 min. M1 was detected using multiple reaction monitoring (*m/z* 444.3 → 98.1) with a set collision energy of 40 V as previously described [12]. To detect impurities, we performed additional MS scans within the range of *m/z* 100-1000 using the same LC-MS gradient and instrument parameters.

6.2.7 *Application of analytical tools to elucidate the identity of M1*

Liquid chromatography-linear trap quadrupole-orbitrap (LTQ-OT). MS analysis of pilot sample fractions was conducted at UW. Samples were analyzed using a Waters (Milford, MA) Acquity HPLC coupled to a Finnigan (Hemel Hempstead, UK) linear trap quadrupole (LTQ) in-line with a Thermo Fisher Scientific (San Jose, CA) linear trap quadrupole-orbitrap (LTQ-OT). Samples were separated using an Agilent Zorbax SB-C8 (2.1 x 30 mm x 3.5 µm) guard column coupled to an Agilent Zorbax SB-Aq (2.1 x 50 mm x 1.8 µm) analytical column. Both columns were heated to 60 °C. The aqueous and organic mobile phases consisted of 0.2% acetic acid in water (mobile phase A) and 0.2% acetic acid in methanol (mobile phase B), respectively. The method consisted of a flow rate of 0.6 mL/min and a gradient elution of 30% B, a linear increase to 54% B by 3 min, a rapid increase to 100% B by 3.1 min where it was held until 4.5 min, and decrease back to initial conditions by 4.6 min, where it was allowed to equilibrate until 8 minutes. The injection volume was 5 µL of sample. The instrument was calibrated on the same day as sample analysis and found to have an error of –0.523 ppm with respect to the reference mass. The scan window ranged from *m/z* 100-600 and resolution was set at 15,000 or 60,000 for LTQ MS^2

and MS^3 experiments and 100,000 to obtain the accurate mass of the parent by Fourier-transform MS. Collision energies were varied between 45, 50, 55, and 60 V.

MS analyses of sample fractions from the large preparation were conducted at BMS. The samples were analyzed using an Agilent 1290 infinity HPLC system coupled to a LTQ-Orbitrap mass spectrometer (Thermo Fisher Scientific). Chromatographic separation was performed with a Waters Atlantis C18 (2.1 x 150 mm x 5 µm) column at a flow rate of 0.25 mL/min. The column was eluted with water containing 0.1% formic acid and acetonitrile. The HPLC separation used a linear gradient program of 10% B for 2 min, 10-40% B for 18 min, 40%-90% for 2 min, 90% for 3 min before returning to 10%. The HPLC eluent was directly coupled to a LTQ/Orbitrap. MS analysis was conducted with an electrospray ionization source. The capillary tempurature was 275 °C, the source voltage was 4 kV. Three scan events were used as follows: (1) *m/z* 200-600 full scan MS operated at a target mass resolution of 30,000, (2) target MS^2 scan of *m/z* 444.3 with a mass resolution of 7,500 and (3) data–dependent MS^3 scan with a mass resolution of 7,500 on the most intense ion from the MS^2 scan.

NMR Analysis. Following C-18 HPLC semi-purification, fractions were prepared for NMR analysis. Fractions 1-10 from the initial 2 L of urine were collected with equal retention times over the elution period of the M1 peak (about 1.1 min range, about 15-20 mL final volume per fraction per day) as monitored by MS. This was done over 2 separate days and the abundance of M1 in each fraction was verified by LC-MS/MS as described above. Fractions with similar M1 abundances were pooled and evaporated to dryness under nitrogen. It was thought that the ammonium acetate present in the residue would be problematic once reconstituted for the NMR analysis. In order to eliminate the ammonium acetate in the fractions, each fraction was re-extracted with MTBE. Briefly, 350 µL of HPLC-grade water was added to each tube in order to reconstitute the sample, then 800 μL of MTBE was added. The entire sample was transferred to a glass tube and capped. The sample was then agitated on a horizontal shaker for 20 minutes and then aqueous and organic phases were allowed to separate. Twenty microliters of the organic phase was transferred to a clean LC insert for LC-MS/MS analysis and 1.2 mL of the organic phase was transferred to a new glass tube for NMR analysis. Both aliquots were evaporated to dryness under nitrogen. The aliquots set aside for LC-MS/MS analysis were reconstituted in 20 μL 0.4% acetic acid. The remaining moisture in the NMR samples was removed by a Speed-Vap solvent evaporation system. Fractions 1-10 were subject to NMR analysis in parallel with LC-MS/MS analysis.

NMR was performed by the Northwest Metabolomics Research Center using a Bruker (Billerica, MA) AVANCE III 800 MHz equipped with an HCN cryoprobe spectrometer equipped with a room temperature probe, suitable for ^{1}H inverse detection with Z-gradients at 298 K. This instrument can be used to analyze samples with low concentrations. The dried residues of HPLC fractions were dissolved in 200 μL phosphate buffer prepared in deuterated water (0.1M; pH =7.4) containing 0.1 mM quantitative and chemical shift reference, TSP (3-(trimethylsilyl) propionic-2,2,3,3-d_4 acid sodium salt) and the solutions transferred to 3 mm NMR tubes for analysis. One-dimensional ^{1}H NMR spectra were obtained using a one pulse sequence that included residual water signal suppression from a pre-saturation pulse during the relaxation delay. For each sample, 32k data points were acquired using a spectral width of 9600 Hz and a relaxation delay of 3 s. The data were processed using a spectral size of 32k points and by multiplying with an exponential window function equivalent to a line broadening of 0.3 Hz. The resulting spectra were phase and baseline corrected and referenced with respect to the internal TSP signal. Bruker Topspin version 3.1 software package was used for NMR data acquisition and processing, respectively.

MS2 and MS3experiments performed at BMS. Ten fractions, α-κ, extracted by MTBE and having undergone a two-step semi-purification, were analyzed by LC-MS/MS for relative abundance of M1. The four fractions with the highest relative abundance of M1, fractions γ – ζ, were sent on dry ice overnight to Bristol-Myers Squibb (BMS) for MS^2 and MS^3 analysis.

6.2.8 *Data analysis*

Analysis of LC-MS/MS data was performed using Agilent Mass Hunter Qualitative Analysis (version B.05.00). Analysis of LC-UV/MS data was performed using Agilent ChemStation. Thermo Xcalibur 2.2 was used for the analysis of LTQ-OT data, the visual inspection of mass spectral data, and for elemental formula predictions based on accurate *m/z*. Criteria for elemental formula predictions included an odd number of nitrogens according to the nitrogen rule of mass spectrometry and an error less than 5 ppm from the observed *m/z*. Predicted elemental formulas were queried for matching formulas of known endogenous compounds in NIST database (webbook.nist.gov/chemistry) searches.

6.3 **Results**

6.3.1 *M1 abundance in pilot sample preparations*

As outlined in Figure 6-1, the pilot experiment was used to determine whether acetonitrile protein precipitation and semi-purification of M1 using a single column chemistry would be sufficient for MS^n experiments. A total of 1000 µL urine was prepared and pooled. After an initial fraction collection, fractions A through J were analyzed by LC-MS/MS in order to identify the fraction(s) containing M1. M1 was highest in fraction G and lower in fraction H (approximately

5×10^4 and 2×10^4 cps, respectively). We chose fraction G to separate and collect sub-fractions in order to obtain a sample with high M1 abundance and fewer contaminants. There were greater than 1500 mass features present in fraction G as determined by a MS scan. Using an isocratic method to separate fraction G, we obtained sub-fractions G1-G10. LC-MS/MS analysis indicated that sub-fraction G7 contained the highest abundance of M1 among sub-fractions. Fraction G7 was selected for LTQ-OT experiments.

6.3.2 *High-resolution MS of M1 and MS^2 by LTQ*

Fourier-transform MS (MS^1) analysis of sub-fraction G7 at 100,000 resolution revealed the accurate *m/z* of M1 to be *m/z* 444.3109. On this system, M1 retention time was 1.52 min. Spectra from *m/z* 443 – 447 indicated that the putative M1+1 ion, *m/z* 445.3142 was 13% of M1 abundance, and the M1+2 ion, *m/z* 446.3272 was 1.8% of M1 abundance (Figure 6-2). Due to the isotopic pattern of the spectra, halides such as bromine and chlorine are unlikely to be present in M1. According to the nitrogen rule, since M1 has an odd nominal mass, then M1 is likely to contain an odd number of nitrogens. Using the accurate *m/z* and the expected organic elements (carbon, hydrogen, oxygen and nitrogen), one elemental formula, $C_{27}H_{42}O_4N$, was predicted. As shown in Table 6-1 and Figure 6-3, the predicted *m/z* and spectra of $C_{27}H_{42}O_4N$ (0.33 ppm error) closely matched that of observed M1. Including phosphorous or sulfur in addition to the expected organic elements yielded three predicted elemental formulas: $C_{21}H_{43}O_3N_5P$, $C_{15}H_{44}O_2N_9P_2$, and $C_{20}H_{42}O_2N_7S$. Predicted *m/z* and spectra closely match that of the observed M1 (Tables 6-1, Figures 6-4, 6-5 and 6-6).

LTQ analysis of the sub-fraction G7 (444.3 →) at 15,000 resolution and a collision energy of 45 V yielded the product ion spectra shown in Figure 6-7. The product ions *m/z* 150.1, 206.2

and 370.3 (predicted formulas of $C_{10}H_{16}N$, $C_{14}H_{24}N$, and $C_{24}H_{36}O_2N$, respectively) were observed previously on a LC-QTOF system [12]. The MS^2 analysis using this LTQ system revealed product ions that included *m/z* 426.3 (predicted formula $C_{27}H_{40}O_3N$), a loss of 18 mass units from M1, suggesting the loss of water. Losses of 72, 73 and 74 mass units to *m/z* 372.3, 371.3 and 370.3 (predicted formulas of $C_{24}H_{38}O_2N$, $C_{24}H_{37}O_2N$, and $C_{24}H_{36}O_2N$, respectively) may indicate subsequent or related losses of hydrogens. Additionally, a loss of 88 was observed to yield a product ion of *m/z* 356.3 (predicted formula of $C_{23}H_{34}O_2N$). These formulas do not appear to correspond to known endogenous CYP2D6 substrates as determined by a database search. A system peak of *m/z* 200.4 was observed throughout the course of the run and is unlikely to be a product ion of M1. These MS^2 fragmentation spectra were confirmed by collaborators at BMS (Figure 6-15).

6.3.3 *Selection of appropriate scale-up methodology*

To separate M1 from interfering compounds in the urine, we considered solid phase extraction or liquid-liquid extraction steps. Due to the large volume of urine to be used, solid phase extraction was deemed to be too impractical and we proceeded to test four organic solvents with differing polarities—hexane, MTBE, toluene:methylene chloride and ethyl acetate—as candidate liquid-liquid extraction solvents. Peak area ratios of M1/MDZ were compared for each solvent. Although MDZ would likely have different extraction efficiencies than M1 in the four solvents, we assumed that the peak area ratio would give a rough approximation of a preferential extraction solvent for M1. The absolute raw M1 peak height was greatest in the sample extracted using MTBE and followed by the sample extracted using ethyl acetate (Table 6-2). M1 was extracted poorly by toluene:methylene chloride and hexane. Peak height ratio of M1/MDZ among samples was highest for the sample which used MTBE, followed closely by ethyl acetate and then by toluene:methylene chloride and hexane. Due to the apparent preference of M1 for MTBE over the other solvents tested, this solvent was chosen for subsequent M1 liquid-liquid extractions.

With the aim of further chemical purification, the effect of acidification and basification of the urine prior to organic extraction by MTBE was investigated. The additions of acid (1 M hydrochloric acid or 1 M acetic acid) or base (1 M sodium hydroxide or saturated sodium borate) to urine were compared to the addition of deionized water prior to liquid-liquid extraction. In each instance, the addition of acid or base resulted in a reduction (with the addition of acetic acid) or elimination (with the addition of hydrochloric acid and both bases) of M1 when analyzed by LC-MS/MS (data not shown), thus these approaches were abandoned.

6.3.4 *Large scale extraction of M1*

Approximately five liters of urine were used in the large scale MTBE extraction of M1. After chemical extraction, other impurities in the sample were reduced by the use of a HPLC C-18 (4.6 mm) semi-preparative column and monitored simultaneously by UV and MS detectors. The C-18 reverse phase column was chosen because the stationary phase is typically reliable for small molecule retention. There was no apparent UV signal for M1 in the wavelengths monitored. However, using UV detection, we were able to avoid retention time windows where there were impurities overlapping with M1 elution. A slowly increasing LC elution gradient was designed to collect M1 in fractions (fractions 1-10) where there were minimal UV signals from impurities (Figure 6-8). However, following pooling and concentration of the resulting fractions from the HPLC C-18 method, reinjection of the pooled sample onto the same semi-preparative column showed a large UV peak in the same retention time window as M1 (Figure 6-9). The large increase in UV absorbance in the M1 retention time window was likely due to the impurities now detectable following pooling and concentration of the fractions.

An orthogonal method was needed to separate the impurities from M1. A PFP column was selected for this purpose as the stationary phase is quite different from the C-18 column stationary phase used in the previous semi-purification step. Interestingly, there was a large effect of the choice of organic mobile phases used for M1 peak elution with this column. When using methanol as mobile phase B, M1 eluted at 100% B and was deemed as not useful in separating M1 from other impurities. When using acetonitrile as mobile phase B, M1 eluted at approximately 7.9 min when the gradient was less than 70% B. M1 eluted separately from the UV absorbing impurities, which eluted before 5 minutes (Figure 6-10). Fractions were collected as described and sent to BMS for MS^n and NMR analysis.

6.3.5 *MS^3 analysis of pilot and large scaled semi-purified samples*

LTQ MS^3 analyses were attempted on sub-fraction G7 prepared during the pilot experiments. MS^3 fragmentation of m/z 444.3→372.3→, m/z 444.3→371.3→, m/z 444.3→356.3→ (CE = 50, 45, 45 V) was problematic due to a low signal-to-noise ratios (<3). MS^3 fragmentation of m/z 444.3→426.4→ (CE = 45 V) yielded spectra shown in Figure 6-11. This signal-to-noise ratio was reasonable (≥3), but confirmation of these spectra may be needed due to low signal intensities. The most abundant product ion, m/z 382.5 results from a loss of m/z 44 from m/z 426.4, which suggests a possible loss of CO_2. Also notable is a loss of m/z 28 from m/z 426 to m/z 398.6, which could be a loss of CO. However, both losses of CO_2 and CO from the molecule are unlikely.

Using the semi-purified fractions that were sent to BMS for MS^n analysis, our collaborators were able to obtain the MS^3 fragmentation spectra of *m/z* 444.3→372.3→ (Figure 6-12). This spectral pattern supports the relationship of *m/z* 370.3 and 371.3 ions with *m/z* 372.3.

6.3.6 *NMR*

Following chemical extraction and C-18 semi-purification, aliquots of fractions 1-10 were analyzed for relative abundance of M1 by LC-MS/MS (Figure 6-13). At the same time, aliquots of fractions 1-10 were also analyzed by ^{1}H NMR (Figure 6-14). NMR results were inconsistent with LC-MS/MS results. Following NMR, we did not observe a peak that was highest in fraction 2 and subsequently decreasing through fraction 10, as was seen in the abundance of M1 by LC-MS/MS. The NMR data were deemed uninterpretable for structural information of M1, likely due to the presence of interfering compounds.

6.4 **Discussion**

Previously, a unique unknown ion, M1, was detected in human urine and plasma as a biological molecule responsive to alterations in CYP2D6 activity ([12] and Chapter 4). The chemical identity of M1 is needed for further investigation of M1 as an endogenous biomarker of CYP2D6 activity. This study provides clues to the structural identity of M1. Semi-purification and enrichment of M1 from urine samples was developed using liquid-liquid extraction and semi-preparative C-18 and PFP HPLC columns. Based on accurate *m/z* 444.3109, four elemental formulas containing an odd number of nitrogens within 5 ppm of the accurate *m/z* were predicted. MS^2 and MS^3 spectrum obtained from fraction collection and semi-purification of M1 revealed unique fragments that may be useful in M1 structural elucidation. Our collaborators at BMS were able to confirm MS^1 spectra and accurate *m/z* of M1 (*m/z* 444.3109) on their system (data not shown). Spectra from MS^2 analysis of M1 at BMS (Figure 6-15) yielded a spectra quite similar to the one obtained at UW (Figure 6-7a). Notable differences between these two spectra are that ion *m/z* 426.3 observed at UW (Figure 6-7a) was low or absent in the analysis by BMS (Figure 6-15), and the low abundance ion *m/z* 326.3 observed at BMS was absent in the spectra obtained at UW. As the ion *m/z* 426.3 observed in MS^2 analysis at UW was not reproduced by BMS, it might be a contaminant in the pilot sub-fraction G7 analyzed at UW, which was removed upon large scale extraction of the fractions provided to BMS. Further confirmation of related ions *m/z* 426.3 and 326.3 are needed. Based on the proposed elemental formulas, MS^n, and searches using metabolomics database, the identity of M1 is still unclear. Additional experiments with M1 fractions at higher concentrations may provide additional fragmentation information.

NMR analyses at UW showed inconsistent results with MS^n results. The purity and abundance of M1 in the NMR sample had a profound effect on the resulting spectrum. It is likely that the fractions used for NMR analysis were not enriched with M1 to the extent needed, and that M1 NMR signals were obscured by contaminants in the sample. Clearly, future analysis by NMR would necessitate more pure and concentrated M1 fractions. This might be accomplished by using larger urine volumes, adding additional purification steps or employing different isolation methods for M1 such as ion exchange columns, or supercritical fluid chromatography/MS.

Identification of the M1 structure by MS and NMR techniques might lead to the determination of its parent compound. Moreover, upon the elucidation of the structure of M1 and its parent, authentic standards could be purchased or synthesized, and a targeted LCMS assay for the quantitation of M1 and its parent could be developed. In addition, structural elucidation could lead to *in vitro* studies identifying the primary enzymatic routes of metabolism and provide information on whether the parent is metabolized to M1 solely by CYP2D6 or if there are other enzymes involved. Furthermore, *in vitro* kinetic studies of M1 and its parent will inform *in vivo* predictions of the utility of these endogenous biomarkers in detecting CYP2D6 drug interactions or specific CYP2D6 genotypes. *In vivo* characterization of the disposition of M1 and its parent would include the determination of the endogenous half-life of M1 and its parent, and inter- and intra-individual variation in their urinary and plasma concentrations. Upon characterization and validation of M1 and its parent, these endogenous compounds could provide CYP2D6 phenotyping information for past, current and future studies without designing additional phenotyping arms to ascertain CYP2D6 activity. It is possible that M1 and its parent could be included in a standard panel of endogenous biomarkers that screen for drug interactions in first-in-human studies, or for selecting appropriate doses of drugs primarily metabolized by CYP2D6.

6.5 **Acknowledgements**

We would like to thank Dr. Sibylle Heidelberger and Dr. Nagana Gowda for their expert consulting in LTQ-OT and NMR data interpretation, respectively. We are grateful to our collaborators at BMS, Dr. Weiqi Chen for MS^n of M1 fractions and also Dr. Justin Lutz and Dr. Jinping Gan. We would like to thank Brian Phillips for assistance with LC-MS method development and Dr. Danny Shen for allowing us to use the LC-MS/UV and fraction collector. We are grateful to Dr. Kenneth Thummel and Dr. Danny Shen for loaning us the semi-preparative columns. We acknowledge Tauri Senn and AJ Sommers for their contribution to the technical work.

6.6 References

1. Wishart DS: Advances in metabolite identification. *Bioanalysis* 3(15), 1769-1782 (2011).

2. Gu H, Gowda GA, Neto FC, Opp MR, Raftery D: RAMSY: ratio analysis of mass spectrometry to improve compound identification. *Analytical chemistry* 85(22), 10771-10779 (2013).

3. Sumner LW, Amberg A, Barrett D *et al.*: Proposed minimum reporting standards for chemical analysis Chemical Analysis Working Group (CAWG) Metabolomics Standards Initiative (MSI). *Metabolomics : Official journal of the Metabolomic Society* 3(3), 211-221 (2007).

4. Corcoran O, Spraul M: LC-NMR-MS in drug discovery. *Drug discovery today* 8(14), 624-631 (2003).

5. Prasad B, Garg A, Takwani H, Singh S: Metabolite identification by liquid chromatography-mass spectrometry. *TrAC Trends in Analytical Chemistry* 30(2), 360-387 (2011).

6. Wolfender JL, Marti G, Thomas A, Bertrand S: Current approaches and challenges for the metabolite profiling of complex natural extracts. *Journal of chromatography. A* 1382, 136-164 (2015).

7. Molinski TF: NMR of natural products at the 'nanomole-scale'. *Natural product reports* 27(3), 321-329 (2010).

8. Wei S, Zhang J, Liu L *et al.*: Ratio analysis nuclear magnetic resonance spectroscopy for selective metabolite identification in complex samples. *Analytical chemistry* 83(20), 7616-7623 (2011).

9. Jhajra S, Prasad B, Shah J, Singh S: High-resolution MS for drug metabolite identification. *Applications of High-Resolution Mass Spectrometry in Drug Discovery and Development*, 22-40 (2013).

10. Holcapek M, Kolarova L, Nobilis M: High-performance liquid chromatography-tandem mass spectrometry in the identification and determination of phase I and phase II drug metabolites. *Analytical and bioanalytical chemistry* 391(1), 59-78 (2008).

11. Rousu T, Herttuainen J, Tolonen A: Comparison of triple quadrupole, hybrid linear ion trap triple quadrupole, time-of-flight and LTQ-Orbitrap mass spectrometers in drug discovery phase metabolite screening and identification in vitro--amitriptyline and verapamil as model compounds. *Rapid communications in mass spectrometry : RCM* 24(7), 939-957 (2010).

12. Tay-Sontheimer J, Shireman LM, Beyer RP *et al.*: Detection of an endogenous urinary biomarker associated with CYP2D6 activity using global metabolomics. *Pharmacogenomics* 15(16), 1947-1962 (2014).

6.7 Tables and Figures

Table 6.1 Predicted molecular formula containing carbon, hydrogen, oxygen, nitrogen and phosphorus or sulfur for accurate *m/z* 444.3109

Elemental Formula	Theoretical *m/z*	Delta PPM
$C_{27}H_{42}O_4N$	444.3108	-0.327
$C_{21}H_{43}O_3N_5P$	444.3098	1.996
$C_{15}H_{44}O_2N_9P_2$	444.3088	4.319
$C_{20}H_{42}O_2N_7S$	444.3115	-1.375

Table 6.2 LC-MS/MS signal intensity of midazolam and M1 following chemical extraction from urine

Extraction Solvent	MDZ Peak Height	M1 Peak Height	Peak Height Ratio
MTBE	10068	3383	0.34
Ethyl acetate	5855	1841	0.31
7:3 toluene:methylene chloride	6556	139	0.021
Hexane	8000	15	0.0019

MTBE, methyl tert-butyl ether
MDZ, midazolam

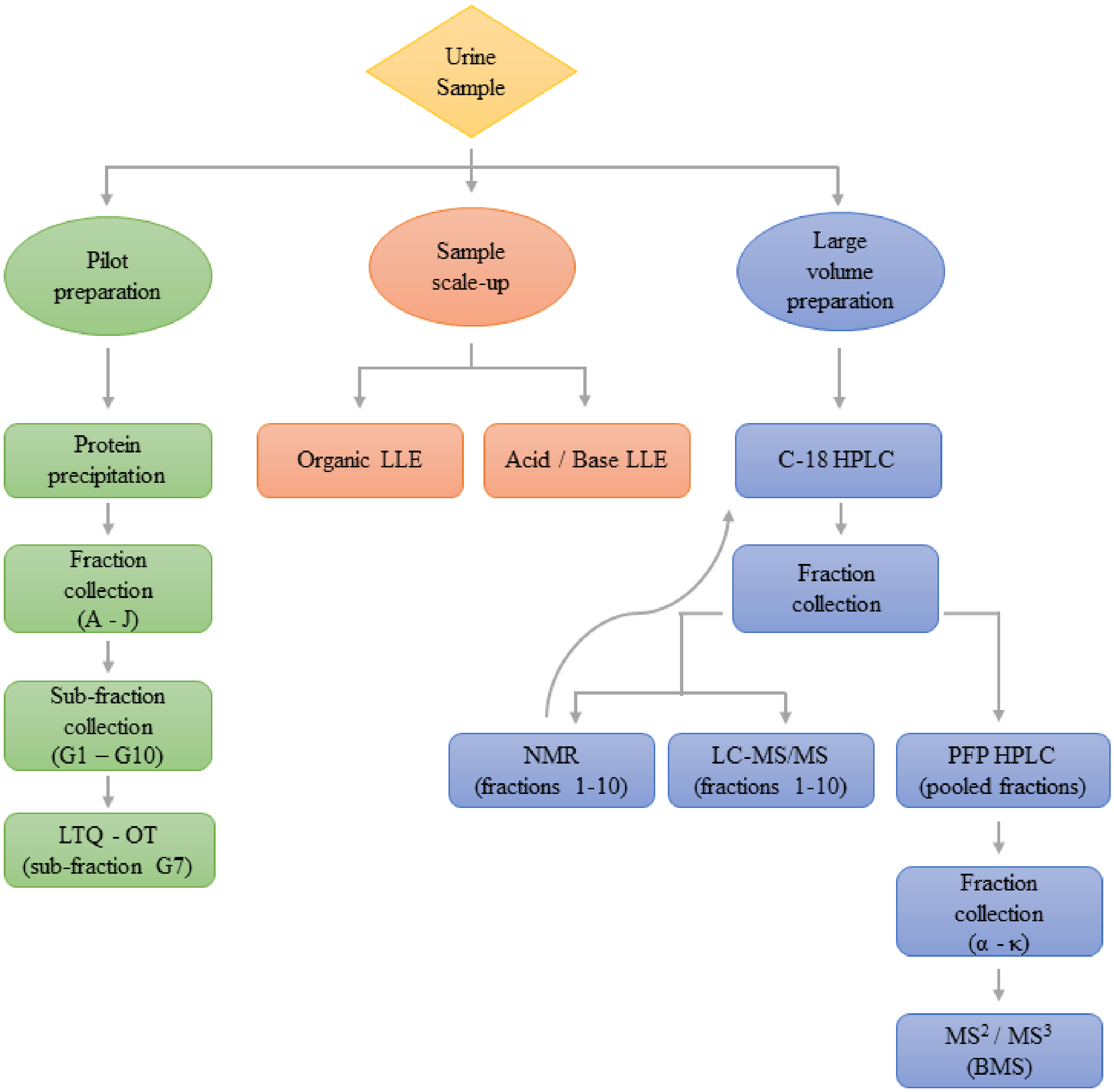

Figure 6.1 Schematic of experimental design for the semi-purification and attempted structural identification of M1. LLE, liquid-liquid extraction; PFP, pentylfluorophenyl

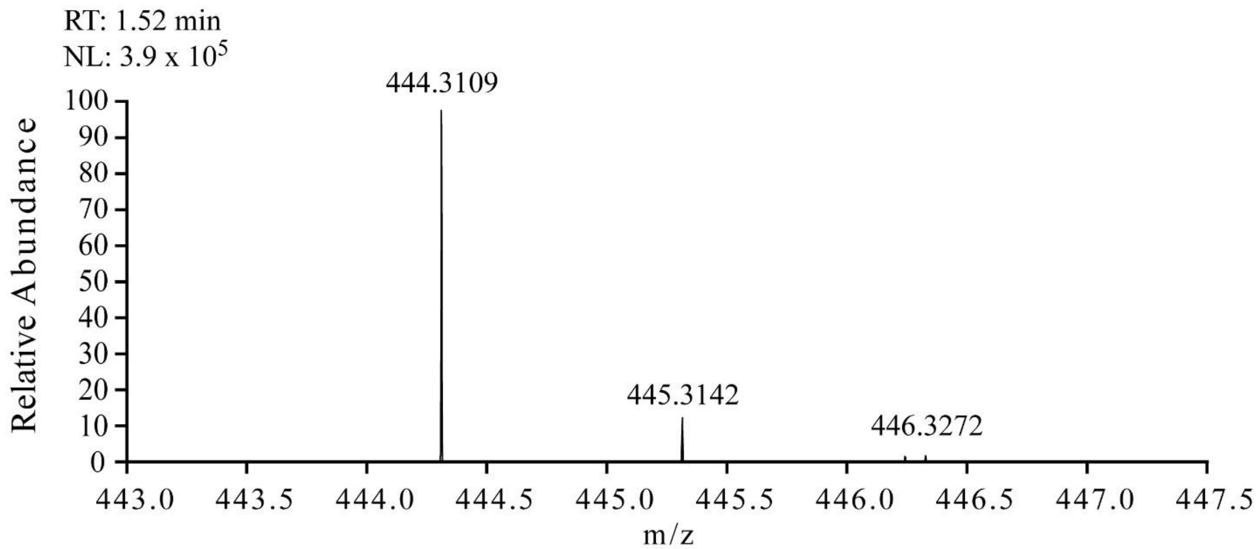

Figure 6.2 High-resolution MS^1 spectra of M1 using Fourier-transform MS (orbitrap). Ionization was performed using positive electrospray ionization mode at 100,000 resolution. The retention time of M1 was 1.52 min.

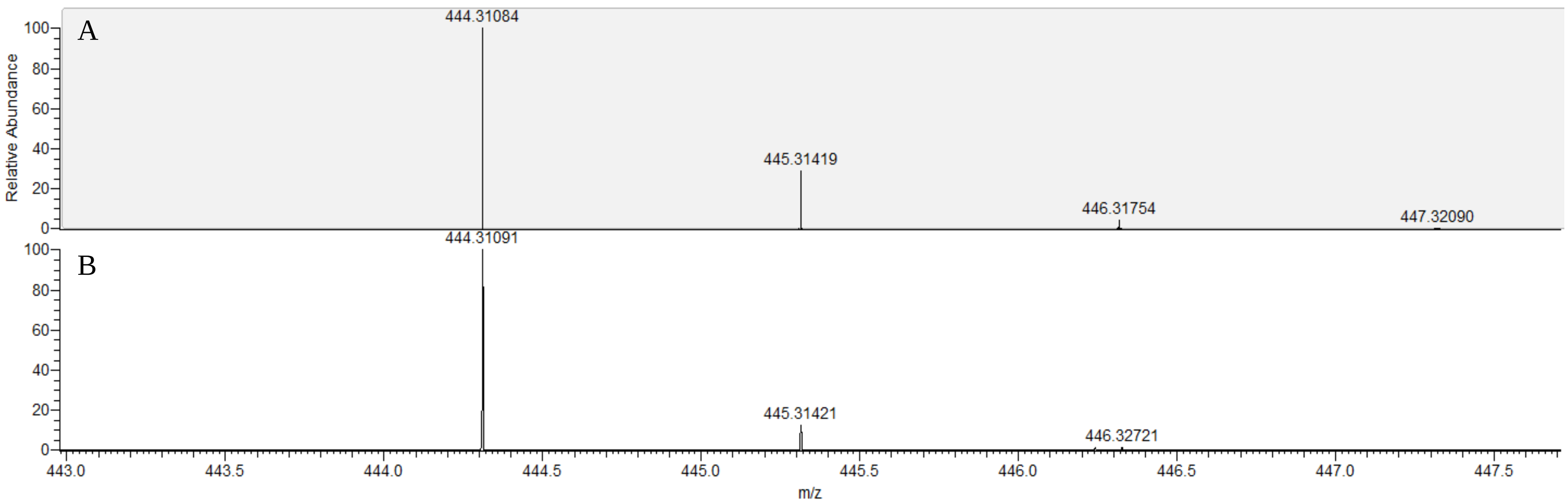

Figure 6.3 The MS[1] spectra for A) simulated ion with elemental formula $C_{27}H_{42}O_4N$ and B) observed M1.

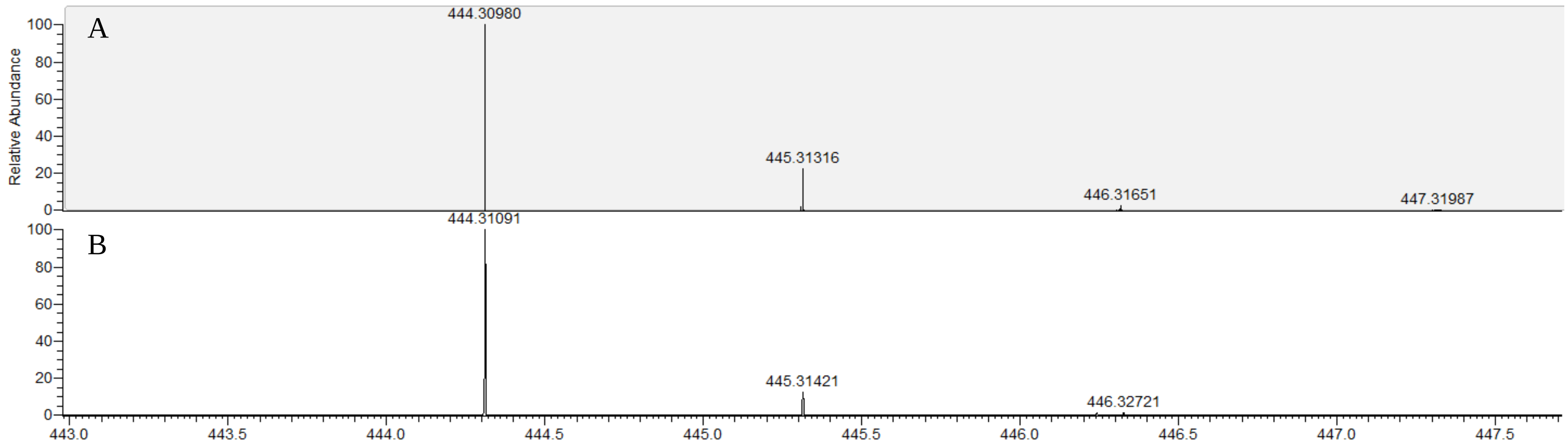

Figure 6.4 The MS^1 spectra for A) simulated ion with elemental formula $C_{21}H_{43}O_3N_5P$ and B) observed M1.

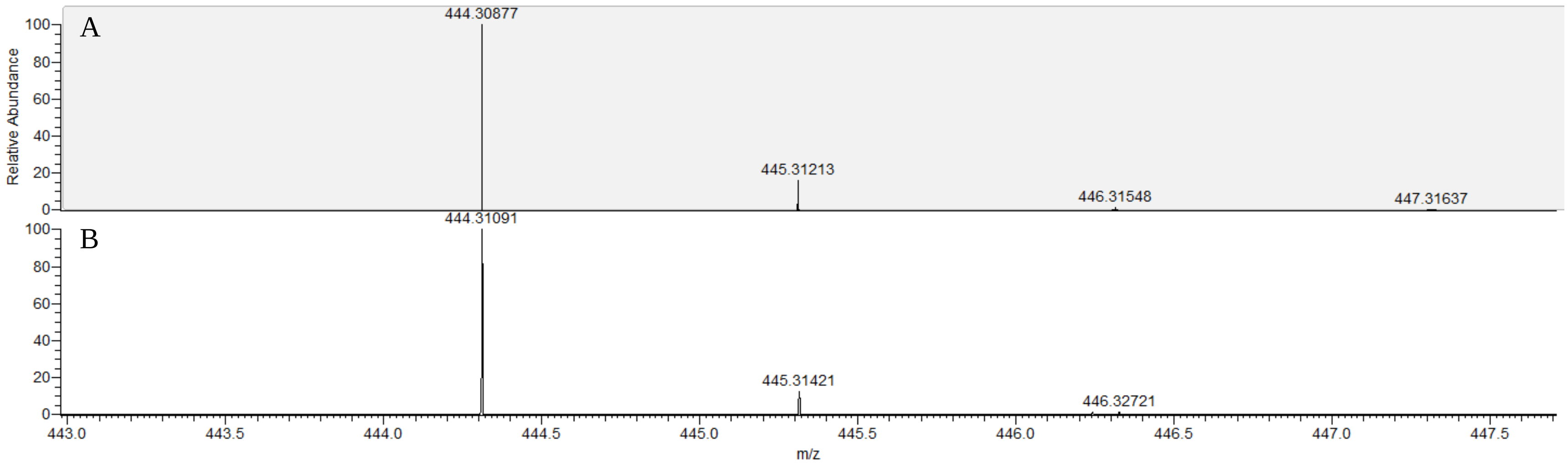

Figure 6.5 The MS[1] spectra for A) simulated ion with elemental formula $C_{15}H_{44}O_2N_9P_2$ and B) observed M1.

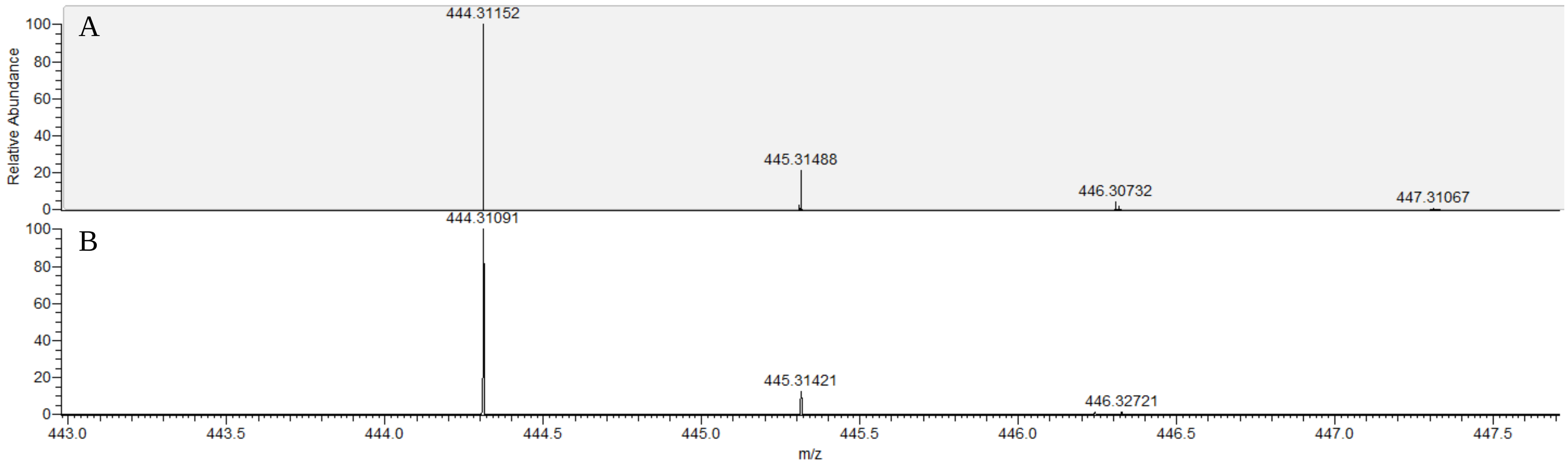

Figure 6.6 The MS^1 spectra for A) simulated ion with elemental formula $C_{20}H_{42}O_2N_7S$ and B) observed M1.

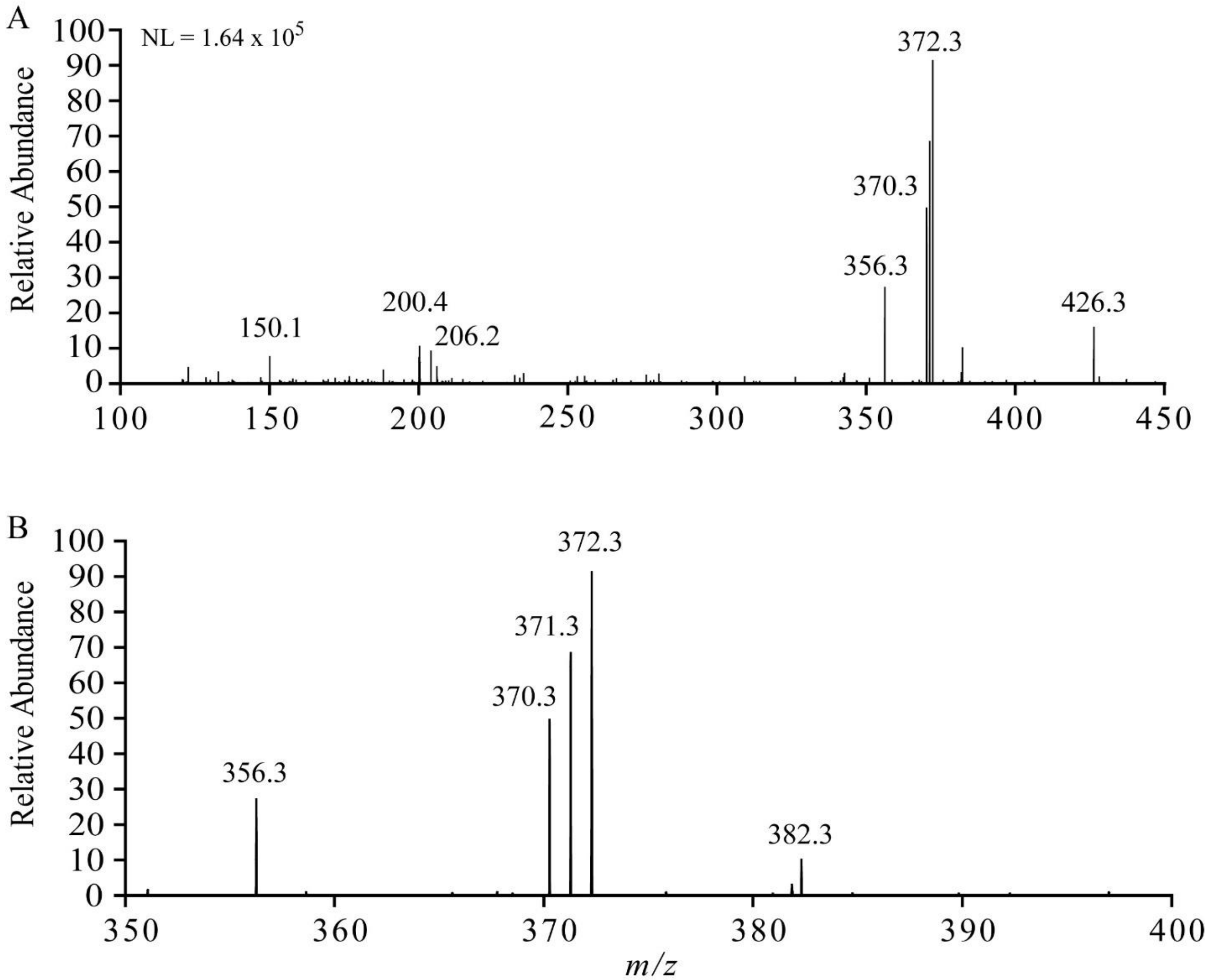

Figure 6.7 MS^2 spectra of A) M1 (*m/z* 444 →) using LTQ at 15,000 resolution in the range of *m/z* 100-450, B) shows a more detailed spectra in the range of *m/z* 350-400. *m/z* 200.35 is observed throughout the course of the run and is likely a system peak.

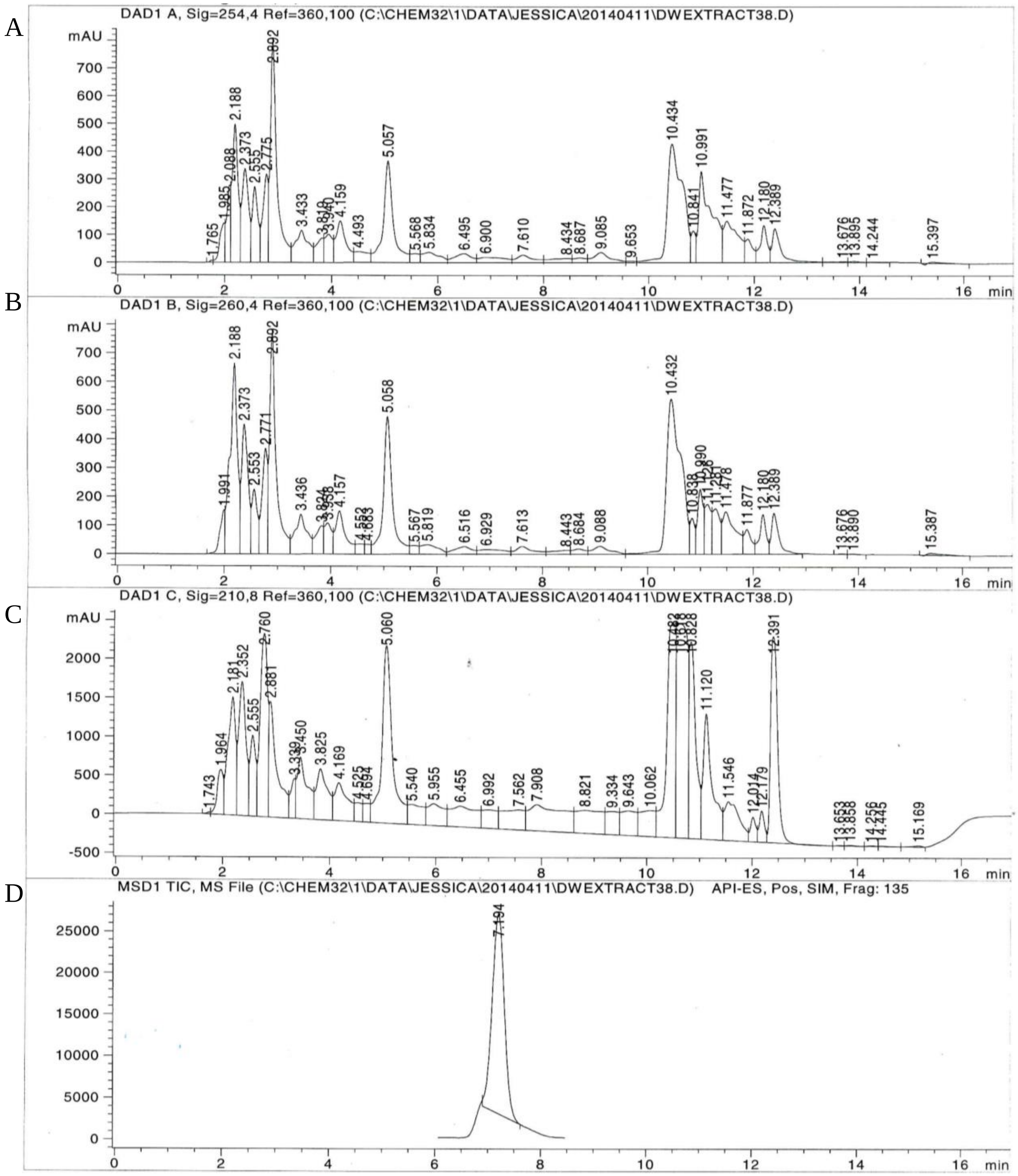

Figure 6.8 LC-UV and LC-MS chromatograms of concentrated, methyl tert-butyl extracted urine sample. A C-18 semi-preparative column was used to separate the sample. UV wavelengths at A) 254 nm, B) 260 nm and C) 210 nm and D) selected ion monitoring of *m/z* 444.3 (M1) by LC-MS are shown. Fractions were collected over the retention time window of the M1 peak shown in D.

A

B

C

D

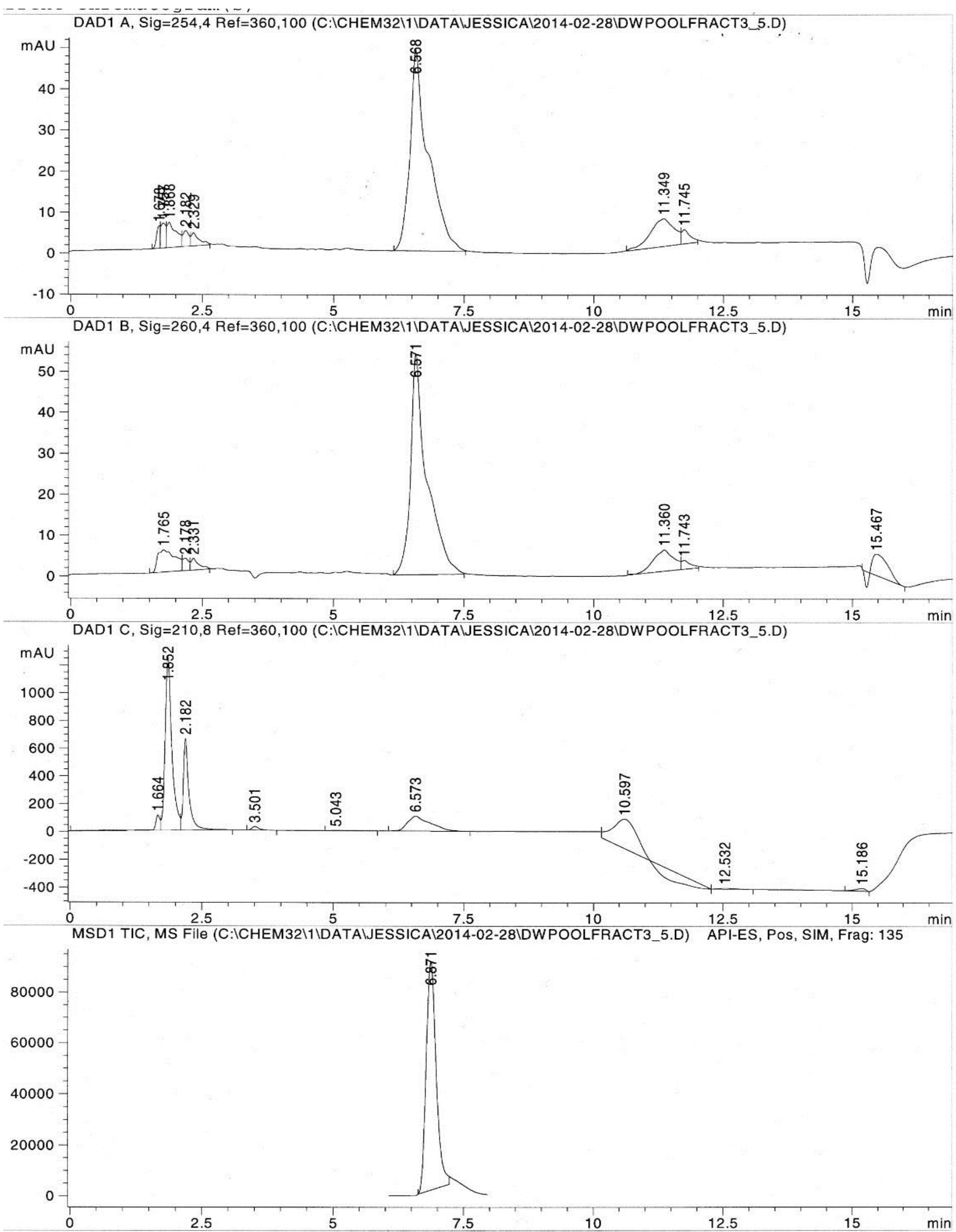

Figure 6.9 LC-UV and LC-MS chromatograms of pooled, concentrated sample following separation and fraction collection by C-18 semi-preparative column. Sample separation shown was achieved using the same C-18 column used prior to sample fraction collection. UV wavelengths at A) 254 nm, B) 260 nm and C) 210 nm and D) selected ion monitoring of *m/z* 444.3 (M1) by LC-MS are shown.

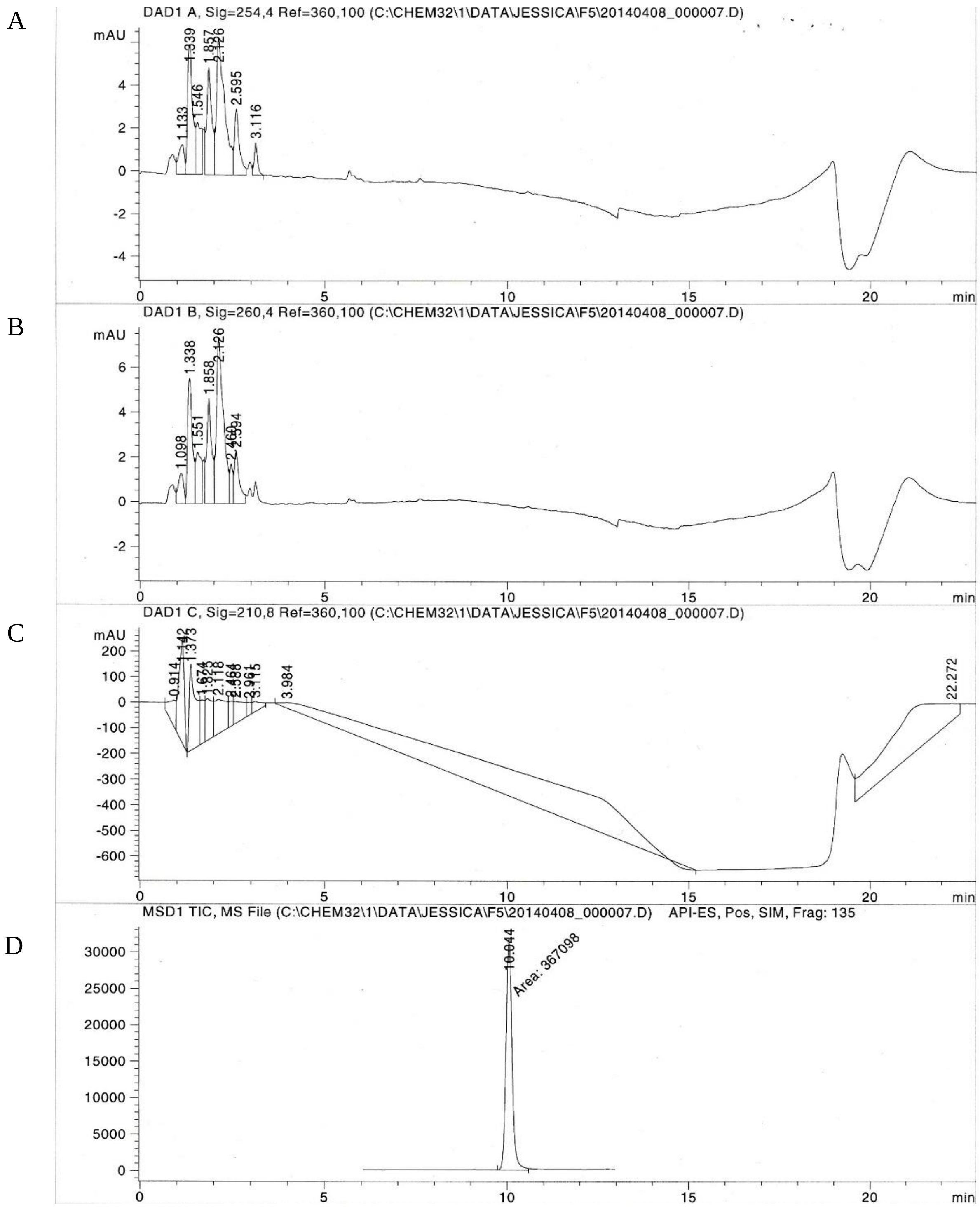

Figure 6.10 LC-UV and LC-MS chromatograms of concentrated, pooled fraction samples. A pentylfluorophenyl column was used to separate the sample following sample separation by C-18 and fraction collection. UV wavelengths at A) 254 nm, B) 260 nm and C) 210 nm and D) selected ion monitoring of *m/z* 444.3 (M1) by LC-MS are shown.

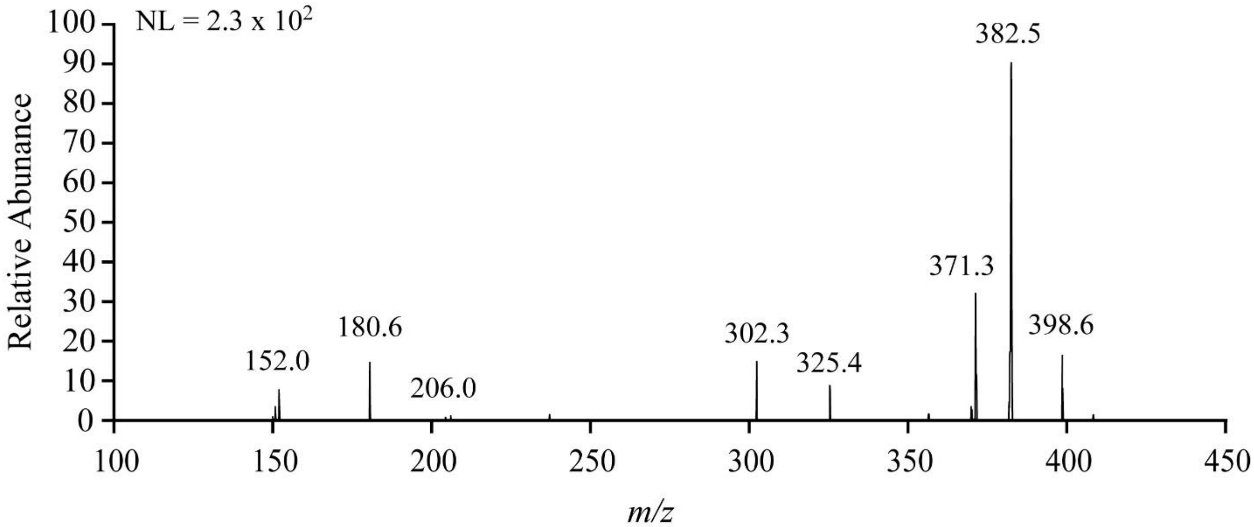

Figure 6.11 MS^3 spectra of M1 (*m/z* 444 → 426 →) using LTQ from *m/z* 100-450.

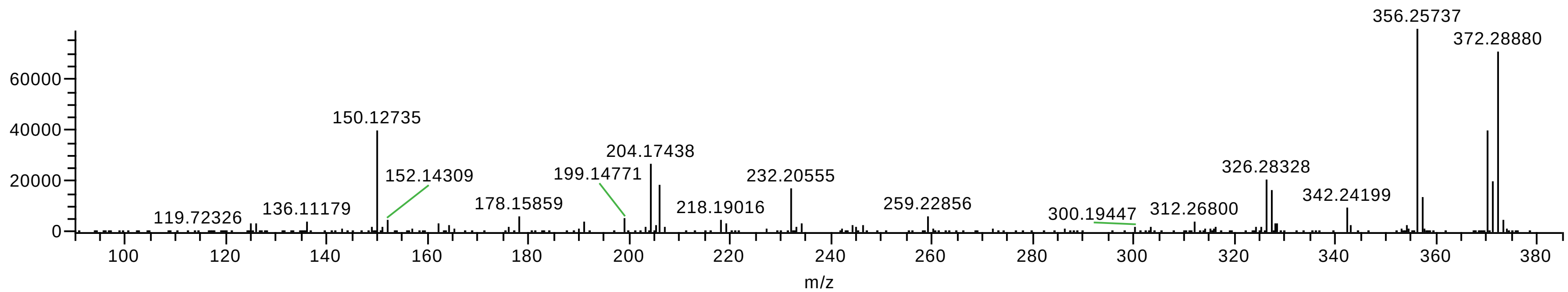

Figure 6.12 MS^3 spectra of M1 (*m/z* 444 → 372 →) from *m/z* 100-380. LC-MS^3 was performed by collaborators at Bristol Myers-Squibb using semi-purification fraction samples containing M1.

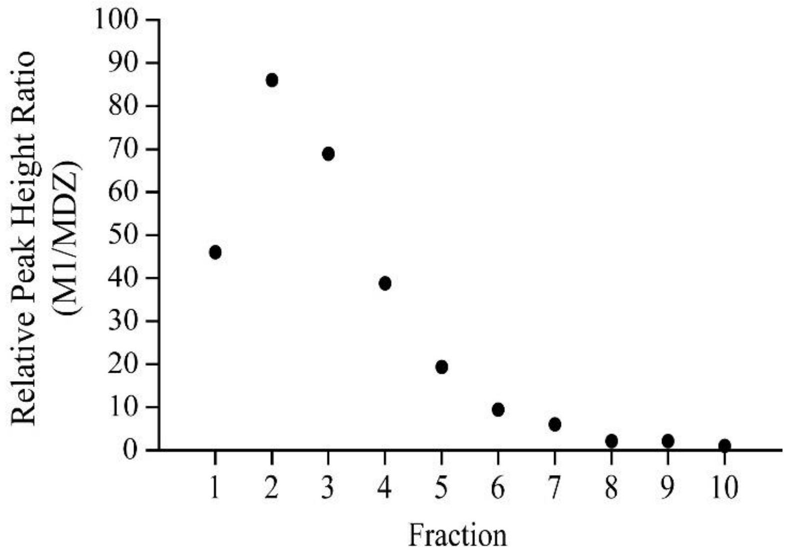

Figure 6.13 Relative M1/midazolam (MDZ) peak height ratio in fractions 1-10 as semi-quantitatively measured by LC-MS/MS.

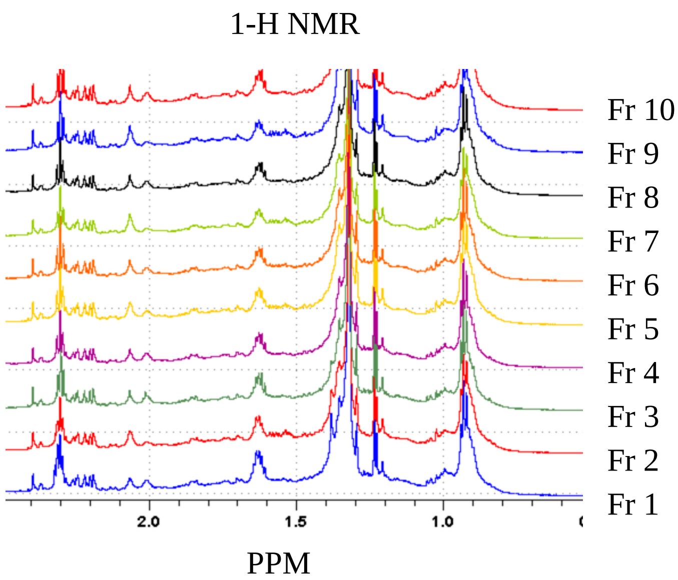

Figure 6.14 ^{1}H NMR analysis of fractions 1-10 following separation by a C-18 semi-preparative column. Analysis was performed by the Northwest Metabolomics Research Center.

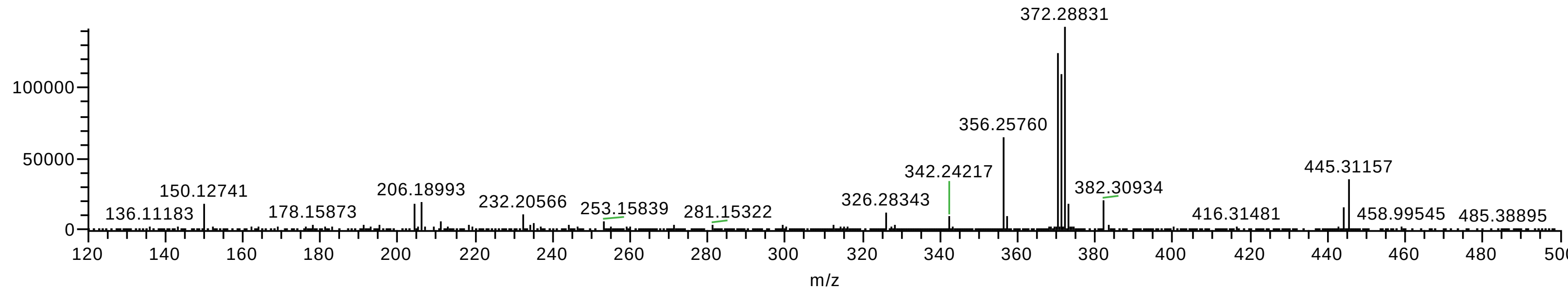

Figure 6.15 MS^2 spectra of M1 (*m/z* 444 →). Analysis was performed by collaborators at Bristol Myers-Squibb using a semi-pure fraction sample containing M1.

Chapter 7. Conclusions

The endocannabinoid, anandamide (AEA) is a CYP2D6 substrate *in vitro* [1, 2] and concentrations have been shown to differ between CYP2D6 humanized mice and wild-type mice [3]. In Chapter 2, our goal was to determine if AEA and its CYP2D6-mediated metabolites, 14,15-epoxyeicosatrienoic acid ethanolamide (14,15-EET-EA) and 20-hydroxyeicosatetraenoic acid ethanolamide (20-HETE-EA) might be endogenous biomarkers of human CYP2D6 activity. We developed a liquid chromatography-tandem mass spectrometry (LC-MS/MS) assay for the simultaneous quantification of AEA, 14,15-EET-EA, and 20-HETE-EA in human plasma. Calibration curve and plasma samples were prepared using a liquid-liquid extraction procedure and analyzed using LC-MS/MS operated in positive electrospray ionization mode. The lower limit of quantification was 0.1 nM for 20-HETE-EA and 0.05 nM for AEA and 14,15-EET-EA. The intraday variability in the accuracy and precision was less than 15% for all analytes. We measured AEA and its metabolites in clinical plasma samples taken from healthy volunteers at baseline and after receiving multiple doses of fluoxetine, a potent CYP2D6 inhibitor. 14,15-EET-EA and 20-HETE-EA were undetectable in the clinical plasma samples. Plasma AEA concentrations did not differ between the baseline and fluoxetine inhibition phases ($P = 0.61$). To our knowledge, this is the first study to investigate the *in vivo* potential of AEA and its metabolites as biomarkers of CYP2D6 activity. Although 20-HETE-EA and 14,15-EET-EA were formed during *in vitro* incubations [1, 2], improving the detection of these metabolites may be necessary to allow quantification in plasma or urine.

In addition to endocannabinoids, other compounds found in the brain have been shown to be CYP2D6 substrates. *In vitro* evidence suggests that trace amines, 5-methoxytryptamine (5-MT) [4], 5-methoxy-*N*,*N*-dimethyltryptamine (5-MeO-DMT) [5], and pinoline [5, 6] are substrates of CYP2D6. We developed a LC-MS/MS method to simultaneously quantify these compounds and the reported CYP2D6 mediated products of 5-MT and 5-MeO-DMT, serotonin and bufotenine in urine. The final sample preparation used SPE and samples were reconstituted in water for symmetrical analyte peak chromatography. We tested the analytical method in two pilot urine samples. Though serotonin and 5-MT were quantifiable, the quality control samples failed, suggesting that the variability in the assay needs to be reduced. Bufotenine was detectable, but far lower than reported literature values, and 5-MeO-DMT and pinoline were not detected. Clearly, additional work needs to be done to improve the assay robustness and reliability prior to assessing the clinical utility of these compounds as CYP2D6 biomarkers.

Analyzing metabolic differences between groups in a shotgun approach has been beneficial in biomarker discovery [7-9]. We applied metabolomics to detect novel urinary biomarkers of CYP2D6 activity as described in Chapter 4 [10]. We identified M1, an ion with *m/z* 444.3 and a retention time of 6.5 min, in a training set of pediatric urine samples. M1 was negatively correlated with dextromethorphan metabolic ratio (spot urine, corrected $P = 6.5 \times 10^{-4}$). Additionally, M1 was absent in CYP2D6 poor metabolizer subjects and present in all other CYP2D6 phenotypes, thus M1 is likely a product of a reaction catalyzed by CYP2D6. This was verified in a second set of pediatric samples using a targeted approach to semi-quantitate M1 abundance. The urinary creatinine/M1 abundance was decreased by 9.56-fold in adults after potent inhibition by fluoxetine treatment as compared to baseline. Creatinine/M1 abundance also correlated with the urinary dextromethorphan metabolic ratio in these adult subjects ($P = 0.012$).

To further validate M1 as a biomarker of CYP2D6 activity, we investigated the relationship between urinary M1 abundance and the oral clearance of metoprolol, dextromethorphan and atomoxetine in Chapter 5. CYP2D6 activity, as determined by log-transformed metoprolol oral clearance, was increased in women during late pregnancy as compared to postpartum ($P = 0.005$). Although the urinary log-transformed M1/creatinine did not differ among pregnancy and postpartum visits, the log-transformed M1/creatinine and log metoprolol oral clearance were correlated ($P < 0.0001$). The log-transformed M1/creatinine was correlated with log atomoxetine oral clearance ($P < 0.0001$) and was different between *CYP2D6* activity score groups among children with ADHD (ANOVA $P < 0.001$). Finally, in the adult subjects, plasma M1 correlated with log dextromethorphan oral clearance ($P = 0.024$).

Overall, M1 appears to reflect CYP2D6 activity *in vivo* as assessed by various probes. M1 is correlated with CYP2D6 activity in urine (Chapter 4) and plasma (Chapter 5). M1 alone may not sensitive enough to reflect small, but significant changes in CYP2D6 activity, as in the case of CYP2D6 induction by pregnancy. This situation may change with the identification of the parent of M1 and the use of a metabolic ratio of the parent compound and M1.

The structural identity of M1 is yet unknown. In order to extract M1 from approximately 5 L of human urine, we used a methyl tert-butyl ether liquid-liquid extraction followed by a two-step HPLC fraction collection using semi-preparative C-18 and pentylfluorophenyl columns. High-resolution mass spectrometry was used to confirm the accurate *m/z* of M1 as 444.3109. From this accurate *m/z*, we obtained four predicted elemental formulas with *m/z* within 5 ppm of *m/z* of M1. MS^2 and MS^3 spectra were obtained using linear trap quadrupole mass spectrometry. Accurate *m/z* (MS^1) and MS^2 were confirmed by collaborators on a separate MS instrument. Nuclear magnetic resonance (NMR) analysis was unsuccessful, likely due to lack of sufficient amounts of M1 at the purity required for this type of analysis. Additional purification steps and a larger starting volume of urine may be needed for identification of M1 by these techniques.

This body of work provides some of the first studies of endogenous compounds as biomarkers of CYP2D6 *in vivo*. Further evaluation of reported ethanolamides and indolethanolamides are needed for confirmation that these would be useful ascertaining CYP2D6 activity. We showed that M1, a molecule found in urine and plasma, was associated with the oral clearance of three probe drugs, dextromethorphan, metoprolol and atomoxetine. We studied M1 in a variety of populations including healthy adults and children, women studied during pregnancy and postpartum, and children with ADHD. Differentiation between CYP2D6 phenotypes by M1 is currently limited to poor and non-poor metabolizers. We believe that the identification of M1 and its parent and subsequent calculation of a parent-to-metabolite metabolic ratio may lead to a more sensitive indicator of CYP2D6 activity. Sufficiently powered and well-designed studies are needed in order to fully validate M1 as a biomarker of CYP2D6 enzyme activity.

Discovery and implementation of endogenous biomarkers in the population, especially if found in urine, might provide a simple, non-invasive, safe, and time-effective means of personalizing drug therapy. Data suggest that M1 reflects CYP2D6 activity in both urine and plasma; therefore, it may be useful for future large-scale pharmacogenomic phenotyping studies, and also when studying banked plasma or urine samples. Upon validation, the use of such biomarkers not only in the general population, but also in vulnerable populations such as children and pregnant women, would provide benefits for general personalized medicine. Endogenous biomarkers may also be useful in first-in-human studies to determine whether a new chemical entity has the potential for drug-drug interactions. Finally, the exploration of the *in vivo* fate of these endogenous compounds will increase our understanding of the physiological role of CYP2D6 in health and disease.

References

1. Snider NT, Sikora MJ, Sridar C, Feuerstein TJ, Rae JM, Hollenberg PF: The endocannabinoid anandamide is a substrate for the human polymorphic cytochrome P450 2D6. *The Journal of pharmacology and experimental therapeutics* 327(2), 538-545 (2008).

2. Sridar C, Snider NT, Hollenberg PF: Anandamide oxidation by wild-type and polymorphically expressed CYP2B6 and CYP2D6. *Drug metabolism and disposition: the biological fate of chemicals* 39(5), 782-788 (2011).

3. Cheng J, Zhen Y, Miksys S *et al.*: Potential role of CYP2D6 in the central nervous system. *Xenobiotica; the fate of foreign compounds in biological systems*, (2013).

4. Yu AM, Idle JR, Byrd LG, Krausz KW, Kupfer A, Gonzalez FJ: Regeneration of serotonin from 5-methoxytryptamine by polymorphic human CYP2D6. *Pharmacogenetics* 13(3), 173-181 (2003).

5. Yu AM, Idle JR, Herraiz T, Kupfer A, Gonzalez FJ: Screening for endogenous substrates reveals that CYP2D6 is a 5-methoxyindolethylamine O-demethylase. *Pharmacogenetics* 13(6), 307-319 (2003).

6. Jiang XL, Shen HW, Yu AM: Pinoline may be used as a probe for CYP2D6 activity. *Drug metabolism and disposition: the biological fate of chemicals* 37(3), 443-446 (2009).

7. Wang X, Zhang A, Han Y *et al.*: Urine metabolomics analysis for biomarker discovery and detection of jaundice syndrome in patients with liver disease. *Molecular & cellular proteomics : MCP* 11(8), 370-380 (2012).

8. Sreekumar A, Poisson LM, Rajendiran TM *et al.*: Metabolomic profiles delineate potential role for sarcosine in prostate cancer progression. *Nature* 457(7231), 910-914 (2009).

9. Quinones MP, Kaddurah-Daouk R: Metabolomics tools for identifying biomarkers for neuropsychiatric diseases. *Neurobiology of disease* 35(2), 165-176 (2009).

10. Tay-Sontheimer J, Shireman LM, Beyer RP *et al.*: Detection of an endogenous urinary biomarker associated with CYP2D6 activity using global metabolomics. *Pharmacogenomics* 15(16), 1947-1962 (2014).